

APPENDIX I

SANTOS, L., SYKES, R. I., KARAMCHANDANI, P., SEIGNEUR, C., LURMANN, F., AND R. ARNDT, 1999: SECOND-ORDER PUFF MODEL WITH AQUEOUS-PHASE CHEMISTRY AND AEROSOLS, DRAFT FINAL REPORT PREPARED FOR EPRI, SCE, AND CALIFORNIA ENERGY COMMISSION

SANTOS, L. AND R. I. SYKES, 1999: FILE FORMATS (MODEL TECHNICAL DOCUMENTATION). DRAFT FINAL REPORT PREPARED FOR EPRI, SCE, AND CALIFORNIA ENERGY COMMISSION

Second-order Closure Puff Model with Aqueous-Phase Chemistry and Aerosols

Second-order Closure Puff Model with Aqueous-Phase Chemistry and Aerosols

Final Report, Draft: September 9, 1999

Prepared by
Lynne Santos and R. Ian Sykes
ARAP Group, Titan Research & Technology

Prakash Karamchandani and Christian Seigneur
Atmospheric and Environmental Research, Inc.

and

Fred Lurmann and Richard Arndt
Sonoma Technology, Inc.

Prepared for
EPRI
Southern California Edison
California Energy Commission

EPRI Project Managers
Mary Ann Allan
Naresh Kumar

TABLE OF CONTENTS

1. INTRODUCTION.....	1
2. SELECTION OF MODULES.....	4
2.1 Selection of the Aerosol Thermodynamic Model	4
2.2 Selection of the Aqueous-Phase Chemistry Module.....	5
3. IMPLEMENTATION OF MODULES.....	18
3.1 Development of Interfaces	18
3.2 Modifications to SCICHEM and the Aerosol Equilibrium and Aqueous Chemistry Modules.....	20
3.2.1 Multicomponent Input File.....	24
3.2.2 Meteorology scenario file.....	32
3.2.3 Meteorology Input Files	32
4. MODEL TESTING.....	35
4.1 Background and Purpose	35
4.2 Test Conditions	36
4.3 Baseline Results	41
4.3.1 Baseline Case Results Without Clouds	41
4.3.2 Baseline Case Results With Clouds	42
4.4 Sensitivity Study Results	52
4.4.1 Sensitivity Results Without Clouds	75
4.4.2 Sensitivity Results With Clouds.....	80
5. SUMMARY AND RECOMMENDATIONS.....	87
5.1. Summary of Model Testing	87
5.1. Recommendations.....	89
6. REFERENCES.....	93

FIGURES

Figure 3-1. Sample species section of the IMC file.....	27
Figure 3-2. Sample aqueous section of the IMC file.	31
Figure 4-1. SCICHEM baseline simulation: Calculated surface concentration (ppm) of SO ₂	43
Figure 4-2. SCICHEM baseline simulation: Calculated surface concentration (µg/m ³) of particulate sulfate.	44
Figure 4-3. SCICHEM baseline simulation: Calculated surface concentration (ppm) of NO.	45
Figure 4-4. SCICHEM baseline simulation: Calculated surface concentration (ppm) of NO ₂	46
Figure 4-5. SCICHEM baseline simulation: Calculated surface concentration (ppm) of Ozone.	47
Figure 4-6. SCICHEM baseline simulation: Calculated surface concentration (µg/m ³) of particulate nitrate.....	48
Figure 4-7. SCICHEM aqueous-phase baseline simulation: Calculated surface concentration (ppm) of SO ₂	49
Figure 4-8. SCICHEM aqueous-phase baseline simulation: Calculated surface concentration (µg/m ³) of particulate sulfate.....	50
Figure 4-9. SCICHEM aqueous-phase baseline simulation: Calculated surface concentration (µg/m ³) of particulate nitrate.	51
Figure 4-10. Downwind surface concentrations of NO _x , ozone, PAN, HNO ₃ and aerosol nitrate for NO _x emissions	78

TABLES

Table 2-1.	Species included in the aqueous-phase chemistry module.....	9
Table 2-2.	Henry's law constants for the gaseous species considered in the aqueous-phase chemistry module.....	10
Table 2-3.	Equilibrium reactions included in the aqueous-phase chemical mechanism.	11
Table 2-4.	Kinetic reactions included in the aqueous-phase chemical mechanism.....	12
Table 3-1.	SCICHEM species types.	26
Table 3-2.	Required species names for the aerosol equilibrium module and aqueous-phase chemistry module	28
Table 3-3.	Additional meteorological variables and corresponding units recognized in SCICHEM.	33
Table 4-1.	Baseline test case meteorological and emissions input parameters.	37
Table 4-2.	Baseline ambient concentrations for the test simulations.	38
Table 4-3.	Input parameter variations for model test simulations.	40
Table 4-4.	Estimated surface concentrations (ppb) of Tracer and SO ₂ at 12:00L at 5 km, 25 km, and 50 km downwind of the major point source for the 41 test simulations.	53
Table 4-5.	Estimated surface concentrations (ppb) of Tracer and SO ₂ at 16:00L at 5 km, 25 km, and 50 km downwind of the major point source for the 41 test simulations.	54
Table 4-6.	Estimated surface concentrations (ppb) of Tracer and SO ₂ at 20:00L at 5 km, 25 km, and 50 km downwind of the major point source for the 41 test simulations.	55
Table 4-7.	Estimated surface concentrations (ppb) of NO and NO ₂ at 12:00L at 5 km, 25 km, and 50 km downwind of the major point source for the 41 test simulations.	56
Table 4-8.	Estimated surface concentrations (ppb) of NO and NO ₂ at 16:00L at 5 km, 25 km, and 50 km downwind of the major point source for the 41 test simulations.	57
Table 4-9.	Estimated surface concentrations (ppb) of NO and NO ₂ at 20:00L at 5 km, 25 km, and 50 km downwind of the major point source for the 41 test simulations.	58

Table 4-10. Estimated surface concentrations (ppb) of Ozone and H ₂ O ₂ at 12:00L at 5 km, 25 km, and 50 km downwind of the major point source for the 41 test simulations.	59
Table 4-11. Estimated surface concentrations (ppb) of Ozone and H ₂ O ₂ at 16:00L at 5 km, 25 km, and 50 km downwind of the major point source for the 41 test simulations.	60
Table 4-12. Estimated surface concentrations (ppb) of Ozone and H ₂ O ₂ at 20:00L at 5 km, 25 km, and 50 km downwind of the major point source for the 41 test simulations.	61
Table 4-13. Estimated surface concentrations (ppb) of HNO ₃ and NH ₃ at 12:00L at 5 km, 25 km, and 50 km downwind of the major point source for the 41 test simulations.	62
Table 4-14. Estimated surface concentrations (ppb) of HNO ₃ and NH ₃ at 16:00L at 5 km, 25 km, and 50 km downwind of the major point source for the 41 test simulations.	63
Table 4-15. Estimated surface concentrations (ppb) of HNO ₃ and NH ₃ at 20:00L at 5 km, 25 km, and 50 km downwind of the major point source for the 41 test simulations.	64
Table 4-16. Estimated surface concentrations (µg/m ³) of sulfate aerosol particle at 12:00L at 5 km, 25 km, and 50 km downwind of the major point source for the 41 test simulations.	65
Table 4-17. Estimated surface concentrations (µg/m ³) of sulfate aerosol particle at 14:00L at 5 km, 25 km, and 50 km downwind of the major point source for the 41 test simulations.	66
Table 4-18. Estimated surface concentrations (µg/m ³) of sulfate aerosol particle at 16:00L at 5 km, 25 km, and 50 km downwind of the major point source for the 41 test simulations.	67
Table 4-19. Estimated surface concentrations (µg/m ³) of sulfate aerosol particle at 18:00L at 5 km, 25 km, and 50 km downwind of the major point source for the 41 test simulations.	68
Table 4-20. Estimated surface concentrations (µg/m ³) of sulfate aerosol particle at 20:00L at 5 km, 25 km, and 50 km downwind of the major point source for the 41 test simulations.	69
Table 4-21. Estimated surface concentrations (µg/m ³) of nitrate and ammonium aerosol particles at 12:00L at 5 km, 25 km, and 50 km downwind of the major point source for the 41 test simulations.	70

Table 4-22. Estimated surface concentrations ($\mu\text{g}/\text{m}^3$) of nitrate and ammonium aerosol particles at 14:00L at 5 km, 25 km, and 50 km downwind of the major point source for the 41 test simulations.	71
Table 4-23. Estimated surface concentrations ($\mu\text{g}/\text{m}^3$) of nitrate and ammonium aerosol particles 16:00L at 5 km, 25 km, and 50 km downwind of the major point source for the 41 test simulations.	72
Table 4-24. Estimated surface concentrations ($\mu\text{g}/\text{m}^3$) of nitrate and ammonium aerosol particles at 18:00L at 5 km, 25 km, and 50 km downwind of the major point source for the 41 test simulations.	73
Table 4-25. Estimated surface concentrations ($\mu\text{g}/\text{m}^3$) of nitrate and ammonium aerosol particles at 20:00L at 5 km, 25 km, and 50 km downwind of the major point source for the 41 test simulations.	74
Table 4-26. Noontime concentrations with different NO_x emission rates.	76
Table 4-27. Noontime concentrations 25 km downwind with different temperature and relative humidity.	80
Table 4-28. Sulfate and Nitrate Aerosol Concentrations for Sensitivity Cases.	81

1. INTRODUCTION

Reactive plume models are often used to estimate the local or short- to medium-range (i.e., up to a few hundred km) impacts of power plants or smelters on air quality. Issues of interest typically include ozone and particulate matter concentrations above the National Ambient Air Quality Standards (NAAQS), visibility degradation, and acid deposition. For example, the second-generation Reactive and Optics Model of Emissions (ROME; Seigneur et al., 1997) has been recently applied to examine the impacts of power plants on visibility in the Dallas-Fort Worth area (Seigneur et al., 1999) and the Grand Canyon (Karamchandani et al., 1998). Examples of other plume models include the first-generation Reactive Plume Model (RPM; Stewart and Liu, 1981) and PLMSTAR model (Godden and Lurmann, 1983), and the CALPUFF model (Scire et al., 1997; Vimont, 1998).

All the currently available reactive plume models, including those mentioned above, have some shortcomings either in their treatment of physical phenomena, or in their treatment of chemical processes. For example, most models employ a simplified treatment of plume dispersion processes, and important physical phenomena, such as the effect of wind shear on plume dispersion and the effect of plume overlaps (e.g., under conditions of reversal flow or merging of adjacent plumes), are not (or poorly) represented by these models. None of the models includes a treatment of the effect of atmospheric turbulence on nonlinear chemical kinetics.

The newer second-generation models, such as ROME and CALPUFF, attempt to address some of these shortcomings. For example, ROME incorporates an advanced treatment of plume dispersion based on a second-order closure algorithm (Sykes and Gabruk, 1997), that has been found to provide better agreement with field measurements of power plant plumes than first-order closure and Pasquill-Gifford-Turner algorithms (Gabruk et al., 1999; Seigneur et al., 1999). ROME also has a fairly complete and comprehensive treatment of the processes governing the chemistry of power plant plumes, including gas-phase chemistry, liquid-phase chemistry, gas-particle thermodynamic equilibrium and aerosol particle dynamics. However, ROME does not account for wind shear effects.

This can be a serious limitation when applying the model for relatively long transport distances. On the other hand, the CALPUFF model is a non-steady-state puff dispersion model that uses a puff-splitting algorithm to account for vertical wind shear. However, its treatment of chemistry is highly simplified. Moreover, CALPUFF includes a relatively simple treatment of dispersion (first-order closure) compared to second-order schemes that have been demonstrated to be more realistic (e.g., Gabruk et al., 1999; Seigneur et al., 1999).

More realistic puff dispersion models have been developed as a part of EPRI and Defense Threat Reduction Agency work over the last few years. The Second-order Closure Integrated Puff model, SCIPUFF, is a state-of-the-science Lagrangian transport and diffusion model for atmospheric dispersion applications. The model uses a collection of three-dimensional Gaussian puffs to represent an arbitrary time-dependent concentration field. Second-order turbulence closure is used to parameterize turbulent diffusion in the model, providing a direct connection between measurable velocity statistics and the predicted dispersion rates. This allows an accurate treatment of dispersion and the influence of turbulence on chemical rates. The model also incorporates generalized puff splitting/merging algorithms to account for wind shear effects and describe multiple sources. The model has recently been enhanced to incorporate detailed gas-phase chemistry mechanisms. The combined puff-chemistry model, referred to as SCICHEM, was recently evaluated using data from the 1995 Southern Oxidants Study (SOS) Nashville/Middle Tennessee Ozone Study (Karamchandani et al., 1999).

Prior to this study, SCICHEM lacked a treatment of chemical transformations in the aqueous phase. This can be a serious shortcoming since a significant amount of chemical conversion can occur in cloud or fog droplets. For example, the application of ROME to the Dallas-Fort Worth region showed that aqueous conversion played an important role in converting power plant SO₂ emissions to sulfate. SCICHEM also did not include a treatment of thermodynamic partitioning of species such as nitrate between the gas (nitric acid) and particle (e.g., ammonium nitrate) phases. Because of the different removal rates of these species from the atmosphere, this limitation can introduce errors under conditions where a significant fraction of the nitrate is present in the particle phase.

Before SCICHEM could be generally applied to study the impacts of NO_x and SO₂ emissions from existing and proposed plants for research and policy-relevant applications, it was necessary to correct these deficiencies. In the study described in this report, we have added capabilities to SCICHEM to simulate liquid-phase chemistry and gas-particle thermodynamic equilibrium. We used existing modules for aqueous-phase chemistry and aerosol thermodynamics and incorporated them in SCICHEM. The enhanced model was then tested for a range of conditions to determine if model results were physically and chemically consistent. The following sections describe: our rationale for selecting the modules that were implemented; details of the implementation; results from model testing; and recommendations for additional improvements and testing.

2. SELECTION OF MODULES

The guiding principle for selection of the SCICHEM aerosol thermodynamic module and aqueous-phase chemistry module was that they should be readily available and have state-of-the-science representation of the relevant processes. This is consistent with the treatment of the other governing physical and chemical processes in the model, such as dispersion and gas-phase chemistry.

2.1 Selection of the Aerosol Thermodynamic Model

The objective was to identify an aerosol thermodynamic module that could be used to estimate the equilibrium phase distribution of sulfuric acid, sulfate, nitric acid, nitrate, ammonia, ammonium, sodium, chloride, and hydrochloric acid for a single aerosol size section. Several recent studies have inter-compared and evaluated aerosol thermodynamic modules (Kumar et al., 1998; Ansari and Pandis, 1999; Zhang et al., 1999). The results of these studies were used to guide the selection of a module for SCICHEM.

Zhang et al. (1999) conducted a comprehensive quantitative evaluation of five thermodynamic equilibrium modules that are currently used in three-dimensional air quality particulate matter (PM) models. The five modules that were tested by Zhang et al. (1999) include MARS-A (Binkowski and Shankar, 1995), SEQUILIB (Pilinis and Seinfeld, 1987), SCAPE2 (Meng et al., 1995), EQUISOLV II (Jacobson, 1999) and AIM2 (Clegg et al., 1998a; 1998b). Zhang et al. (1999) concluded that the SCAPE2 and EQUISOLV II modules contained a state-of-the-science representation of aerosol chemistry and thermodynamics and were applicable for a wide range of conditions. The SCAPE2 software is publicly available, whereas EQUISOLV is copyrighted. The simpler MARS-A module has a limited range of applicability, and the version of SEQUILIB tested was unstable or gave abnormal results for many conditions. Although

the AIM2 module also has a comprehensive treatment of the relevant processes, it cannot simulate alkaline systems.

Kumar et al. (1998) intercompared three aerosol thermodynamic modules, SCAPE2, ISORROPIA (Nenes et al., 1999), and SEQUILIB 2.1, against reference numerical solutions obtained by pure minimization of the Gibbs Free Energy (GFEM) in the aerosol thermodynamic system (i.e., a gold standard). They found that all three modules compared well against the reference solutions and that ISORROPIA was numerically much faster than the other schemes under most conditions. The modules were also compared against gas/aerosol ambient concentration data obtained in the California's San Joaquin Valley in winter. Overall, both SCAPE2 and ISORROPIA compared well against the observations. However, SCAPE2 includes thermodynamic data for carbonate, calcium, potassium, and manganese, which are not included in the other modules. There was marginal evidence that inclusion of these extra species improved the performance of SCAPE2 compared to ISORROPIA in the San Joaquin Valley applications.

Ansari and Pandis (1999) extended the comparative evaluation of SCAPE2, ISORROPIA, SEQUILIB, and GFEM to a large number of simulation cases. Their conclusions were qualitatively consistent with those of Zhang et al. (1999) and Kumar et al. (1998).

Based on the reviews summarized above, SCAPE2 offers a comprehensive treatment of gas/particle chemical composition and thermodynamics, good accuracy, reasonable computational efficiency, and no copyright restrictions. Therefore, we selected SCAPE2 for incorporation into SCICHEM.

2.2 Selection of the Aqueous-Phase Chemistry Module

The requirements for the aqueous-phase chemistry module were that it should be readily available in a package with a robust numerical solver and that it should provide a relatively complete representation of the aqueous sulfur chemistry and the chemistry of the compounds that affect the sulfur chemistry. Because the solubility of SO₂ and the

oxidation rates of dissolved SO₂ depend on the acidity of the liquid, the selected aqueous chemistry mechanism needs to include a fairly long list of species that can affect the acidity of atmospheric droplets. Based on these specifications, the following four aqueous-phase chemical mechanisms were considered in our review:

- CMU Mechanism (Strader et al., 1998),
- MaTChM Mechanism (Zhang et al., 1998)
- ROME Mechanism (Seigneur and Saxena, 1988)
- RADM-II Mechanism (Walcek and Taylor, 1986)

All of the mechanisms are designed for estimation of sulfate production from SO₂ in atmospheric liquid water and include the three dominant pathways for S(IV) oxidation: hydrogen peroxide, ozone, and oxygen catalyzed by iron and manganese.

The CMU and MaTChM mechanisms incorporate the highest level of chemical detail and are very similar. The CMU mechanism includes 17 gas-aqueous equilibrium reactions, 18 aqueous equilibrium reactions, and 99 aqueous-phase kinetic reactions among 18 gas-phase species and 28 aqueous-phase species. The CMU mechanism is an updated version of the Pandis and Seinfeld (1989) mechanism. Zhang et al. (1998) compared the MaTChM mechanism to the Pandis and Seinfeld (1989) mechanism and found several missing reactions and outdated rate constants in the latter. The CMU mechanism of Strader et al. (1998) includes the updates recommended by Zhang et al. (1998). Thus, these two mechanisms are essentially equivalent.

The ROME mechanism is less detailed than the first two mechanisms. It incorporates the principal reactions controlling aqueous-phase sulfate formation in most circumstances and includes some updated reaction rates from those reported by Seigneur and Saxena (1988). It is probably a good choice for an alternate, more condensed mechanism for SCICHEM, but not for the primary mechanism. The RADM-II mechanism, which is also used in the SAQM, MAQSIP, and CMAQ/Models-3 three-dimensional air quality models, is the least detailed of the mechanisms. The RADM-II mechanism was

developed at a time when computers required representation of the chemistry with absolutely the fewest number of species. For example, it does not include chlorine chemistry, or organic acids that can be important in less polluted environments. The lack of chemical detail makes this mechanism undesirable for SCICHEM.

The CMU and MaTChM mechanisms are well suited for use in SCICHEM. We have run the CMU mechanism using the software module developed by Strader et al. (1998). We did not obtain or test the MaTChM model software. Strader et al. (1998) tested 7 numerical solvers and found the VODE solver to be the fastest for a range of conditions. The MaTChM model uses the LSODE solver that Strader et al. (1998) found to be three times slower than VODE. Strader et al. (1998) also tried to identify the minimum number of species that needed to be integrated in the module to increase the computational efficiency. We believe that the CMU module is computationally more efficient than the MaTChM module, but have not actually performed side-by-side comparisons of the two modules. Given that the mechanisms in the CMU and MaTChM modules are similar, and that the CMU implementation appears to be more efficient, we selected the CMU module for implementation in SCICHEM.

A detailed description of the CMU aqueous-phase mechanism is provided in Seinfeld and Pandis (1998) and Strader et al. (1998). The scope of the mechanism is summarized in the following tables.

- Table 2-1 lists the aqueous-phase and gas-phase species, along with their treatment, in the CMU module.
- Table 2-2 lists the Henry's law constants for the gaseous species considered in the CMU module.
- Table 2-3 lists the aqueous-phase dissociation or equilibrium reactions included in the CMU mechanism.
- Table 2-4 lists the aqueous-phase kinetic reactions included in the CMU mechanism. These are separated into the oxygen-hydrogen reactions, the carbonate reactions, the

chlorine reactions, the nitrite and nitrate reactions, the organic reactions, and the sulfur reactions.

The mechanism was implemented with options for controlling what aqueous-phase chemistry is actually used in a particular simulation. While the aqueous-phase mechanism is virtually imbedded in the code, rather than read-in from the input files, the SCICHEM implementation allows the user to include or ignore (1) the chlorine chemistry, and (2) the iron and manganese catalyst oxidation of dissolved SO₂. These options are provided because these portions of the chemistry often have only small effects on the results and sometimes present very stiff numerical conditions that use significant amounts of computer time. In general, however, we recommend that the full aqueous-phase chemical mechanism be used for reactive plume simulations.

Table 2-1. Species included in the aqueous-phase chemistry module.

Aqueous-Phase Species	Treatment	Gas-Phase Species	Treatment
S(IV)	Dynamic	SO ₂	Dynamic
S(VI)	Dynamic	H ₂ SO ₄	Dissolution
N(III)	Henry's law	HNO ₂	Henry's law
N(V)	Dynamic	HNO ₃	Dissolution
CO ₂	Henry's law	CO ₂	Constant
H ₂ O ₂	Dynamic	H ₂ O ₂	Dynamic
HCHO	Dynamic	HCHO	Henry's law
HCOOH	Dynamic	HCOOH	Henry's law
NO	Constant	NO	Constant
NO ₂	Constant	NO ₂	Constant
O ₃	Constant	O ₃	Constant
PAN	Constant	PAN	Constant
HCl	Dynamic	HCl	Dissolution
OH	Steady-state	OH	Steady-state
HO ₂	Steady-state	HO ₂	Steady-state
NO ₃	Steady-state	NO ₃	Steady-state
NH ₃	Dynamic	NH ₃	Dynamic
CH ₃ O ₂	Constant	CH ₃ O ₂	Constant
SO ₄ ⁻	Steady-state		
SO ₅ ⁻	Steady-state		
HSO ₅ ⁻	Dynamic		
HMSA	Dynamic		
CO ₃ ⁻	Steady-state		
Na ⁺	Constant		
Fe ³⁺	Constant		
Mn ²⁺	Constant		

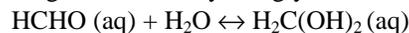
Table 2-2. Henry's law constants for the gaseous species considered in the aqueous-phase chemistry module.

Gas-Phase Species ^a	Henry's Law Constant (M atm ⁻¹ , at 298 K) ^b
SO ₂	1.23
HNO ₂	49
HNO ₃	2.1 x 10 ⁵
CO ₂	3.4 x 10 ⁻²
H ₂ O ₂	7.5 x 10 ⁴
HCHO ^c	2.5
HCOOH	3.6 x 10 ³
NO	1.9 x 10 ⁻³
NO ₂	1.0 x 10 ⁻²
O ₃	1.1 x 10 ⁻²
PAN	2.9
HCl	727
OH	25
HO ₂	2.0 x 10 ³
NO ₃	2.1 x 10 ⁵
NH ₃	62
CH ₃ O ₂ ^d	6

^a The values given reflect only the physical solubility of the gas regardless of the subsequent fate of the dissolved species. The above constants do not account for dissociation or other aqueous-phase transformations. See Table 2-3 for the dissociation reactions.

^b For data on the temperature dependence of these constants, see Pandis and Seinfeld (1989).

^c Formaldehyde, upon dissolution in water, undergoes hydrolysis to yield the gem-diol, methylene glycol.



If this reaction is included, the effective Henry's law constant of formaldehyde becomes 6.3×10^3 (Seinfeld and Pandis, 1998). The mechanism implemented here includes the effect of this reaction.

^d For the SAPRC98 chemical mechanism, the total alkyl peroxy radicals (RO₂) can be used as an upper-limit estimate of CH₃O₂. For the CB-IV mechanism, the CH₃O₂ concentration is estimated as the sum of the XO₂ and TO₂ radicals.

Table 2-3. Equilibrium reactions included in the aqueous-phase chemical mechanism.

Equilibrium Reaction	K_{298} (M or $M \text{ atm}^{-1}$) ^a	$-\Delta H / R(K)$	Reference
$SO_2 \cdot H_2O \leftrightarrow HSO_3^- + H^+$	1.3×10^{-2}	1960	Smith and Martell (1976)
$HSO_3^- \leftrightarrow SO_3^{2-} + H^+$	6.6×10^{-8}	1500	Smith and Martell (1976)
$H_2SO_4(aq) \leftrightarrow HSO_4^- + H^+$	1000		Perrin (1982)
$HSO_4^- \leftrightarrow SO_4^{2-} + H^+$	1.02×10^{-2}	2720	Smith and Martell (1976)
$H_2O_2(aq) \leftrightarrow HO_2^- + H^+$	2.2×10^{-12}	-3730	Smith and Martell (1976)
$HNO_3(aq) \leftrightarrow NO_3^- + H^+$	15.4	8700 ^b	Schwartz (1984)
$HNO_2(aq) \leftrightarrow NO_2^- + H^+$	5.1×10^{-4}	-1260	Schwartz and White (1981)
$CO_2 \cdot H_2O \leftrightarrow HCO_3^- + H^+$	4.3×10^{-7}	-1000	Smith and Martell (1976)
$HCO_3^- \leftrightarrow CO_3^{2-} + H^+$	4.68×10^{-11}	-1760	Smith and Martell (1976)
$NH_4OH \leftrightarrow NH_4^+ + OH^-$	1.7×10^{-5}	-450	Smith and Martell (1976)
$H_2O \leftrightarrow H^+ + OH^-$	1.0×10^{-14}	-6710	Smith and Martell (1976)
$HCHO(aq) \xrightleftharpoons{H_2O} H_2C(OH)_2(aq)$	2.53×10^3	4020	Le Hanaf (1968)
$HCOOH(aq) \leftrightarrow HCOO^- + H^+$	1.8×10^{-4}	-20	Martell and Smith (1977)
$HCl(aq) \leftrightarrow H^+ + Cl^-$	1.74×10^6	6900	Marsh and McElroy (1985)
$Cl_2 \leftrightarrow Cl + Cl^-$	5.26×10^{-6}		Jayson et al. (1973)
$NO_3(g) \leftrightarrow NO_3(aq)$	2.1×10^5	8700	Jacob (1986)
$HO_2(aq) \leftrightarrow H^+ + O_2^-$	3.50×10^{-5}		Perrin (1982)
$HOCH_2SO_3^- \leftrightarrow ^-OCH_2SO_3^- + H^+$	2.00×10^{-12}		Sorensen and Anderson (1970)

^aThe temperature dependence is represented by

$$K = K_{298} \exp \left[\frac{-\Delta H}{R} \left(\frac{1}{T} - \frac{1}{298} \right) \right]$$

where K is the equilibrium constant at temperature T (in K).

^b Value for equilibrium: $HNO_3(g) \leftrightarrow NO_3^- + H^+$.

Table 2-4. Kinetic reactions included in the aqueous-phase chemical mechanism.

Oxygen-Hydrogen Chemistry			
	Reaction	k_{298}^a	$-E/R(K)$
1.	$H_2O_2 \xrightarrow{h\nu} 2 OH$	e	
2.	$O_3 \xrightarrow{h\nu, H_2O} H_2O_2 + O_2$	e	
3.	$OH + HO_2 \rightarrow H_2O + O_2$	7.0×10^9	-1500
4.	$OH + O_2^- \rightarrow OH^- + O_2$	1.0×10^{10}	-1500
5.	$OH + H_2O_2 \rightarrow H_2O + HO_2$	2.7×10^7	-1700
6.	$HO_2 + HO_2 \rightarrow H_2O_2 + O_2$	8.6×10^5	-2365
7.	$HO_2 + O_2^- \xrightarrow{H_2O} H_2O_2 + O_2 + OH^-$	1.0×10^8	-1500
8.	$O_2^- + O_2^- \xrightarrow{2H_2O} H_2O_2 + O_2 + 2OH^-$	<0.3	
9.	$HO_2 + H_2O_2 \rightarrow OH + O_2 + H_2O$	0.5	
10.	$O_2^- + H_2O_2 \rightarrow OH + O_2 + OH^-$	0.13	
11.	$OH + O_3 \rightarrow HO_2 + O_2$	2×10^9	
12.	$HO_2 + O_3 \rightarrow OH + 2 O_2$	$< 1 \times 10^4$	
13.	$O_2^- + O_3 \xrightarrow{H_2O} OH + 2 O_2 + OH^-$	1.5×10^9	-1500
14.	$OH^- + O_3 \xrightarrow{H_2O} H_2O_2 + O_2 + OH^-$	70	
15.	$HO_2^- + O_3 \rightarrow OH + O_2^- + O_2$	2.8×10^6	-2500
16.	$H_2O_2 + O_3 \rightarrow H_2O + 2 O_2$	$7.8 \times 10^{-3} [O_3]^{0.5}$	

Table 2-4. Kinetic reactions included in the aqueous-phase chemical mechanism (continued).

Carbonate Chemistry			
	Reaction	k_{298}	$-E/R(K)$
17.	$HCO_3^- + OH \rightarrow H_2O + CO_3^-$	1.5×10^7	-1910
18.	$HCO_3^- + O_2^- \rightarrow HO_2^- + CO_3^-$	1.5×10^6	0
19.	$CO_3^- + O_2 \xrightarrow{H_2O} HCO_3^- + O_2 + OH^-$	4.0×10^8	-1500
20.	$CO_3^- + H_2O_2 \rightarrow HO_2 + HCO_3^-$	8.0×10^5	-2820

Chlorine Chemistry			
	Reaction	k_{298}	$-E/R(K)$
21.	$Cl^- + OH \rightarrow ClOH^-$	4.3×10^9	-1500
22.	$ClOH^- \rightarrow Cl^- + OH$	6.1×10^9	0
23.	$ClOH^- \xrightarrow{H^+} Cl + H_2O$	$2.1 \times 10^{10} [H^+]$	0
24.	$Cl \xrightarrow{H_2O} ClOH^- + H^+$	1.3×10^3	0
25.	$HO_2 + Cl_2^- \rightarrow 2 Cl^- + O_2 + H^+$	4.5×10^9	-1500
26.	$O_2^- + Cl_2^- \rightarrow 2 Cl^- + O_2$	1.0×10^9	-1500
27.	$HO_2 + Cl \rightarrow Cl^- + O_2 + H^+$	3.1×10^9	-1500
28.	$H_2O_2 + Cl_2^- \rightarrow 2 Cl^- + HO_2 + H^+$	1.4×10^5	-3370
29.	$H_2O_2 + Cl \rightarrow Cl^- + HO_2 + H^+$	4.5×10^7	0
30.	$OH^- + Cl_2^- \rightarrow 2 Cl^- + OH$	7.3×10^6	-2160

Table 2-4. Kinetic reactions included in the aqueous-phase chemical mechanism (continued).

Nitrite and Nitrate Chemistry			
	Reaction	k_{298}	$-E/R(K)$
31.	$NO + NO_2 \xrightarrow{H_2O} 2 NO_2^- + 2H^+$	2.0×10^8	-1500
32.	$NO_2 + NO_2 \xrightarrow{H_2O} NO_2^- + NO_3^- + 2 H^+$	1.0×10^8	-1500
33.	$NO + OH \rightarrow NO_2^- + H^+$	2.0×10^{10}	-1500
34.	$NO_2 + OH \rightarrow NO_3^- + H^+$	1.3×10^9	-1500
35.	$HNO_2 \xrightarrow{h\nu} NO + OH$	e	
36.	$NO_2^- \xrightarrow{h\nu, H_2O} NO + OH + OH^-$	e	
37.	$HNO_2 + OH \rightarrow NO_2 + H_2O$	1.0×10^9	-1500
38.	$NO_2^- + OH \rightarrow NO_2 + OH^-$	1.0×10^{10}	-1500
39.	$HNO_2 + H_2O_2 \xrightarrow{H^+} NO_3^- + 2 H^+ + H_2O$	$6.3 \times 10^3 [H^+]$	-6693
40.	$NO_2^- + O_3 \rightarrow NO_3^- + O_2$	5.0×10^5	-6950
41.	$NO_2^- + CO_3^- \rightarrow NO_2 + CO_3^{2-}$	4.0×10^5	0
42.	$NO_2^- + Cl_2^- \rightarrow NO_2 + 2 Cl^-$	2.5×10^8	-1500
43.	$NO_2^- + NO_3 \rightarrow NO_2 + NO_3^-$	1.2×10^9	-1500
44.	$NO_3^- \xrightarrow{h\nu, H_2O} NO_2 + OH + OH^-$	e	
45.	$NO_3 \xrightarrow{h\nu} NO + O_2$	e	
46.	$NO_3 + HO_2 \rightarrow NO_3^- + H^+ + O_2$	4.5×10^9	-1500
47.	$NO_3 + O_2^- \rightarrow NO_3^- + O_2$	1.0×10^9	-1500
48.	$NO_3 + H_2O_2 \rightarrow NO_3^- + H^+ + HO_2$	1.0×10^6	-2800
49.	$NO_3 + Cl^- \rightarrow NO_3^- + Cl$	1.0×10^8	-1500

Table 2-4. Kinetic reactions included in the aqueous-phase chemical mechanism (continued).

Organic Chemistry			
	Reaction	k_{298}	$-E/R(K)$
50.	$H_2C(OH)_2 + OH \xrightarrow{O_2} HCOOH + HO_2 + H_2O$	2.0×10^9	-1500
51.	$H_2C(OH)_2 + O_3 \rightarrow Products$	0.1	0
52.	$HCOOH + OH \xrightarrow{O_2} CO_2 + HO_2 + H_2O$	2.0×10^8	-1500
53.	$HCOOH + H_2O_2 \rightarrow Product + H_2O$	4.6×10^{-6}	-5180
54.	$HCOOH + NO_3 \xrightarrow{O_2} NO_3^- + H^+ + CO_2 + HO_2$	2.1×10^5	-3200
55.	$HCOOH + O_3 \rightarrow CO_2 + HO_2 + OH$	5.0	0
56.	$HCOOH + Cl_2 \xrightarrow{O_2} CO_2 + HO_2 + 2 Cl^- + H^+$	6.7×10^3	-4300
57.	$HCOO^- + OH \xrightarrow{O_2} CO_2 + HO_2 + OH^-$	2.5×10^9	-1500
58.	$HCOO^- + O_3 \rightarrow CO_2 + OH + OH_2^-$	100.0	0
59.	$HCOO^- + NO_3 \xrightarrow{O_2} NO_3^- + CO_2 + HO_2$	6.0×10^7	-1500
60.	$HCOO^- + CO_3 \xrightarrow{O_2, H_2O} CO_2 + HCO_3^- + HO_2 + OH^-$	1.1×10^5	-3400
61.	$HCOO^- + Cl_2 \xrightarrow{O_2} CO_2 + HO_2 + 2 Cl^-$	1.9×10^6	-2600
62.	$CH_3C(O)O_2NO_2 \rightarrow NO_3^- + Products$	4.0×10^{-4}	0
63.	$CH_3O_2 + HO_2 \rightarrow CH_3OOH + O_2$	4.3×10^5	-3000
64.	$CH_3O_2 + O_2 \xrightarrow{H_2O} CH_3OOH + O_2 + OH^-$	5.0×10^7	-1600

Table 2-4. Kinetic reactions included in the aqueous-phase chemical mechanism (continued).

Sulfur Chemistry			
	Reaction	k_{298}	$-E/R(K)$
65. ^b	$S(IV) + O_3 \rightarrow S(IV) + O_2$	2.4×10^4 3.7×10^5 1.5×10^9	-5530 -5280
66. ^b	$S(IV) + H_2O_2 \rightarrow S(IV) + H_2O$	7.5×10^7	-4430
67. ^b	$S(IV) + \frac{1}{2} O_2 \xrightarrow{Mn^{2+}, Fe^{3+}} S(IV)$	(Complex expression from Martin et al., 1991)	
68.	$SO_3^{2-} + OH \xrightarrow{O_2} SO_5^- + OH^-$	5.2×10^9	-1500
69.	$HSO_3^- + OH \xrightarrow{O_2} SO_5^- + H_2O$	4.5×10^9	-1500
70.	$SO_5^- + HSO_3^- \xrightarrow{O_2, H_2O} HSO_5^- + SO_5^-$	2.5×10^4	-3100
	$SO_5^- + SO_3^{2-} \xrightarrow{O_2} HSO_5^- + SO_5^- + OH^-$	2.5×10^4	-2000
71.	$SO_5^- + O_2 \xrightarrow{H_2O} HSO_5^- + OH^- + O_2$	1.0×10^8	-1500
72.	$SO_5^- + HCOOH \xrightarrow{O_2} HSO_5^- + CO_2 + HO_2$	200	-5300
73.	$SO_5^- + HCOO^- \xrightarrow{O_2} HSO_5^- + CO_2 + O_2^-$	1.4×10^4	-4000
74.	$SO_5^- + SO_5^- \rightarrow 2 SO_4^- + O_2$	6.0×10^8	-1500
75.	$HSO_5^- + HSO_3^- + H^+ \rightarrow 2 SO_4^{2-} + 3H^+$	7.1×10^6	-3100
76.	$HSO_5^- + OH \rightarrow SO_5^- + H_2O$	1.7×10^7	-1900
77.	$HSO_5^- + SO_4^- \rightarrow SO_5^- + SO_5^{2-} + H^+$	$< 1.0 \times 10^5$	0
78.	$HSO_5^- + NO_2^- \rightarrow HSO_4^- + NO_3^-$	0.31	-6650
79.	$HSO_5^- + Cl^- \rightarrow SO_4^{2-} + Product$	1.8×10^{-3}	-7050
80.	$SO_4^- + HSO_3^- \xrightarrow{O_2} SO_4^{2-} + H^+ + SO_5^-$	1.3×10^9	-1500
81.	$SO_4^- + SO_3^{2-} \xrightarrow{O_2} SO_4^{2-} + SO_5^-$	5.3×10^8	-1500
82.	$SO_4^- + HO_2 \rightarrow SO_4^{2-} + H^+ + O_2$	5.0×10^9	-1500
83.	$SO_4^- + O_2^- \rightarrow SO_4^{2-} + O_2$	5.0×10^9	-1500

Table 2-4. Kinetic reactions included in the aqueous-phase chemical mechanism (continued).

Sulfur Chemistry (continued)			
	Reaction	k_{298}	$-E/R(K)$
84.	$SO_4^- + OH^- \rightarrow SO_4^{2-} + OH$	8.0×10^7	-1500
85.	$SO_4^- + H_2O_2 \rightarrow SO_4^{2-} + H^+ + HO_2$	1.2×10^7	-2000
86.	$SO_4^- + NO_2^- \rightarrow SO_4^{2-} + NO_2$	8.8×10^8	-1500
87.	$SO_4^- + HCO_3^- \rightarrow SO_4^{2-} + H^+ + CO_3^-$	9.1×10^6	-2100
88.	$SO_4^- + HCOO^- \xrightarrow{O_2} SO_4^{2-} + CO_2 + HO_2$	1.7×10^8	-1500
89.	$SO_4^- + Cl^- \rightarrow SO_4^{2-} + Cl$	2.0×10^8	-1500
90.	$SO_4^- + HCOOH \xrightarrow{O_2} SO_4^{2-} + H^+ + CO_2 + HO_2$	1.4×10^6	-2700
91. ^b	$S(IV) + CH_3C(O)O_2NO_2 \rightarrow S(VI)$	6.7×10^{-3}	0
92.	$S(IV) + HO_2 \rightarrow S(VI) + OH$	1.0×10^6	0
	$S(IV) + O_2 \xrightarrow{H_2O} S(VI) + OH + OH^-$	1.0×10^5	0
93.	$HSO_3^- + NO_3^- \rightarrow NO_3^- + H^+ + SO_3^- + SO_3^-$	1.0×10^8	0
94.	$2 NO_2 + HSO_3^- \xrightarrow{H_2O} SO_4^{2-} + 3H^+ + 2 NO_2^-$	2.0×10^6	0
95a. ^c	$S(IV) + N(III) \rightarrow S(IV) + Product$	1.4×10^2	0
95b. ^d	$3 HSO_3^- + NO_2^- \rightarrow OH^- + Product$	4.8×10^3	-6100
96.	$HCHO + HSO_3^- \rightarrow HOCH_2SO_3^-$	7.9×10^2	-4900
	$HCHO + SO_3^{2-} \xrightarrow{H_2O} HOCH_2SO_3^- + OH^-$	2.5×10^7	-1800
97.	$HOCH_2SO_3^- + OH^- \rightarrow SO_3^{2-} + HCHO + H_2O$	3.6×10^3	-4500
98.	$HOCH_2SO_3^- + OH^- \xrightarrow{O_2} SO_5^- + HCHO + H_2O$	2.6×10^8	-1500
99.	$HSO_3^- + Cl_2 \xrightarrow{O_2} SO_5^- + 2 Cl^- + H^+$	3.4×10^8	-1500
	$SO_3^{2-} + Cl_2 \xrightarrow{O_2} SO_5^- + 2 Cl^-$	3.4×10^8	-1500

^a In appropriate units of M and s⁻¹.

^b Reaction with “nonelementary” rate expression; see Seinfeld and Pandis (1998) for expressions.

^c For pH ≤ 3.

^d For pH > 3.

^e Solar radiation dependent.

3. IMPLEMENTATION OF MODULES

This section describes the interface routines that were developed, and the modifications that were made to SCICHEM and the aerosol equilibrium and aqueous-phase chemistry modules to accommodate these modules within the SCICHEM framework. To ensure that the implementation was correct, we compared results from simulations performed with the modules inside SCICHEM with results from the stand-alone versions of the modules.

3.1 Development of Interfaces

The interfaces that were added consist of initialization routines and driver routines for both the aerosol thermodynamics and aqueous-phase chemistry modules. The initialization routines are used to set up species pointers and cross-referencing arrays and are called at the beginning of a SCICHEM simulation. The driver routines handle the transformation of information between SCICHEM and the modules and are called at every simulation time step. These routines perform any conversions required between the variables carried in SCICHEM and the variables required by the modules.

The aerosol driver routine transmits the following information from SCICHEM to the aerosol equilibrium (SCAPE2) module:

- Total sulfate (particulate sulfate + newly formed gas-phase sulfuric acid) concentration,
- Total nitrate (particulate nitrate + nitric acid) concentration,
- Total ammonia (particulate ammonium + ammonia) concentration,
- Total chloride (particulate chloride + hydrogen chloride) concentration,
- Particulate sodium, potassium, calcium, and magnesium concentration,
- Carbon dioxide concentration,

- Cloud size; and
- Temperature and relative humidity.

SCAPE2 returns the following information to SCICHEM via the driver routine:

- Final particulate sulfate concentration (gas-phase sulfuric acid is set to zero),
- Final particulate nitrate and gas-phase nitric acid concentrations,
- Final particulate ammonium and gas-phase ammonia concentrations,
- Final particulate chloride and gas-phase hydrogen chloride concentrations,
- Particulate water concentration,
- Aerosol density; and
- Aerosol acidity

The aqueous-phase chemistry driver routine transfers the following information from SCICHEM to the chemistry module:

- Time step for chemistry calculations.
- Temperature, pressure, liquid water content, precipitation rate, NO_2 photolysis rate.
- Gas-phase concentrations of sulfur dioxide, ammonia, nitric acid, hydrogen chloride, hydrogen peroxide, formaldehyde, formic acid, nitrous acid, ozone, nitric oxide, nitrogen dioxide, PAN, and carbon dioxide.
- Gas-phase concentrations of radicals such as OH, HO_2 , NO_3 , and CH_3O_2 (aqueous-phase radical chemistry is performed during the day, as determined by the NO_2 photolysis rate).
- Concentrations of particulate sulfate, nitrate, ammonium, sodium, chloride, and crustal material for each aerosol particle size section. The concentrations of iron and manganese, the trace metals that catalyze the aqueous-phase oxidation of SO_2 by oxygen to sulfate, are proportional to the crustal material concentration.

At the end of the aqueous-phase chemistry time step, the following information is returned to SCICHEM from the aqueous driver routine:

- Final gas-phase concentrations of sulfur dioxide, ammonia, nitric acid, hydrogen chloride, hydrogen peroxide, formaldehyde, formic acid, nitrous acid, ozone, nitric oxide, nitrogen dioxide and PAN. Note that relatively insoluble species (such as ozone or nitric oxide) are treated as constant during the aqueous-phase chemistry calculations. Thus, their final concentrations are the same as their initial concentrations.
- Final concentrations of particulate sulfate, nitrate, ammonium, sodium, chloride, and crustal material for each aerosol particle size section.
- Effective deposition velocities for wet removal of soluble gaseous species such as SO_2 , H_2O_2 , and formaldehyde.

3.2 Modifications to SCICHEM and the Aerosol Equilibrium and Aqueous Chemistry Modules

In order to implement the aerosol equilibrium and aqueous-phase chemistry modules within SCICHEM, additional variables were added to the SCICHEM input files, including the multicomponent input file (*ProjectName.IMC*, referred to as the IMC file hereafter) and the meteorological data files. Flags were added to the IMC file to specify whether or not aerosol thermodynamics or aqueous chemistry should be simulated. A section was added to the IMC file to specify several parameters that are used in the aqueous-phase module. Other changes to the IMC file include the specification of aerosol particle parameters such as the aerosol particle density, the number of aerosol particle size sections, and the section boundaries. The various size sections are combined for the aerosol equilibrium calculation, but are treated separately in other calculations, such as in the aqueous chemistry module and the washout and deposition calculations. Note that although the code is generalized to handle multiple aerosol particle size sections, only one size section is currently allowed (by setting the maximum number of size sections to one in a single PARAMETER statement). The generalized code is

intended to provide the framework for future model improvement (i.e., addition of modules to SCICHEM to simulate aerosol particle dynamics and growth).

The new meteorological variables that were added include two-dimensional fractional cloud cover, two-dimensional liquid precipitation rate, and three-dimensional cloud liquid water content. Like the other meteorological variables in SCICHEM, these new variables can be specified in either the observational or MEDOC gridded file format. These variables were also added to the interpolation schemes in SCICHEM that are used to calculate meteorological quantities at the puff location.

As in the case of the aerosol particle size sections, the code has been generalized to read and interpolate multiple cloud droplet size sections. However, because the current aqueous chemistry module is a bulk module, the maximum number of cloud droplet size sections is currently limited to one via a PARAMETER statement. The generalized code allows for future development, such as implementation of an aqueous chemistry module that can be used for multiple cloud/fog droplet sizes.

SCICHEM was modified to include wet deposition of gases and wet and dry deposition of aerosol particles as sink terms in the multi-component species calculations. Wet scavenging coefficients for the gas-phase species were added to the IMC file as additional model inputs. These coefficients are only used to calculate gaseous wet deposition when the aqueous-chemistry option is not selected. When the flag for aqueous-phase chemistry is activated, the specified wet scavenging coefficients are ignored, and the aqueous-phase module returns effective deposition velocities to SCICHEM.

For aerosol particles, a different procedure is used to calculate dry and wet deposition. We have used existing algorithms already available in SCICHEM that were developed for the particle material type.

The dry deposition module for particles is based on the approach of Slinn (1982), who assumes the deposition velocity is equal to a collection efficiency multiplied by the momentum deposition velocity,

$$v_d = E u_*^2 / u_r$$

where u_* is the surface friction velocity and u_r is the wind speed at the reference height, z_r . The total collection efficiency, E , is defined in terms of individual collection mechanism efficiencies, such as the efficiency of the viscous sublayer flow (within a millimeter of the surface elements), particle interception and particle impaction. Individual collection mechanism efficiencies are defined specifically for a vegetative canopy or for a rough surface. Further details of the particle dry deposition model can be found in Sykes et al. (1998).

The particle wet deposition model is based on Seinfeld's (1986) definition of the particle wet scavenging coefficient,

$$\omega_s = \int_0^{\infty} \frac{\pi}{4} D_r^2 V_r N_r E dD_r$$

where D_r is the raindrop diameter, V_r is the raindrop fall velocity, N_r is the raindrop size distribution, and E is the collision efficiency. Similar to the dry deposition of particles onto the surface, the collision efficiency with rain drops is defined in terms of individual efficiencies as defined by Seinfeld (1986), such as that due to Brownian motion, interception and inertial impaction. The Marshall and Palmer (1948) raindrop distribution is assumed. Further details of the particle wet deposition model can be found in Sykes et al. (1998).

Another modification to the SCICHEM input files is that gas-phase species emission rates can now be specified in grams per second in addition to the *species_units*-m³ per second rates that were assumed in previous versions. The *species_units* (either ppm or molecules/cm³) are specified in the IMC file under the Control Section and the additional variable, *emission_units*, was added there. When importing or re-running projects run by an earlier version of the model, it is assumed that the emission rates are specified in *species_units*-m³, therefore, no changes to the input files are necessary. Molecular weights were added to the IMC file under the Species Section to allow for the conversion

from *emission_units* to *species_units*. Note that aerosol particle species emissions are always assumed to be in g/s and the resulting concentrations are displayed in $\mu\text{g}/\text{m}^3$.

Details of the additional variables added to the SCICHEM input files are provided in the sub-sections below. Note that the discussion is only limited to changes to these files related to the implementation of the aqueous-phase chemistry and aerosol thermodynamic modules. The SCICHEM File Formats Document provides complete details on the preparation of the input files for a SCICHEM simulation.

In addition to the above modifications related to SCICHEM inputs, other modifications to SCICHEM include the addition of calls to the interface routines between SCICHEM and the new modules at appropriate locations. These include calls for stepping both the puff concentrations and the ambient species concentrations (if *step_ambient* is specified as *true* in the IMC file – see the SCICHEM File Formats Document). The aerosol equilibrium module (if *aerosol* is specified as *true* in the IMC file – see below) is called after the gas-phase chemistry step. Next, if the aqueous-phase chemistry option is selected, the aqueous-phase chemistry calculations are performed followed by another call to the aerosol module (if *aerosol* is *true*). Even if the ambient is not being advanced (*step_ambient* is *false*), the aerosol equilibrium module is still called for the ambient species, so that the ambient species will be in equilibrium as well.

The modifications to the modules primarily involved addition of code to calculate quantities required by SCICHEM. For example, washout ratios for wet removal of gaseous species were calculated in the aqueous-phase module and converted to effective deposition velocities for SCICHEM. In addition, we have made substantial modifications to the aqueous-phase chemistry module code independent of the implementation modifications. These modifications involve bug fixes, streamlining of the code, and reducing the hardwiring in the code to the extent possible within the limited resources of this study.

3.2.1 Multicomponent Input File

Multicomponent Control Section

Additions to this section include flags for selecting aerosol equilibrium and aqueous-phase chemistry calculations, the number of aerosol particle size sections, the aerosol particle size section boundaries, aerosol particle density, and the units for the emission rates of gas-phase species. Note that if the aqueous-phase chemistry option is selected, it is necessary to provide cloud liquid water content in the meteorological input files. Although the aqueous-phase chemistry option does not require that the aerosol equilibrium calculations be selected, it is necessary to specify aerosol species in the species section of the IMC file (see Table 3-2 below in the description of the species section). If the aerosol module is not used in conjunction with the aqueous module, the aerosol concentrations will be obtained from the background and/or emitted aerosols.

The additional namelist parameters in the control section are listed below:

- aqueous* - Specifies whether or not aqueous-phase chemistry will be performed (LOGICAL). Must have certain species defined in the species section, as described in the species section. If set to *true*, the species names will be checked to determine if the aqueous module can be used and if so, aqueous-phase chemistry will be performed in addition to gas-phase chemistry and/or aerosol equilibrium calculations. Cloud liquid water content must be provided in a meteorological input file (Observations or Gridded). The default is *false*.

- aerosol* - Specifies whether or not aerosol equilibrium calculations will be performed (LOGICAL). Must have certain species defined in the species section, as described in the species section. If set to *true*, the species names will be checked to determine if the aerosol module can be used and if so, aerosol equilibrium calculations will be performed in addition to gas-phase and/or aqueous-phase chemistry. The default is *false*.

- nsec_aer* - Number of sections of aerosol particles (INTEGER*4). Used with *aerosol* or *aqueous* set to *true*. The default is 1. Currently, the maximum number of sections allowed is also equal to 1. This can be changed easily for future model development by changing a single PARAMETER statement in the model code.
- secbnds_aer* - Section boundaries (m) of the aerosol particles (REAL*4). Used with *aerosol* or *aqueous* set to *true*. The defaults are defined to give a geometric mean aerosol diameter of 4.0e-7 m (0.4 microns). Must specify *nsec_aer*+1 boundaries.
- rho_aer* - Density (kg/m³) of the aerosol particles. Used with *aerosol* set to *true*. The default is 1000.
- emission_units* - Gas-phase species emission rate units (CHARACTER*80). Options are either 'ppm-m³/s', 'molecules-m³/cm³-s', or 'g/s'. Emission rates for the release specified in *rel_mc* in the SCN file. The default is 'ppm-m³/s'. For projects run with earlier versions of the model that are re-run or imported, the emission rate is *species_units*- m³/s and it is not necessary to edit the IMC file to include this parameter. Note that emission rates of aerosol particle species are always assumed to be in g/s.

Multicomponent species section

The species section was expanded to include the specification of particle materials, wet scavenging coefficients and molecular weights. Each line of the species section gives the species name, the species type (F, S, P, A, or E), the ambient concentration (ppm or molecules/cm³), the absolute tolerance (ppm or molecules/cm³), the dry deposition velocity (m/s) (used only for gases), the wet scavenging coefficient (s⁻¹) (used only for gases and only if the *aqueous* flag in the control section is *false*), and the molecular weight (g/mole) (used only for emitted gases). There are no defaults for these parameters. The species types are shown in Table 3-1. An example of a species section is shown in Figure 3-1.

Table 3-1. SCICHEM species types.

<i>F</i>	Fast	Species concentrations change rapidly and species rate equations will be integrated using LSODE.
<i>S</i>	Slow	Species concentrations change slowly and will be integrated explicitly using a predictor-corrector scheme.
<i>P</i>	Particle	Species concentrations are determined through aerosol equilibrium. Species name must match one of the aerosol particle names set by aerosol module.
<i>E</i>	Equilibrium	Species concentrations are assumed to be at steady-state.
<i>A</i>	Ambient	Species concentrations do not change by the reaction, such as H ₂ O or O ₂ .

The wet scavenging coefficient, s (s⁻¹), is used to define the scavenging rate, sr (s⁻¹), as:

$$sr = s (R/R_0)$$

where R is the precipitation rate in mm/hr and R_0 is the reference precipitation rate of 1 mm/hr. The scavenging rate is applied to the gas-phase species after the gas-phase chemistry has been advanced. If the aqueous-phase chemistry module is turned on, the specified wet scavenging coefficient will be ignored and the aqueous-phase chemistry module will return effective removal velocities to SCICHEM.

Molecular weights are used to convert the gas-phase emissions to the desired species units. Emission rates that are provided in 'g/s' will be converted to either 'ppm-m³/s' or 'molecules-m³/cm³-s' using the molecular weight, depending on whether *species_units* has been set to ppm or molecules/cm³, respectively. It is not essential to provide molecular weights for non-emitted species, however, since species emission rates are not checked initially to identify emitted species versus non-emitted species, all 'Fast' and 'Slow' species must have non-zero molecular weights provided on the IMC file. Molecular weights are not required for equilibrium species or for particle species, since equilibrium concentrations are determined from the 'Fast' and 'Slow' species concentrations and aerosol particle species concentrations are always assumed to be in μg/m³ and the emission rates in g/s.

#Species	Type	Ambient	Atol	Dep	Wet Scav	MW
NO	F	0.0	1.e-8	0.00	0.000	30.01
O3	F	0.1	1.e-8	0.00	0.000	48.00
NO2	F	0.0	1.e-8	0.00	0.000	46.01
HNO3	F	0.0	1.e-8	0.02	6.e-5	63.00
RCHO	F	0.50	1.e-8	0.00	0.000	99.99
RH	S	12.0	1.e-8	0.00	0.000	99.99
PAN	F	0.0	1.e-8	0.00	0.000	121.0
OH	F	0.0	1.e-12	0.00	0.000	99.99
HO2	E	0.0	1.e-12	0.00	0.000	99.99
RO2	E	0.0	1.e-12	0.00	0.000	99.99
C2O3	E	0.0	1.e-12	0.00	0.000	99.99
H2O	A	-1.0	1.e-6	0.00	0.000	99.99

Figure 3-1. Sample species section of the IMC file.

In the example species section shown in Figure 3-1, only HNO₃ has a nonzero deposition velocity and wet scavenging coefficient and therefore, there will be no deposition or scavenging of any species other than HNO₃. HNO₃ is modeled as a fast species with a background concentration of zero and a relative tolerance of 1.e-8. The deposition velocity is 0.02 m/s and the wet scavenging coefficient is 6.e-5 s⁻¹. The ambient H₂O concentration is set to -1.0, indicating that it will be set internally using the humidity given in the meteorological input files or a default value of 30% relative humidity. Molecular weights of non-emitted, equilibrium and ambient species have been set to an arbitrary value of 99.99.

If either the aerosol equilibrium option is selected (*aerosol* is equal to *true* in the control section) or the aqueous-phase chemistry is turned on (*aqueous* is equal to *true* in the control section), or both, the species shown in Table 3-2 must appear in the species section, even if they do not all appear in the gas-phase mechanism (for example the aerosol species).

For multiple particle sections (*nsec_aer* greater than 1), the aerosol species names must appear in the species section of the IMC file with the section number. For example, when three sections are desired (*nsec_aer* is equal to 3), the user must list CRUS01, CRUS02, and CRUS03 and likewise for the other aerosol particles. Note that *nsec_aer* will specify the number of sections for all the aerosol particle species. The species list will be

searched for aerosol_name01 to aerosol_namensec_aer using the format (A,i2.2) where the aerosol_name refers to CRUS, ASO4, ANO3, ANH4, ANA, ACL, AMG, ACA, or APOT. However, recall that currently, the maximum number of aerosol particle sections is 1. For *nsec_aer* equal to 1, the user may optionally leave off the section number from the name. The required names for either aqueous chemistry or aerosol equilibrium will be as they appear in Table 3-2.

Table 3-2. Required species names for the aerosol equilibrium module and aqueous-phase chemistry module

Chemical	Required Species Name
Sulfur dioxide (SO ₂)	SO2
Hydrogen peroxide (H ₂ O ₂)	H2O2
Formaldehyde (HCHO)	FORM
Formic Acid (HCOOH)	FA
Nitrous acid (HNO ₂)	HONO
Nitric Oxide (NO)	NO
Nitrogen Dioxide (NO ₂)	NO2
Ozone (O ₃)	O3
Peroxyacyl Nitrate (CH ₃ C(O)OONO ₂)	PAN
Carbon Dioxide(CO ₂)	CO2
Hydroxyl Radical (OH)	OH
Hydroperoxy Radical (HO ₂)	HO2
Nitrate Radical (NO ₃)	NO3
Toluene-hydroxyl radical adduct	TO2
NO-to-NO ₂ operation	XO2
Crustal Material (particulate) ¹	CRUS01 or CRUS ²
Aerosol Sulfate ¹	ASO401 or ASO4 ²
Aerosol Nitrate ¹	ANO301 or ANO3 ²
Aerosol Ammonia ¹	ANH401 or ANH4 ²
Aerosol Sodium ¹	ANA01 or ANA ²
Aerosol Chloride ¹	ACL01 or ACL ²
Aerosol Magnesium ¹	AMG01 or AMG ²
Aerosol Calcium ¹	ACA01 or ACA ²
Aerosol Pottasium ¹	APOT01 or APOT ²
Sulfuric Acid (H ₂ SO ₄)	SA
Nitric Acid (HNO ₃)	HNO3
Ammonia (NH ₃)	NH3
Hydrogen chloride (HCl)	HCL

Note: ¹ Aerosol particles must be specified as species type “P” (particle).

² For *nsec_aer* equal to 1, the section number may be optionally removed from

the aerosol particle names.

Multicomponent Aqueous Section

The aqueous section of the multicomponent input (IMC) file specifies parameters that will be used in the aqueous-phase module (using *aqueous* in the control section set to true). The aqueous variables may be provided as an option and this section does not even have to appear on the IMC file. If it does not appear on the file, the default values will be used in the aqueous module. The following variables may be specified:

- debug* - Debug flag (LOGICAL). If set to true, messages from the aqueous module will be printed to the log file. The default is false.
- lradical* - Choice of whether or not to use aqueous-phase free radical chemistry (LOGICAL). If set to true, the aqueous-phase free radical chemistry will be performed during the daytime hours. Otherwise, it is not performed at all. The default is true.
- dactiv* - Dry activation diameter (m) (REAL*4). The default is 3.0e-7.
- fdist(1)* - Fraction of mass change that will go to each aerosol particle size section (REAL*4). Must specify *nsec_aer* values. The default is 1. For future applications when *nsec_aer* is greater than 1, the default is to have the mass equally distributed.
- kiron* - Choice of expression for iron and manganese chemistry (INTEGER*4). If *kiron* is 0, there is no iron and manganese chemistry. If *kiron* is 1, the method of Martin and Good (1991) is used. If *kiron* is 2, the method of Martin (1984) is used. The default is 1.
- firon* - Fraction of crustal material that is iron (REAL*4). The default is 1.e-2.
- fman* - Fraction of crustal material that is manganese (REAL*4). The default is 2.e-3.
- chlorine* - Choice of turning off chlorine chemistry (REAL*4). If set to 0, chlorine chemistry will be turned off. The default is 1.0.
- so2min* - Minimum SO₂ concentration (ppm) for the aqueous calculation (REAL*4). The default is 1.0e-6.

- lwcmín* - Minimum liquid water content (g/m³) for the aqueous calculation (REAL*4). The default is 5.0e-2.
- atolx* - Absolute error tolerance for numerical integration (REAL*4). The default is 1.0e-4.
- rtolx* - Relative error tolerance for numerical integration (REAL*4). The default is 1.0e-3.
- dtmaxsec* - Maximum time step (seconds) for numerical integration (REAL*4). The default is 120.
- xtol* - Relative error tolerance for nonlinear solver (REAL*4). The default is 1.0e-3.

The aqueous section namelist begins with “\$AQUEOUS” and end with “\$END”. If parameters are not set under this section, the default values will be assumed. An example of an aqueous section is shown in Figure 3-2.

```
#Aqueous
$AQUEOUS
  debug = .false.
  lradical = .true.,
  dactiv = 3.000000e-07,
  fdist = 1.0,
  kiron = 1,
  firon = 1.000000e-02,
  fman = 2.000000e-03,
  chlorine = 1.00000,
  so2min = 1.000000e-06,
  lwcmín = 5.000000e-02,
  atolx = 1.000000e-04,
  rtolx = 1.000000e-03,
  dtmaxsec = 120.000,
  xtol = 1.000000e-03,
$END
```

Figure 3-2. Sample aqueous section of the IMC file.

3.2.2 Meteorology scenario file

The meteorology scenario file was expanded to include the number of cloud droplet sections and the sizes of the cloud droplet sections. Currently, the maximum number of cloud droplet sections is one, but these parameters were added for future aqueous modules that accept multiple cloud droplet sections. The following parameters were added:

- ncl* - Number of cloud droplet sections on observational or MEDOC type files (INTEGER). The default is zero and the maximum is equal to 1. For future model development, the maximum can be changed by modifying a single PARAMETER statement in the code. This is not currently available for editing with the GUI and, for projects that are created with the GUI, this value may only be changed from the default value by editing the MSC file.
- size_cld(1)* - An array (REAL*4) of cloud liquid droplet sizes (m) corresponding to the droplet sections. Must provide *ncl* sizes. The default is 1.e-5. This is not currently available for editing with the GUI and, for projects that are created with the GUI, this value may only be changed from the default value by editing the MSC file.

3.2.3 Meteorology Input Files

Observation File Format

A meteorological observation input file consists of a header section that specifies the file type, the number of observation variables, their names and units, followed by the numerical data.

Two file types are recognized by SCICHEM, a *SURFACE* file or a *PROFILE* file. A *SURFACE* file has only one observation per time interval for each station and is typically associated with near-surface measurements of wind and/or boundary layer parameters such as surface heat flux or mixing-layer height. A *PROFILE* file generally has more

than one observation height at a station and is used when vertical profiles of wind, temperature, etc. are available, such as from upper air soundings.

Details of the observation file format can be found in the Online Help or the File Formats Document. Additional variable names that were added to the observational input file format are shown in Table 3-3. Precipitation rate is needed for the calculation of wet deposition of gases and washout of aerosol particles. The ‘Precipitation Rate’ variable was added in order to be more flexible than the ‘Precipitation Index’, which only allowed the user to specify light, moderate or heavy rain (or snow). The precipitation rate is assumed to specify liquid precipitation only.

Fractional cloud cover was added as input and will be used for a ‘Calculated’ boundary layer. It is not necessary for the aqueous-phase module. The cloud liquid water content will be used in the aqueous module and must be present as input if the aqueous module is turned on. As mentioned previously, the cloud liquid water content does allow for multiple droplet sizes, but the maximum number of cloud droplet sections currently allowed is restricted to one.

Table 3-3. Additional meteorological variables and corresponding units recognized in SCICHEM.

Variable Description	Specific Name	Units
Precipitation Rate ¹	PRATE	MM/HR
Fractional Cloud Cover ¹	FCC	None
Cloud Liquid Water Content	CLD or CLD1, CLD2, etc.	G/M3

Note: ¹ Variable can be specified as fixed data on a *PROFILE* file.

MEDOC Format

The MEDOC file is used to specify three-dimensional meteorological data. Two-dimensional data may also be specified on this file. A MEDOC file contains a header section followed by numerical data for each time. Details of the MEDOC file format can be found in the Online Help or the File Formats Document. Additional variables that have been added to accommodate aqueous-phase chemistry are the three-dimensional cloud liquid water content, indicated in the header by 'CLD', and the two-dimensional precipitation rate in millimeters per hour, 'PRATE' or 'PRECIP', and fractional cloud cover, 'FCC' or 'CC'. Currently, the cloud liquid water content is general and does not refer to any droplet sizes. However, this can be easily expanded to allow the specification of different droplet sizes.

4. MODEL TESTING

4.1 Background and Purpose

The implementation of modules to simulate additional physical and chemical processes in the SCICHEM model involved major changes to the code. Such modifications require careful testing. Testing was performed at several stages of the implementation to assess whether the software was operating as intended. The program entailed testing by AER and STI of the stand-alone modules (primarily the aqueous-phase module) prior to implementation in the SCICHEM module, testing of the overall model by AER and ARAP before, during, and after the modules were implemented, and testing of the overall model by STI. The purpose of these tests was primarily to assess whether the codes were functioning as intended and responding to changes in model inputs in a manner that was consistent with scientific expectations. No attempt was made to compare model estimates with observed concentrations. Assessment of the new model's performance against observations in real world cases is an essential part of the model development process but was beyond the scope of this particular study.

The first element of the testing program was stand-alone module testing. Significant changes were made to the CMU aqueous-phase chemistry module as a result of the module-testing program. These modifications involved improving the code's ability to conserve mass of sulfur, nitrogen, chlorine, and carbon species and bringing more of the module's parameters up to the module's interface with the host model. No significant changes were needed in the SCAPE2 aerosol thermodynamic/equilibrium module.

The second element of the testing program was testing during the implementation of the modules in the host model. The modification and testing process is inherently iterative. The project team went through numerous iterations to reach a version of the software that was suitable for testing over a range of conditions by STI. Due to the time constraints of the project, the iteration process did continue through the analysis of the test runs described here, and therefore, time did not allow the model developers to completely investigate the anomalous results predicted for some of the test cases.

The third element of the testing program entailed testing the model under hypothetical conditions that used the newly implemented modules for simulating gas-aerosol equilibrium/ thermodynamics and aqueous-phase chemistry. Unfortunately, there are no analytical solutions against which the model could be tested because the SCICHEM model is far too complex and nonlinear. Instead, testing was conducted for typical conditions to assess whether the new model responded to changes in model inputs in a manner that was consistent with scientific expectations. If the model's response (change in surface concentration) was directionally consistent with scientific expectation and quantitatively plausible, the model was judged acceptable. The model performance was judged on an individual species basis. The intent of this type of testing is solely to identify possible flaws in the implementation of the modules that might cause the model to have no response, or have an exaggerated response, to perturbations in important model inputs. This type of testing is necessary but by no means sufficient to fully ascertain that the modules are implemented correctly. Comprehensive testing of the code and of the model performance against observations should be carried out in future studies.

4.2 Test Conditions

The test conditions involve simulation of the transport, dispersion, chemical transformation, and deposition of SO₂ and NO_x emissions from a single source with a relatively tall stack on a typical summer day. One group of tests examines the ability of the model to simulate gas and aerosol species concentrations in the absence of clouds or precipitation. A second group of tests examines the performance of the model before, during, and after plume interaction with clouds and, optionally, with precipitation. All simulations are conducted for a 24-hr period with display of model outputs every 30 minutes.

The conditions for the baseline simulation are summarized in Tables 4-1 and 4-2. To simplify interpretation of the results for chemically reactive species, constant meteorological conditions were specified for the 24-hr period. Vertically uniform

westerly winds at 3 meters per second were specified along with slightly unstable atmospheric conditions, a mixing height of 800 meters, a 20°C air temperature, 50 percent relative humidity, and a latitude of 37 degrees. Constant emissions from a single 100-meter tall stack were specified with 40 grams per second of SO₂ and 20 grams per second of NO_x. The stack effluents were warm (500 K) and buoyant and left the stack with significant momentum (555 m³/s flow rate). These emissions were injected into a flow field with spatially uniform concentrations of the trace gases and aerosols listed in Table 4-2. The principal background species concentrations are 54 ppb of ozone, 2 ppb of NO₂, 100 ppbC of VOC, 200 ppb of CO, 5 ppb of NH₃, 3 ppb of H₂O₂, 1 µg/m³ of sulfate aerosol, 0.5 µg/m³ of nitrate aerosol, 0.52 µg/m³ of ammonium aerosol, and 10 µg/m³ of crustal aerosol. The aerosol particles were assumed to have a mass mean diameter of 0.5 µm and fully activated by clouds. These background species concentrations were treated as constants in all of the test simulations reported here. Initially, selected simulations were made with gas-phase and aqueous-phase chemistry influencing the background species concentrations, but these results were more difficult to interpret than the constant background cases reported here.

Table 4-1. Baseline test case meteorological and emissions input parameters.

Input Parameter	Base Case Value
Wind Speed	3 m/s
Wind Direction	Westerly
Mixing Height	800 m
Temperature	293.15 K
Relative Humidity	50 percent
Precipitation Rate	0
Liquid Water Content	0
Atmospheric Stability	Unstable
Simulation Hours	0000 –2300 hrs
Date	June 21, 1999
Latitude	37 degrees
Time Zone	8
SO ₂ Emissions Rate	40 grams/sec
NO Emissions Rate	18 grams/sec
NO ₂ Emissions Rate	2 grams/sec
Stack Height	100 meters
Stack Effluent Temperature	500 K
Stack Effluent Flow Rate	555 m ³ /sec

Table 4-2. Baseline ambient concentrations for the test simulations.

Species	Concentrations
Gases (ppm)	
NO	1.00E-04
SO2	1.00E-04
NO2	2.00E-03
O3	5.40E-02
OLE	2.00E-03
PAR	6.80E-02
TOL	2.00E-03
XYL	1.00E-03
FORM	1.00E-03
FA	1.00E-06
ALD2	5.00E-04
ETH	2.00E-03
CRES	0.00E+00
MGLY	0.00E+00
OPEN	0.00E+00
PAN	1.00E-05
CO	2.00E-01
HONO	1.00E-05
H2O2	3.00E-03
HNO3	1.00E-05
ISOP	1.00E-03
SA	1.00E-06
HCL	1.00E-06
NH3	5.00E-03
NO3	1.00E-06
N2O5	1.00E-07
C2O3	1.00E-12
XO2	1.00E-12
XO2N	1.00E-12
CRO	1.00E-12
O	1.00E-12
OH	1.00E-12
O1D	1.00E-12
HO2	1.00E-12
ROR	1.00E-12
TO2	1.00E-12
H2O	Determined from RH & T
Aerosols ($\mu\text{g}/\text{m}^3$)	
ASO4	1.000
ANH4	0.520
ANO3	0.500
ANA	0.045
ACL	0.071
CRUS	10.00

Note that in Table 4-2, the aerosol particles are assumed to exist in a single size section with lower and upper bound diameters of 0.025 and 10 μm , mass mean diameter of 0.5 μm , and cloud water activation diameter of 0.2 μm (i.e., aerosols are fully scavenged by cloud water droplets). The concentrations given for the ambient aerosol particle species are not assumed to remain constant. They will be determined internally by the aerosol equilibrium module using the ambient gas phase species concentrations, initial aerosol particle concentrations, and background temperature and relative humidity.

The model testing consisted of one baseline simulation and 40 sensitivity simulations where one or more input parameters were varied from those in the baseline case. Table 4-3 summarizes the input parameter variations. The first group of simulations, Runs 1-16, does not involve clouds, precipitation, or aqueous-phase chemistry, but does include the gas-phase chemistry and gas-particle equilibrium/thermodynamics. These runs are designed to explore the model's response to variations in wind speed, mixing height, SO_2 emissions, NO_x emissions, temperature, and relative humidity. The second group of simulations, Runs 17-40, involves clouds as well as the other processes. Run 19 is essentially a second baseline case with three hours of clouds in the afternoon, a liquid water content (LWC) of 0.1 g/cm^3 and no precipitation. Variations in the cloud duration, liquid water content, precipitation rate, temperature, SO_2 emission rate, and background concentrations of H_2O_2 , NH_3 , ozone, crustal aerosol, sodium chloride, and VOC are simulated in these runs. Thus, while this is a fairly small set of test simulations, it covers variations in the three major types of inputs: emissions, air quality, and meteorology.

Table 4-3. Input parameter variations for model test simulations.

Run No.	Parameter Variations
1	Double wind speed (6 m/s)
2	Half wind speed (1.5 m/s)
3	Double mixing height (1600 m)
4	Half mixing height (400 m)
5	Double SO ₂ emissions (80 g/s)
6	Half SO ₂ emissions (20 g/s)
7	Zero SO ₂ emissions (0)
8	Double NO _x emissions (40 g/s)
9	Half NO _x emissions (10 g/s)
10	Zero NO _x emissions (0)
11	Lower background temperature (278.15 K)
12	Higher background temperature (308.15 K)
13	Freezing background temperature (263.15 K)
14	Lower relative humidity (10 %)
15	High relative humidity 1 (70%)
16	High relative humidity 2 (95%)
17	Run 19 with only one hour of clouds (15-16)
18	2 hrs of clouds (15-17); LWC=0.1 & RH=100% RH
19	3 hrs of clouds (15-18); LWC=0.1 & RH=100% RH
20	Run 19 with LWC = 0.3 g/cm ³
21	Run 20 with aqueous-phase radical chemistry disabled
22	Run 19 with LWC = 0.4 g/cm ³
23	Run 19 with 1 mm/hr precipitation
24	Run 19 with 5 mm/hr precipitation
25	Run 19 with 10 mm/hr precipitation
26	Run 19 with low background temperature (278.15 K)
27	Run 19 with high background temperature (308.15 K)
28	Run 19 with low background H ₂ O ₂ (1e-3 ppb)
29	Run 19 with high background H ₂ O ₂ (10 ppb)
30	Run 19 with low background NH ₃ (0.1 ppb)
31	Run 19 with high background NH ₃ (25 ppb)
32	Run 19 with low background Ozone (10 ppb)
33	Run 19 with high background Ozone (100 ppb)
34	Run 19 with low background CRUS (0.1 µg/m ³)
35	Run 19 with high background CRUS (100.00 µg/m ³)
36	Run 19 with high background NAACL (5 µg/m ³)
37	Run 19 with low background VOCs (10 ppbC)
38	Run 19 with high background VOCs (300 ppbC)
39	Run 19 with zero source 1 SO ₂ Emissions
40	Run 19 with double source 1 SO ₂ Emissions

4.3 Baseline Results

4.3.1 Baseline Case Results Without Clouds

Spatial plots of model estimates of baseline surface concentrations for key species for hours 10, 12, 14, 16, 18, and 20 are shown in Figures 4-1 through 4-6. These displays are generated by the SCICHEM graphical user interface (GUI). The results for SO₂ (Figure 4-1) show that, at a short distance downwind of the source location (x=0, y=35), the surface concentrations reach about 4 ppb, and plume centerline surface concentrations remain in the 1-3 ppb range for about 30 km downwind of the source. Away from the plume centerline and farther downwind, the results show a gradual decrease in SO₂ concentrations towards the assumed background level of 0.1 ppb. The estimated surface concentrations are virtually constant during the simulation, which is expected for the constant emission rate and constant meteorological conditions specified for this case.

The estimated ground-level sulfate concentration (shown in Figure 4-2) reaches 1.2 µg/m³ in the plume in the afternoon hours, which is consistent with the expected slow rate of gas-phase chemical conversion of SO₂ to sulfate aerosol under these conditions. Less conversion to sulfate is evident in the morning and late in the day, reflecting the diurnal cycle of the atmospheric chemistry.

The NO, NO₂, and ozone plots (Figures 4-3, 4-4, and 4-5) show evidence of fairly rapid NO_x oxidation in the simulated plume and formation of ozone downwind of the source. In fact, the plume NO₂ concentrations are mostly lower than the non-reactive background NO₂ concentration of 2 ppb. The estimated maximum surface ozone concentrations occur 70 to 90 km downwind of the source and reach 136 ppb at hour 16 in the afternoon. The simulated ozone production from this single 1.9 tons/day NO_x source is quite efficient under these unstable conditions with the 100 ppbC of background VOCs. Besides contributing to ozone formation, the NO_x emissions also lead to formation of aerosol nitrate (see Figure 4-6). The estimated surface concentrations of aerosol nitrate (NO₃⁻) reach 3.7 µg/m³ about 90 km downwind of the source in the afternoon. The baseline case has a fairly high background ammonia concentration, so that nitric acid

formed in the photo-oxidation of the NO_x emissions can readily form ammonium nitrate under the simulated conditions.

4.3.2 Baseline Case Results With Clouds

Run 19 is the baseline case with clouds. It has clouds throughout the domain from hours 15 to 18. Figure 4-7 shows the estimated surface SO_2 concentrations through the afternoon hours. The SO_2 concentrations in the plume are negligible at hours 15, 16, and 17. It should be noted that the SCICHEM model interpolates the meteorological inputs between hours, so that the effects of the clouds begin at hour 14.5; by hour 15, the SO_2 in the plume is mostly converted to sulfate. Figure 4-8 shows the estimated sulfate concentrations at the surface. At hour 14, the plume sulfate concentrations reach $1.2 \mu\text{g}/\text{m}^3$ far downwind of the source, similar to the baseline case without clouds. For hours 15, 16, and 17, the maximum surface sulfate concentrations are 13.8 to $15.7 \mu\text{g}/\text{m}^3$ just 5 km downwind of the source. Farther downwind, the estimated surface sulfate levels are in the 4 to $10 \mu\text{g}/\text{m}^3$ range along the plume centerline. This simulation reflects the rapid aqueous-phase conversion of SO_2 to sulfate expected in the summer with ample liquid water and with moderately high background concentrations of H_2O_2 , ozone, and ammonia.

The estimated surface concentrations of aerosol nitrate are also enhanced in the simulation with clouds. Figure 4-9 shows that the maximum aerosol nitrate levels are 8 to $9 \mu\text{g}/\text{m}^3$ during the hours with clouds, compared to $4 \mu\text{g}/\text{m}^3$ before and after the clouds. The highest nitrate levels are simulated farther downwind than the highest sulfate levels, because the NO_x emissions must first be converted to nitric acid in gas-phase reactions before conversion to aerosol and aqueous nitrate. Hence, the principal features of the SO_2 , SO_4 , and NO_3 distributions before, during, and after the clouds are physically and chemically plausible and directionally correct.

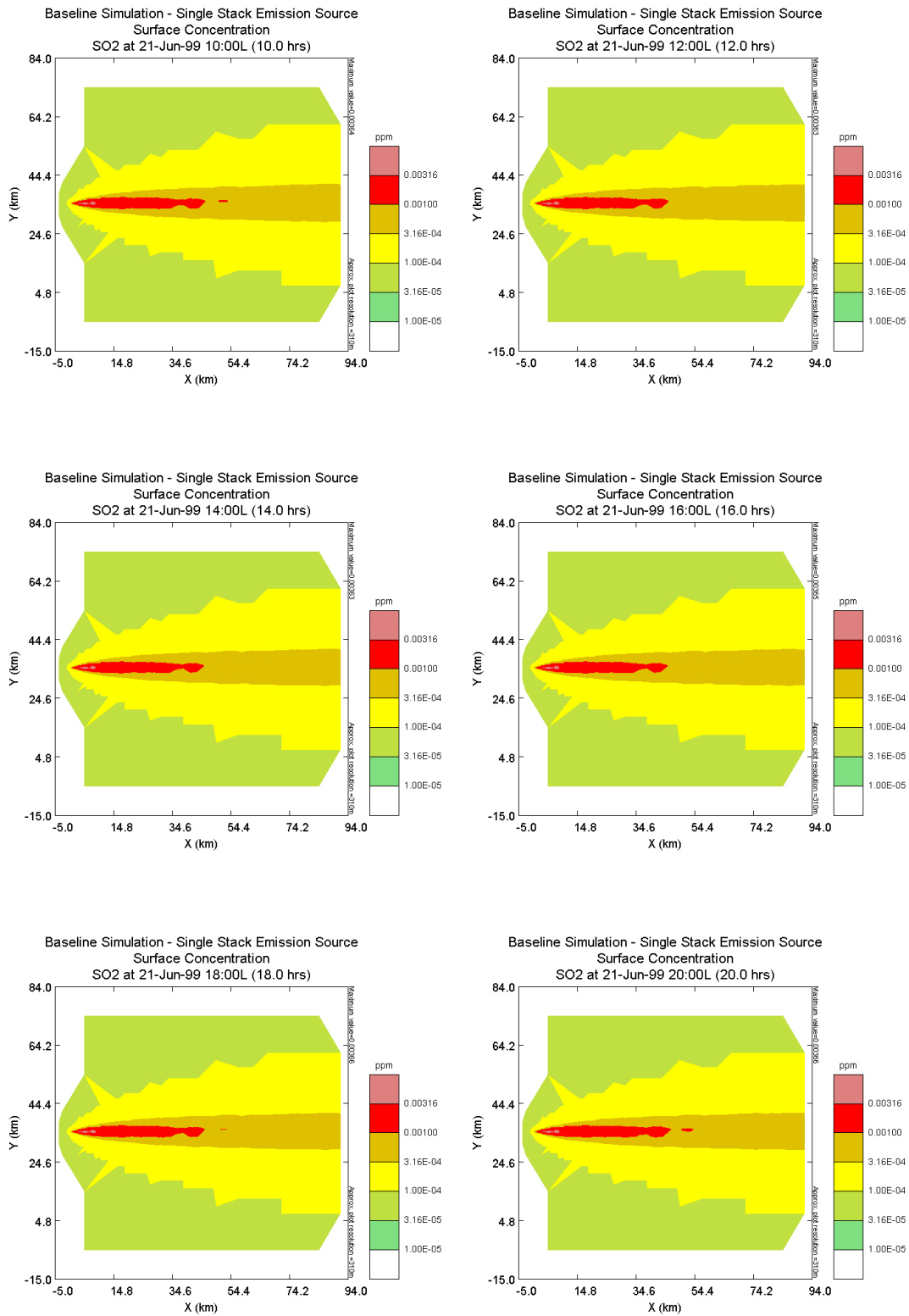


Figure 4-1. SCICHEM baseline simulation: Calculated surface concentration (ppm) of SO₂.

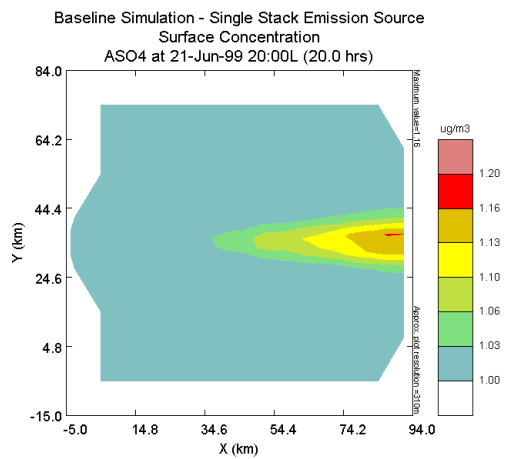
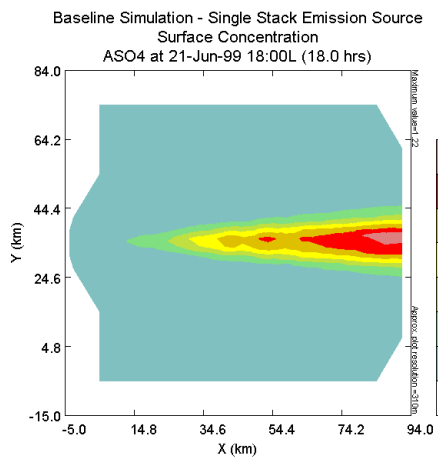
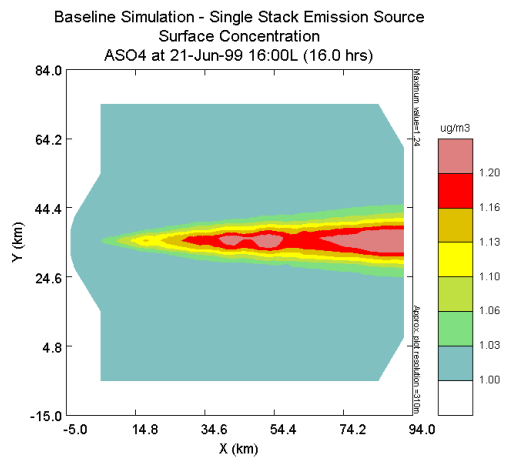
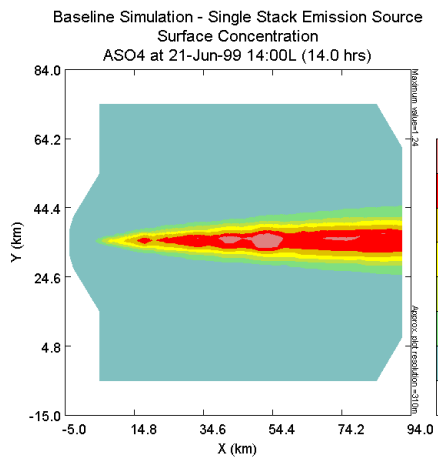
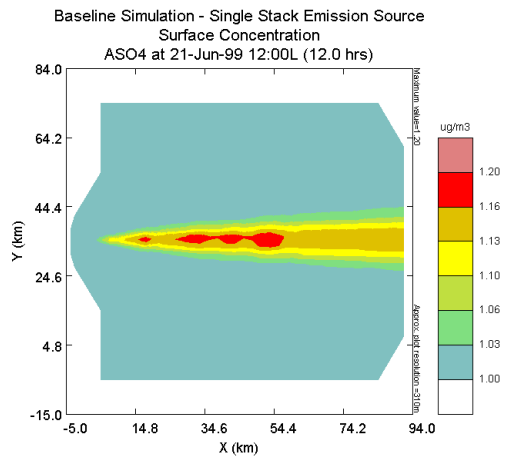
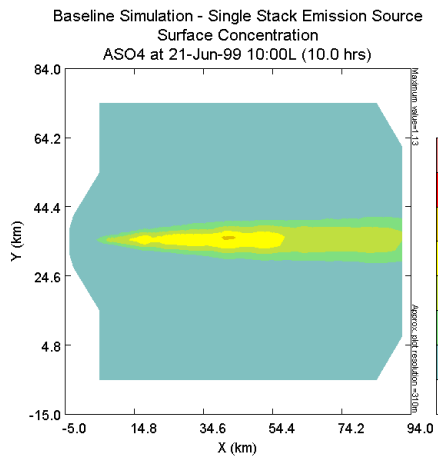


Figure 4-2. SCICHEM baseline simulation: Calculated surface concentration ($\mu\text{g}/\text{m}^3$) of particulate sulfate.

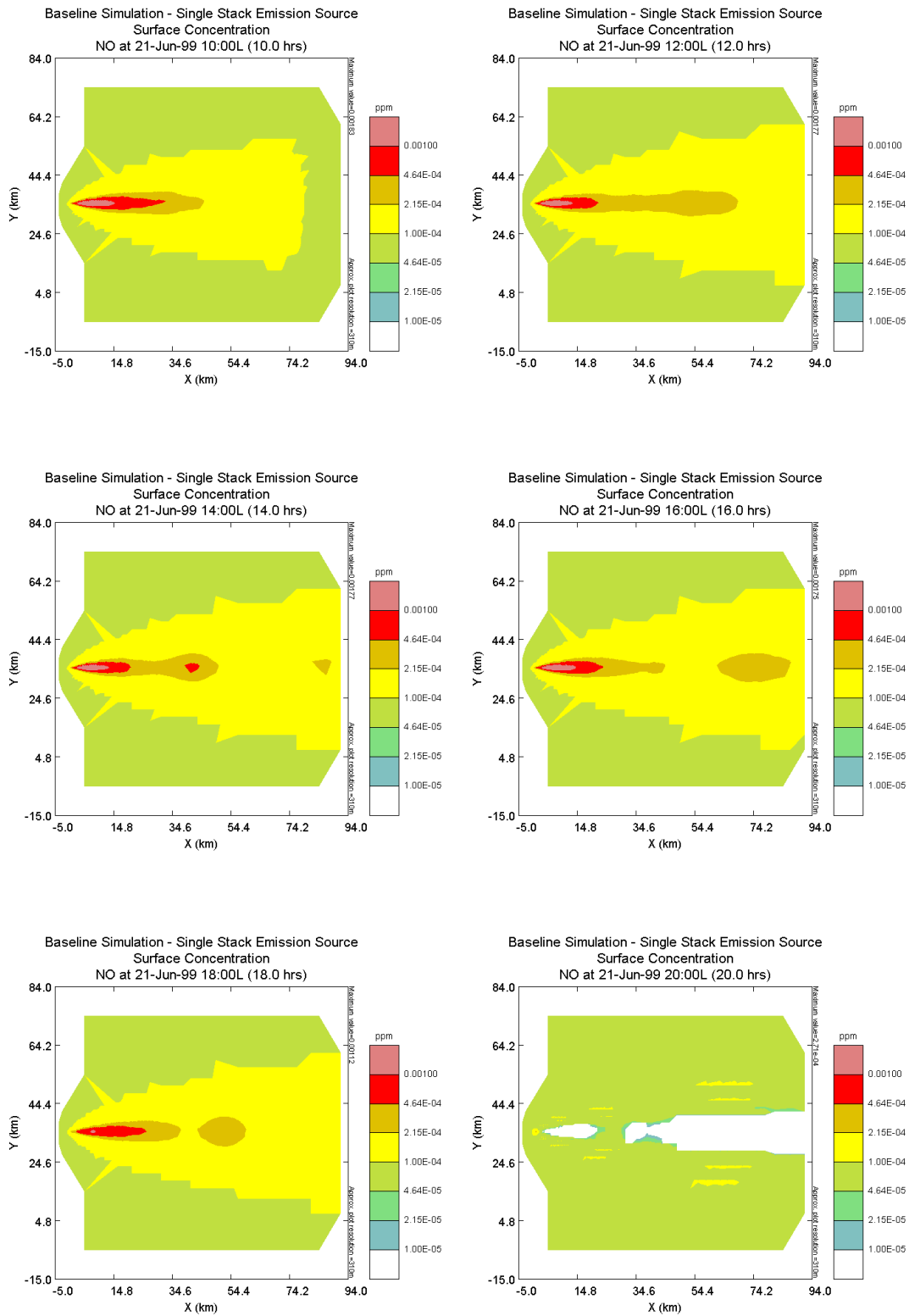


Figure 4-3. SCICHEM baseline simulation: Calculated surface concentration (ppm) of NO.

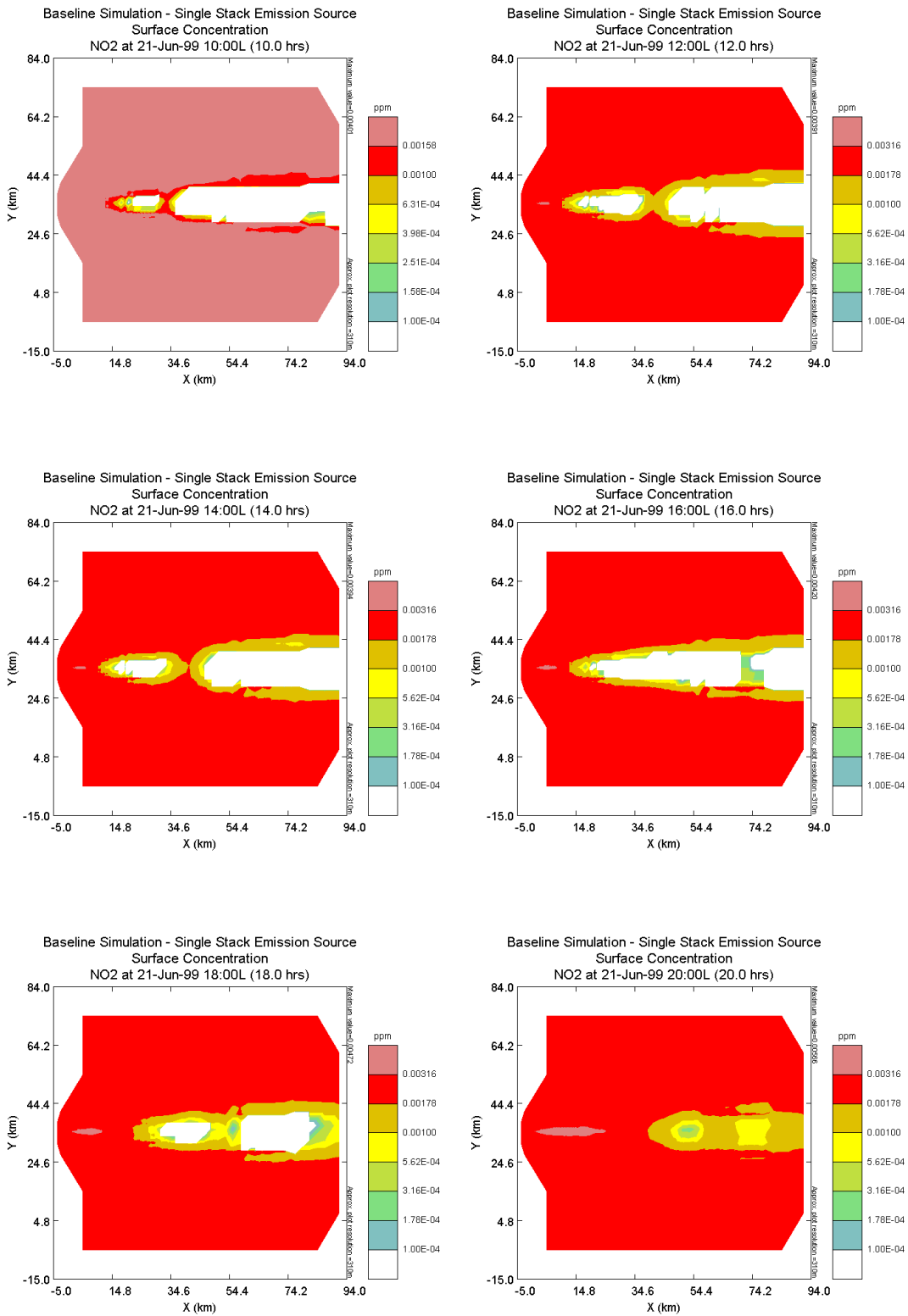


Figure 4-4. SCICHEM baseline simulation: Calculated surface concentration (ppm) of NO₂.

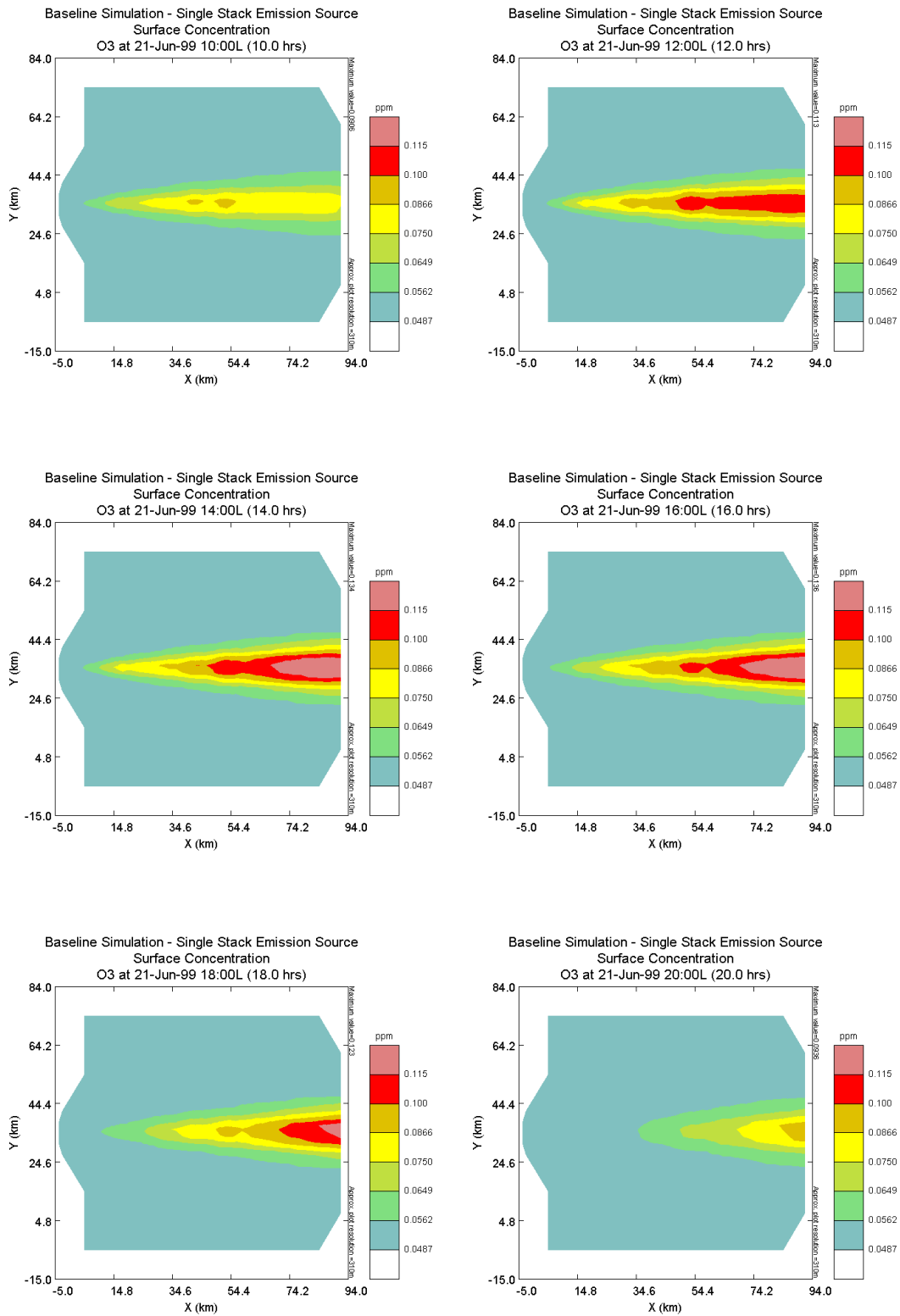


Figure 4-5. SCICHEM baseline simulation: Calculated surface concentration (ppm) of Ozone.

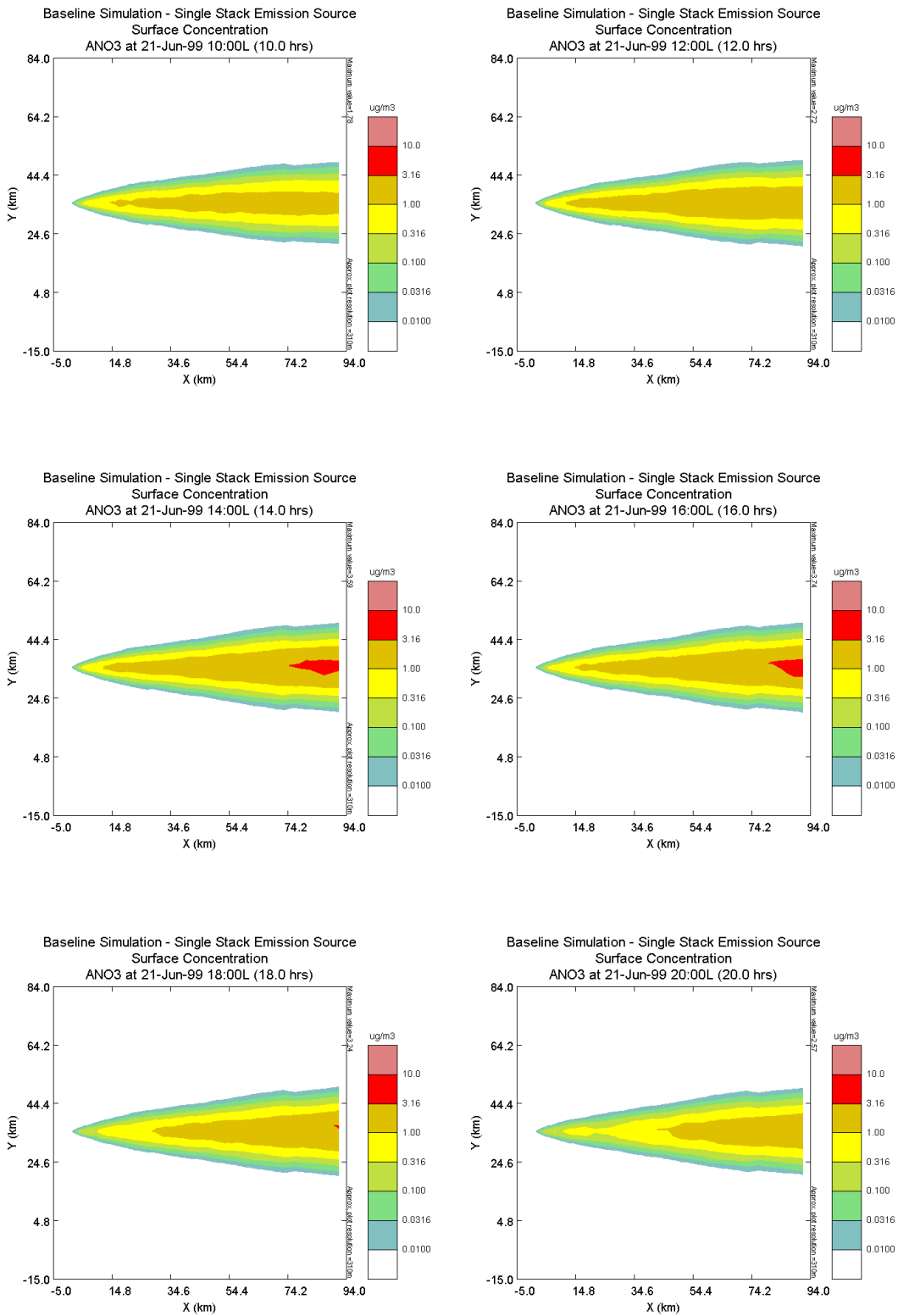


Figure 4-6. SCICHEM baseline simulation: Calculated surface concentration ($\mu\text{g}/\text{m}^3$) of particulate nitrate.

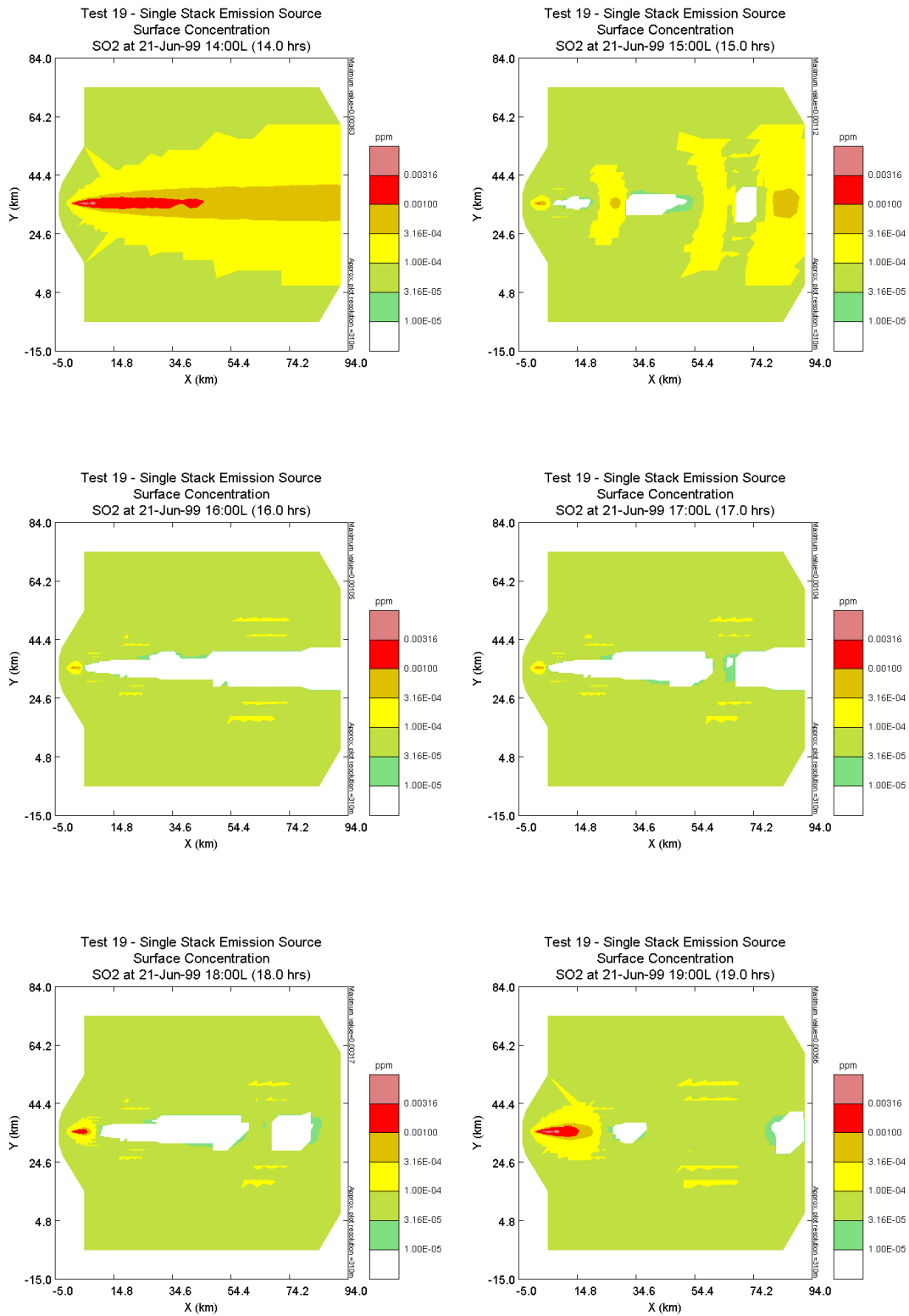


Figure 4-7. SCICHEM aqueous-phase baseline simulation: Calculated surface concentration (ppm) of SO₂.

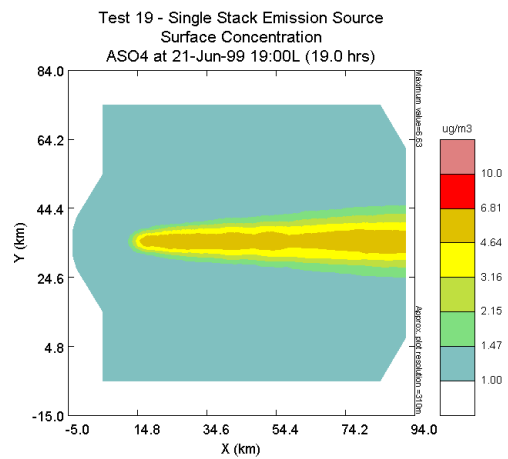
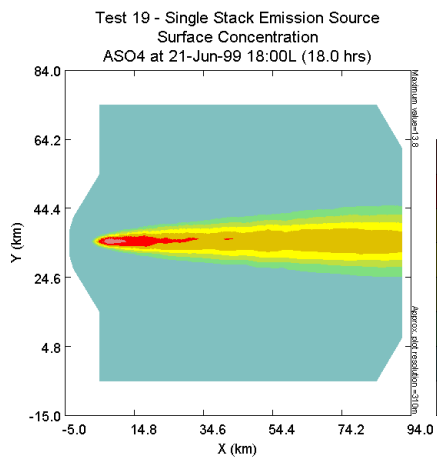
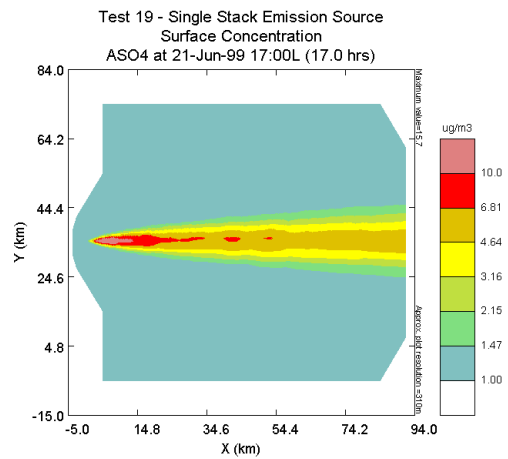
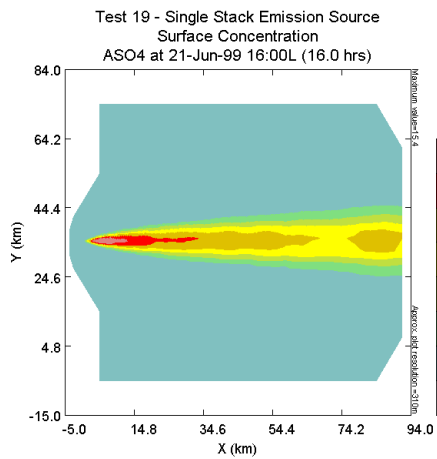
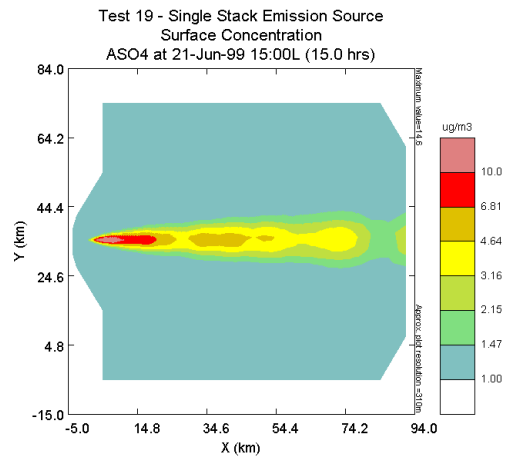
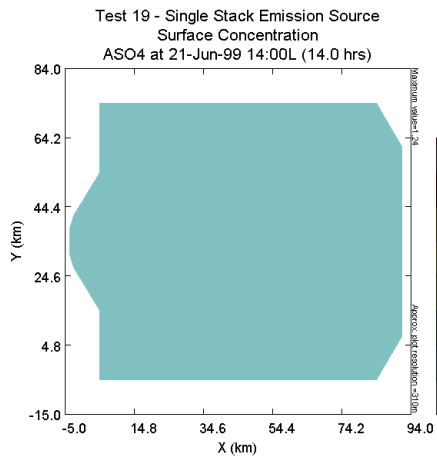


Figure 4-8. SCICHEM aqueous-phase baseline simulation: Calculated surface concentration ($\mu\text{g}/\text{m}^3$) of particulate sulfate.

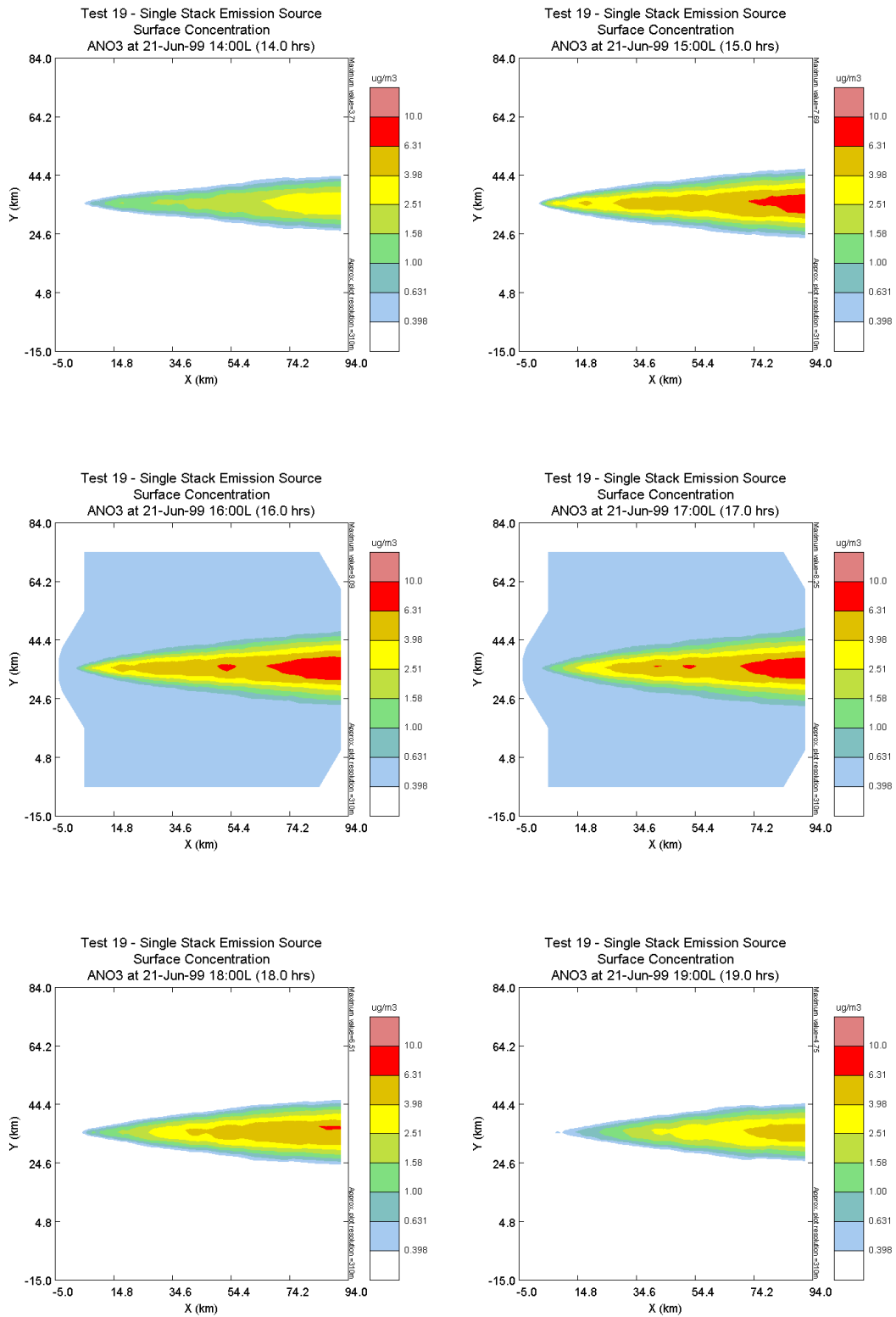


Figure 4-9. SCICHEM aqueous-phase baseline simulation: Calculated surface concentration ($\mu\text{g}/\text{m}^3$) of particulate nitrate.

4.4 Sensitivity Study Results

For comparison of the sensitivity study results to the baseline case results, we focused on the surface concentration estimates between 12 noon and hour 20 at three distances downwind of the source: 5, 25, and 50 km. The surface concentrations of the tracer and SO₂ for hours 12, 16, and 20 are listed in Tables 4-4, 4-5, and 4-6, respectively. Tables 4-7 through 4-15 list the corresponding concentrations of six other gases: NO, NO₂, ozone, H₂O₂, HNO₃, and NH₃. The surface concentrations of sulfate, nitrate, and ammonium aerosol particles downwind of the source are given at 2 hour increments starting at 12 noon in Tables 4-16 through 4-25. Finer time resolution is provided to more clearly illustrate the effects of the clouds on the aerosol particle concentrations.

Table 4-4. Estimated surface concentrations (ppb) of Tracer and SO₂ at 12:00L at 5 km, 25 km, and 50 km downwind of the major point source for the 41 test simulations.

Run	Tracer			SO ₂		
	5 km	25 km	50 km	5 km	25 km	50 km
Baseline	1.94E-07	7.25E-08	4.78E-08	3.93E-03	1.49E-03	9.96E-04
1	1.60E-07	6.59E-08	4.67E-08	3.26E-03	1.38E-03	9.91E-04
2	2.23E-07	8.05E-08	5.30E-08	4.47E-03	1.63E-03	1.10E-03
3	6.34E-08	3.58E-08	2.34E-08	1.35E-03	7.85E-04	5.35E-04
4	6.11E-07	1.59E-07	1.05E-07	1.22E-02	3.18E-03	2.09E-03
5	1.94E-07	7.25E-08	4.78E-08	7.76E-03	2.88E-03	1.90E-03
6	1.94E-07	7.25E-08	4.78E-08	2.01E-03	7.90E-04	5.43E-04
7	1.94E-07	7.25E-08	4.78E-08	9.95E-05	9.41E-05	9.15E-05
8	1.94E-07	7.25E-08	4.78E-08	3.93E-03	1.49E-03	9.97E-04
9	1.94E-07	7.25E-08	4.78E-08	3.93E-03	1.49E-03	1.00E-03
10	1.94E-07	7.25E-08	4.78E-08	3.93E-03	1.49E-03	9.98E-04
11	1.89E-07	7.25E-08	4.72E-08	3.74E-03	1.46E-03	9.72E-04
12	1.93E-07	7.33E-08	4.78E-08	3.98E-03	1.52E-03	1.00E-03
13	1.95E-07	6.97E-08	4.89E-08	3.76E-03	1.38E-03	9.80E-04
14	1.94E-07	7.25E-08	4.78E-08	3.94E-03	1.50E-03	1.01E-03
15	1.94E-07	7.25E-08	4.78E-08	3.92E-03	1.49E-03	9.95E-04
16	1.94E-07	7.25E-08	4.78E-08	3.92E-03	1.48E-03	9.89E-04
17	1.94E-07	7.25E-08	4.78E-08	3.93E-03	1.49E-03	9.97E-04
18	1.94E-07	7.25E-08	4.78E-08	3.93E-03	1.49E-03	9.98E-04
19	1.94E-07	7.25E-08	4.78E-08	3.93E-03	1.49E-03	9.98E-04
20	1.94E-07	7.25E-08	4.78E-08	3.93E-03	1.49E-03	9.98E-04
21	1.94E-07	7.25E-08	4.78E-08	3.93E-03	1.49E-03	9.98E-04
22	1.94E-07	7.25E-08	4.78E-08	3.93E-03	1.49E-03	9.98E-04
23	1.94E-07	7.25E-08	4.78E-08	3.93E-03	1.49E-03	9.98E-04
24	1.94E-07	7.25E-08	4.78E-08	3.93E-03	1.49E-03	9.98E-04
25	1.94E-07	7.25E-08	4.78E-08	3.93E-03	1.49E-03	9.98E-04
26	1.89E-07	7.25E-08	4.72E-08	3.74E-03	1.46E-03	9.71E-04
27	1.93E-07	7.33E-08	4.78E-08	3.98E-03	1.51E-03	1.00E-03
28	1.94E-07	7.25E-08	4.78E-08	3.93E-03	1.49E-03	9.99E-04
29	1.94E-07	7.25E-08	4.78E-08	3.92E-03	1.48E-03	9.91E-04
30	1.94E-07	7.25E-08	4.78E-08	3.93E-03	1.49E-03	9.97E-04
31	1.94E-07	7.25E-08	4.78E-08	3.93E-03	1.49E-03	9.98E-04
32	1.94E-07	7.25E-08	4.78E-08	3.94E-03	1.49E-03	9.90E-04
33	1.94E-07	7.25E-08	4.78E-08	3.92E-03	1.48E-03	9.94E-04
34	1.94E-07	7.25E-08	4.78E-08	3.93E-03	1.49E-03	9.96E-04
35	1.94E-07	7.25E-08	4.78E-08	3.93E-03	1.49E-03	9.96E-04
36	1.94E-07	7.25E-08	4.78E-08	3.93E-03	1.49E-03	9.97E-04
37	1.94E-07	7.25E-08	4.78E-08	3.93E-03	1.46E-03	9.54E-04
38	1.94E-07	7.25E-08	4.78E-08	3.93E-03	1.51E-03	1.02E-03
39	1.94E-07	7.25E-08	4.78E-08	9.95E-05	9.42E-05	9.14E-05
40	1.94E-07	7.25E-08	4.78E-08	7.76E-03	2.88E-03	1.90E-03

Table 4-5. Estimated surface concentrations (ppb) of Tracer and SO₂ at 16:00L at 5 km, 25 km, and 50 km downwind of the major point source for the 41 test simulations.

Run	Tracer			SO ₂		
	5 km	25 km	50 km	5 km	25 km	50 km
Baseline	1.94E-07	7.25E-08	4.78E-08	3.94E-03	1.49E-03	9.87E-04
1	1.63E-07	6.57E-08	4.24E-08	3.33E-03	1.39E-03	9.16E-04
2	2.23E-07	8.04E-08	5.68E-08	4.49E-03	1.61E-03	1.13E-03
3	6.55E-08	3.58E-08	2.19E-08	1.40E-03	7.89E-04	5.05E-04
4	6.11E-07	1.59E-07	1.05E-07	1.22E-02	3.19E-03	2.07E-03
5	1.94E-07	7.25E-08	4.78E-08	7.77E-03	2.89E-03	1.88E-03
6	1.94E-07	7.25E-08	4.78E-08	2.02E-03	7.94E-04	5.38E-04
7	1.94E-07	7.25E-08	4.78E-08	9.97E-05	9.78E-05	9.91E-05
8	1.94E-07	7.25E-08	4.78E-08	3.94E-03	1.50E-03	9.89E-04
9	1.94E-07	7.25E-08	4.78E-08	3.94E-03	1.49E-03	9.88E-04
10	1.94E-07	7.25E-08	4.78E-08	3.93E-03	1.50E-03	9.89E-04
11	1.78E-07	7.25E-08	4.88E-08	3.53E-03	1.47E-03	9.93E-04
12	1.78E-07	6.92E-08	5.04E-08	3.69E-03	1.44E-03	1.03E-03
13	1.92E-07	7.08E-08	4.89E-08	3.70E-03	1.41E-03	9.75E-04
14	1.94E-07	7.25E-08	4.78E-08	3.94E-03	1.51E-03	9.99E-04
15	1.94E-07	7.25E-08	4.78E-08	3.93E-03	1.49E-03	9.85E-04
16	1.94E-07	7.25E-08	4.78E-08	3.93E-03	1.48E-03	9.76E-04
17	1.94E-07	7.25E-08	4.78E-08	3.94E-03	1.49E-03	9.87E-04
18	1.94E-07	7.25E-08	4.78E-08	6.43E-05	5.20E-05	5.37E-05
19	1.94E-07	7.25E-08	4.78E-08	6.48E-05	5.24E-05	6.31E-05
20	1.94E-07	7.25E-08	4.78E-08	5.37E-05	5.31E-05	6.86E-05
21	1.94E-07	7.25E-08	4.78E-08	5.72E-05	5.32E-05	6.32E-05
22	1.94E-07	7.25E-08	4.78E-08	5.65E-05	5.63E-05	6.13E-05
23	1.94E-07	7.25E-08	4.78E-08	6.39E-05	6.71E-05	5.33E-05
24	1.94E-07	7.25E-08	4.78E-08	6.29E-05	5.10E-05	5.55E-05
25	1.94E-07	7.25E-08	4.78E-08	6.31E-05	5.10E-05	5.26E-05
26	1.78E-07	7.25E-08	4.88E-08	5.91E-05	5.05E-05	5.18E-05
27	1.78E-07	6.92E-08	5.04E-08	8.39E-04	4.82E-05	6.01E-05
28	1.94E-07	7.25E-08	4.78E-08	1.07E-04	5.19E-05	4.83E-05
29	1.94E-07	7.25E-08	4.78E-08	6.54E-05	8.02E-05	5.17E-05
30	1.94E-07	7.25E-08	4.78E-08	1.88E-03	2.94E-05	2.07E-05
31	1.94E-07	7.25E-08	4.78E-08	5.69E-05	1.72E-04	1.05E-04
32	1.94E-07	7.25E-08	4.78E-08	1.24E-04	5.12E-05	5.82E-05
33	1.94E-07	7.25E-08	4.78E-08	6.57E-05	5.12E-05	8.31E-05
34	1.94E-07	7.25E-08	4.78E-08	1.03E-03	5.54E-05	7.22E-05
35	1.94E-07	7.25E-08	4.78E-08	9.20E-05	5.37E-05	5.99E-05
36	1.94E-07	7.25E-08	4.78E-08	6.34E-05	5.20E-05	5.01E-05
37	1.94E-07	7.25E-08	4.78E-08	6.33E-05	5.18E-05	4.88E-05
38	1.94E-07	7.25E-08	4.78E-08	6.60E-05	5.17E-05	4.99E-05
39	1.94E-07	7.25E-08	4.78E-08	7.66E-05	7.25E-05	8.36E-05
40	1.94E-07	7.25E-08	4.78E-08	1.44E-03	7.40E-05	5.25E-05

Table 4-6. Estimated surface concentrations (ppb) of Tracer and SO₂ at 20:00L at 5 km, 25 km, and 50 km downwind of the major point source for the 41 test simulations.

Run	Tracer			SO ₂		
	5 km	25 km	50 km	5 km	25 km	50 km
Baseline	1.94E-07	7.25E-08	4.78E-08	3.95E-03	1.53E-03	1.03E-03
1	1.63E-07	6.72E-08	4.55E-08	3.34E-03	1.43E-03	9.99E-04
2	2.23E-07	8.04E-08	5.69E-08	4.51E-03	1.67E-03	1.14E-03
3	6.35E-08	3.52E-08	2.23E-08	1.36E-03	7.97E-04	5.33E-04
4	6.11E-07	1.59E-07	1.05E-07	1.22E-02	3.25E-03	2.15E-03
5	1.94E-07	7.25E-08	4.78E-08	7.79E-03	2.97E-03	1.96E-03
6	1.94E-07	7.25E-08	4.78E-08	2.02E-03	8.17E-04	5.63E-04
7	1.94E-07	7.25E-08	4.78E-08	1.00E-04	1.00E-04	9.78E-05
8	1.94E-07	7.25E-08	4.78E-08	3.95E-03	1.53E-03	1.03E-03
9	1.94E-07	7.25E-08	4.78E-08	3.95E-03	1.53E-03	1.03E-03
10	1.94E-07	7.25E-08	4.78E-08	3.95E-03	1.53E-03	1.03E-03
11	1.88E-07	7.38E-08	4.89E-08	3.74E-03	1.52E-03	1.03E-03
12	1.98E-07	7.35E-08	4.69E-08	4.12E-03	1.59E-03	1.03E-03
13	1.88E-07	7.05E-08	4.91E-08	3.63E-03	1.42E-03	1.01E-03
14	1.94E-07	7.25E-08	4.78E-08	3.95E-03	1.53E-03	1.03E-03
15	1.94E-07	7.25E-08	4.78E-08	3.95E-03	1.53E-03	1.03E-03
16	1.94E-07	7.25E-08	4.78E-08	3.95E-03	1.53E-03	1.02E-03
17	1.94E-07	7.25E-08	4.78E-08	3.95E-03	1.53E-03	1.03E-03
18	1.94E-07	7.25E-08	4.78E-08	3.95E-03	1.09E-03	1.56E-05
19	1.94E-07	7.25E-08	4.78E-08	3.95E-03	1.09E-03	5.37E-05
20	1.94E-07	7.25E-08	4.78E-08	3.95E-03	6.56E-04	8.85E-05
21	1.94E-07	7.25E-08	4.78E-08	3.95E-03	1.09E-03	1.56E-05
22	1.94E-07	7.25E-08	4.78E-08	3.95E-03	1.13E-04	2.10E-05
23	1.94E-07	7.25E-08	4.78E-08	3.95E-03	1.08E-03	8.80E-05
24	1.94E-07	7.25E-08	4.78E-08	3.95E-03	1.08E-03	9.56E-06
25	1.94E-07	7.25E-08	4.78E-08	3.95E-03	1.07E-03	1.40E-05
26	1.88E-07	7.38E-08	4.89E-08	3.74E-03	1.07E-03	2.40E-06
27	1.98E-07	7.35E-08	4.69E-08	4.12E-03	1.31E-03	1.00E-04
28	1.94E-07	7.25E-08	4.78E-08	3.95E-03	1.10E-03	4.94E-05
29	1.94E-07	7.25E-08	4.78E-08	3.95E-03	1.05E-03	9.48E-05
30	1.94E-07	7.25E-08	4.78E-08	3.95E-03	1.34E-03	9.88E-05
31	1.94E-07	7.25E-08	4.78E-08	3.95E-03	9.40E-04	9.55E-05
32	1.94E-07	7.25E-08	4.78E-08	3.95E-03	1.08E-03	6.15E-05
33	1.94E-07	7.25E-08	4.78E-08	3.94E-03	1.09E-03	8.82E-05
34	1.94E-07	7.25E-08	4.78E-08	3.95E-03	1.26E-03	1.84E-05
35	1.94E-07	7.25E-08	4.78E-08	3.95E-03	1.07E-03	1.91E-05
36	1.94E-07	7.25E-08	4.78E-08	3.95E-03	9.90E-04	1.00E-04
37	1.94E-07	7.25E-08	4.78E-08	3.95E-03	1.09E-03	2.20E-05
38	1.94E-07	7.25E-08	4.78E-08	3.95E-03	1.09E-03	2.89E-05
39	1.94E-07	7.25E-08	4.78E-08	1.00E-04	9.99E-05	3.14E-05
40	1.94E-07	7.25E-08	4.78E-08	7.79E-03	2.32E-03	3.44E-05

Table 4-7. Estimated surface concentrations (ppb) of NO and NO₂ at 12:00L at 5 km, 25 km, and 50 km downwind of the major point source for the 41 test simulations.

Run	NO			NO ₂		
	5 km	25 km	50 km	5 km	25 km	50 km
Baseline	1.86E-03	4.18E-04	3.57E-04	3.68E-03	4.17E-04	3.33E-04
1	1.58E-03	8.70E-04	6.58E-04	3.68E-03	7.42E-04	3.04E-04
2	1.62E-03	2.84E-04	2.49E-04	3.76E-03	7.83E-04	7.05E-05
3	8.40E-04	4.83E-04	2.44E-04	2.36E-03	5.03E-04	2.68E-04
4	4.60E-03	7.55E-04	6.05E-04	9.44E-03	1.41E-03	7.65E-04
5	1.87E-03	3.74E-04	9.46E-05	3.67E-03	2.96E-04	4.13E-04
6	1.86E-03	3.72E-04	3.10E-04	3.69E-03	2.98E-04	2.64E-04
7	1.86E-03	3.38E-04	1.28E-04	3.68E-03	3.38E-04	6.45E-04
8	3.10E-03	5.75E-04	2.79E-04	6.35E-03	5.21E-04	1.63E-03
9	1.26E-03	5.11E-04	5.01E-04	2.31E-03	9.62E-04	4.62E-04
10	8.67E-04	2.42E-04	2.86E-05	1.55E-03	3.65E-04	5.76E-04
11	2.32E-03	8.14E-04	4.81E-04	3.21E-03	4.73E-04	1.49E-04
12	1.28E-03	1.35E-04	2.05E-04	3.82E-03	4.22E-04	2.95E-04
13	2.79E-03	1.38E-03	3.44E-04	2.90E-03	5.98E-04	3.06E-04
14	2.06E-03	7.01E-04	6.15E-04	3.73E-03	5.11E-04	4.79E-04
15	1.78E-03	4.79E-04	5.37E-04	3.61E-03	2.65E-04	7.20E-04
16	1.69E-03	2.09E-04	4.82E-04	3.55E-03	4.04E-04	7.94E-04
17	1.86E-03	3.81E-04	4.98E-04	3.67E-03	2.73E-04	2.29E-04
18	1.86E-03	5.24E-04	4.24E-04	3.67E-03	5.06E-04	1.54E-03
19	1.86E-03	5.24E-04	4.24E-04	3.67E-03	5.06E-04	1.54E-03
20	1.86E-03	5.24E-04	4.24E-04	3.67E-03	5.06E-04	1.54E-03
21	1.86E-03	5.24E-04	4.24E-04	3.67E-03	5.06E-04	1.54E-03
22	1.86E-03	5.24E-04	4.24E-04	3.67E-03	5.06E-04	1.54E-03
23	1.86E-03	5.24E-04	4.24E-04	3.67E-03	5.06E-04	1.54E-03
24	1.86E-03	5.24E-04	4.24E-04	3.67E-03	5.06E-04	1.54E-03
25	1.86E-03	5.24E-04	4.24E-04	3.67E-03	5.06E-04	1.54E-03
26	2.32E-03	8.07E-04	3.79E-04	3.19E-03	5.11E-04	2.87E-04
27	1.28E-03	1.17E-04	8.36E-06	3.82E-03	2.77E-04	5.10E-04
28	1.91E-03	4.35E-04	6.30E-04	3.67E-03	9.66E-04	7.62E-04
29	1.77E-03	4.93E-04	8.02E-05	3.60E-03	5.24E-04	6.32E-04
30	1.86E-03	3.43E-04	1.24E-04	3.66E-03	3.99E-04	7.22E-04
31	1.89E-03	3.48E-04	1.28E-04	3.76E-03	3.96E-04	5.48E-04
32	4.61E-03	1.04E-03	1.79E-04	1.35E-03	3.62E-04	6.12E-04
33	1.06E-03	1.82E-04	1.02E-04	4.18E-03	1.68E-04	2.11E-04
34	1.86E-03	4.20E-04	6.42E-05	3.68E-03	4.19E-04	5.05E-04
35	1.86E-03	4.20E-04	6.42E-05	3.68E-03	4.19E-04	5.05E-04
36	1.86E-03	6.07E-04	6.22E-05	3.68E-03	7.31E-04	4.07E-04
37	2.03E-03	6.29E-04	3.34E-04	3.60E-03	3.78E-04	2.76E-04
38	1.58E-03	2.93E-04	1.19E-04	3.73E-03	4.37E-04	1.13E-03
39	1.86E-03	3.74E-04	3.96E-04	3.68E-03	2.75E-04	8.26E-05
40	1.87E-03	3.48E-04	6.39E-05	3.66E-03	3.38E-04	4.82E-04

Table 4-8 Estimated surface concentrations (ppb) of NO and NO₂ at 16:00L at 5 km, 25 km, and 50 km downwind of the major point source for the 41 test simulations.

Run	NO			NO ₂		
	5 km	25 km	50 km	5 km	25 km	50 km
Baseline	1.72E-03	4.62E-04	1.63E-04	4.08E-03	4.35E-04	2.84E-04
1	1.55E-03	1.05E-03	6.06E-04	3.79E-03	1.27E-03	7.08E-04
2	1.59E-03	2.49E-04	1.40E-04	4.28E-03	6.87E-04	8.19E-04
3	7.98E-04	4.85E-04	2.03E-04	2.49E-03	4.94E-04	3.05E-04
4	4.06E-03	8.88E-04	2.13E-04	1.02E-02	1.35E-03	4.03E-04
5	1.73E-03	4.67E-04	1.37E-04	4.05E-03	4.42E-04	6.12E-04
6	1.70E-03	4.74E-04	4.25E-04	4.11E-03	4.12E-04	4.10E-04
7	1.73E-03	4.79E-04	1.89E-04	4.06E-03	1.18E-03	1.69E-03
8	2.78E-03	7.50E-04	2.37E-04	6.95E-03	9.46E-04	2.09E-04
9	1.21E-03	3.95E-04	2.34E-04	2.63E-03	3.58E-04	2.26E-04
10	7.20E-04	3.52E-04	2.11E-04	1.32E-03	3.65E-04	1.10E-03
11	1.95E-03	9.24E-04	2.69E-04	3.51E-03	4.78E-04	3.59E-04
12	1.24E-03	2.18E-04	4.33E-05	4.07E-03	3.60E-04	2.27E-04
13	2.48E-03	1.35E-03	2.84E-04	3.19E-03	5.93E-04	3.25E-04
14	1.81E-03	7.51E-04	4.06E-04	4.08E-03	7.16E-04	1.46E-04
15	1.70E-03	4.50E-04	2.62E-04	4.02E-03	7.09E-04	1.28E-03
16	1.66E-03	3.58E-04	1.31E-04	4.02E-03	3.38E-04	3.22E-04
17	1.72E-03	3.89E-04	4.11E-04	4.02E-03	4.04E-04	1.54E-03
18	1.69E-03	4.94E-04	2.40E-04	4.07E-03	4.52E-04	3.35E-04
19	1.69E-03	4.39E-04	1.71E-04	4.07E-03	3.68E-04	4.41E-04
20	1.67E-03	3.92E-04	2.32E-04	4.06E-03	3.73E-04	6.27E-04
21	1.69E-03	5.67E-04	2.02E-04	4.06E-03	5.92E-04	4.67E-04
22	1.69E-03	3.82E-04	2.09E-04	4.04E-03	3.97E-04	3.49E-04
23	1.69E-03	5.75E-04	2.97E-04	4.07E-03	9.21E-04	1.75E-04
24	1.68E-03	4.45E-04	3.74E-04	4.08E-03	3.50E-04	1.52E-04
25	1.68E-03	4.44E-04	3.59E-04	4.09E-03	3.53E-04	9.41E-05
26	1.95E-03	9.03E-04	3.24E-04	3.49E-03	4.61E-04	2.07E-04
27	1.15E-03	2.70E-04	1.02E-05	3.97E-03	5.09E-04	5.08E-04
28	1.65E-03	4.70E-04	4.19E-04	4.17E-03	4.58E-04	3.99E-04
29	1.63E-03	5.96E-04	2.57E-04	4.07E-03	1.63E-03	2.08E-04
30	1.68E-03	7.45E-04	4.66E-04	4.02E-03	9.37E-04	6.01E-04
31	1.69E-03	4.66E-04	5.17E-04	4.05E-03	1.14E-03	9.92E-04
32	4.46E-03	1.78E-03	4.97E-04	1.63E-03	5.48E-04	3.53E-04
33	9.58E-04	1.89E-04	1.05E-04	4.61E-03	3.46E-04	1.67E-03
34	1.68E-03	5.77E-04	1.66E-04	4.02E-03	5.60E-04	6.05E-04
35	1.63E-03	4.41E-04	1.37E-04	4.20E-03	4.62E-04	3.35E-04
36	1.68E-03	4.62E-04	3.93E-04	4.08E-03	3.45E-04	3.75E-04
37	1.79E-03	7.83E-04	5.81E-04	4.02E-03	6.99E-04	5.07E-04
38	1.51E-03	3.66E-04	2.87E-04	4.13E-03	2.62E-04	3.27E-04
39	1.63E-03	4.67E-04	1.94E-04	4.14E-03	1.12E-03	1.72E-03
40	1.64E-03	6.99E-04	2.84E-04	4.11E-03	1.56E-03	3.03E-04

Table 4-9 Estimated surface concentrations (ppb) of NO and NO₂ at 20:00L at 5 km, 25 km, and 50 km downwind of the major point source for the 41 test simulations.

Run	NO			NO ₂		
	5 km	25 km	50 km	5 km	25 km	50 km
Baseline	5.79E-05	9.06E-05	6.32E-05	5.99E-03	3.33E-03	6.96E-04
1	8.41E-05	4.50E-05	6.23E-05	5.45E-03	3.12E-03	3.02E-03
2	6.77E-05	6.84E-05	5.26E-05	6.42E-03	2.28E-03	9.48E-04
3	6.34E-05	9.12E-05	6.13E-05	3.30E-03	2.62E-03	1.73E-03
4	5.14E-05	7.53E-05	9.13E-05	1.42E-02	4.83E-03	2.03E-03
5	5.80E-05	9.01E-05	6.03E-05	5.99E-03	3.28E-03	7.37E-04
6	5.80E-05	8.93E-05	5.87E-05	6.06E-03	3.33E-03	7.27E-04
7	5.81E-05	8.29E-05	6.86E-05	5.98E-03	3.29E-03	7.14E-04
8	5.80E-05	8.02E-05	7.45E-05	9.82E-03	4.65E-03	1.23E-03
9	5.79E-05	7.38E-05	7.43E-05	4.09E-03	2.55E-03	5.85E-04
10	5.78E-05	6.73E-05	6.65E-05	2.18E-03	1.87E-03	3.79E-04
11	5.79E-05	7.35E-05	5.38E-05	5.78E-03	3.29E-03	1.18E-03
12	7.69E-05	7.94E-05	5.92E-05	6.27E-03	3.18E-03	7.39E-04
13	5.73E-05	6.13E-05	6.01E-05	5.69E-03	3.24E-03	1.74E-03
14	5.79E-05	7.60E-05	6.77E-05	5.95E-03	3.25E-03	9.99E-04
15	6.41E-05	7.96E-05	5.43E-05	6.03E-03	3.27E-03	5.98E-04
16	5.79E-05	9.42E-05	5.76E-05	5.93E-03	3.29E-03	5.48E-04
17	5.79E-05	9.30E-05	8.10E-05	6.01E-03	3.30E-03	1.44E-03
18	5.78E-05	8.49E-05	7.89E-05	6.01E-03	3.36E-03	1.19E-03
19	5.79E-05	9.11E-05	5.34E-05	5.97E-03	3.37E-03	8.57E-04
20	5.79E-05	8.95E-05	9.08E-05	5.98E-03	3.32E-03	1.95E-03
21	5.79E-05	9.60E-05	5.90E-05	5.98E-03	3.38E-03	6.60E-04
22	5.79E-05	9.39E-05	7.46E-05	5.97E-03	3.37E-03	9.16E-04
23	5.79E-05	8.26E-05	6.19E-05	5.98E-03	3.36E-03	1.95E-03
24	5.79E-05	8.32E-05	6.13E-05	5.98E-03	3.38E-03	7.05E-04
25	5.79E-05	8.67E-05	5.46E-05	5.98E-03	3.37E-03	8.19E-04
26	5.53E-05	6.16E-05	6.38E-05	5.73E-03	3.36E-03	1.33E-03
27	7.31E-05	7.86E-05	1.06E-04	6.12E-03	3.35E-03	2.00E-03
28	5.80E-05	7.33E-05	7.03E-05	5.98E-03	3.29E-03	9.88E-04
29	5.79E-05	9.67E-05	7.34E-05	5.99E-03	3.37E-03	1.60E-03
30	6.80E-05	7.72E-05	8.54E-05	6.13E-03	3.36E-03	1.64E-03
31	5.73E-05	8.88E-05	7.51E-05	6.14E-03	3.37E-03	2.00E-03
32	1.16E-04	6.32E-05	8.16E-05	5.96E-03	3.69E-03	2.48E-03
33	5.80E-05	8.07E-05	5.98E-05	5.58E-03	2.89E-03	1.02E-03
34	5.79E-05	7.80E-05	6.98E-05	5.98E-03	3.28E-03	7.30E-04
35	5.79E-05	8.74E-05	6.10E-05	5.98E-03	3.39E-03	7.85E-04
36	6.12E-05	8.52E-05	5.55E-05	5.99E-03	3.43E-03	2.01E-03
37	5.78E-05	8.12E-05	5.95E-05	5.99E-03	3.36E-03	1.33E-03
38	6.31E-05	7.30E-05	7.17E-05	6.04E-03	3.12E-03	5.42E-04
39	5.79E-05	8.13E-05	6.90E-05	5.98E-03	3.34E-03	1.11E-03
40	5.80E-05	7.71E-05	6.63E-05	5.99E-03	3.31E-03	1.20E-03

Table 4-10. Estimated surface concentrations (ppb) of Ozone and H₂O₂ at 12:00L at 5 km, 25 km, and 50 km downwind of the major point source for the 41 test simulations.

Run	Ozone			H ₂ O ₂		
	5 km	25 km	50 km	5 km	25 km	50 km
Baseline	5.78E-02	8.57E-02	1.09E-01	2.94E-03	3.28E-03	4.07E-03
1	5.41E-02	7.26E-02	8.96E-02	3.00E-03	2.95E-03	3.44E-03
2	6.12E-02	9.72E-02	1.24E-01	2.91E-03	3.81E-03	5.03E-03
3	5.58E-02	8.03E-02	1.02E-01	2.99E-03	3.29E-03	4.29E-03
4	5.44E-02	8.13E-02	1.03E-01	2.94E-03	3.01E-03	3.57E-03
5	5.67E-02	8.59E-02	9.97E-02	2.94E-03	3.32E-03	4.59E-03
6	5.78E-02	8.61E-02	1.03E-01	2.94E-03	3.32E-03	4.26E-03
7	5.78E-02	8.64E-02	9.84E-02	2.94E-03	3.36E-03	4.52E-03
8	5.60E-02	8.72E-02	9.99E-02	2.94E-03	3.10E-03	3.85E-03
9	5.86E-02	8.23E-02	1.02E-01	2.95E-03	3.24E-03	3.93E-03
10	5.85E-02	8.11E-02	9.20E-02	2.99E-03	3.60E-03	4.92E-03
11	5.71E-02	8.27E-02	1.03E-01	2.96E-03	2.81E-03	3.23E-03
12	6.07E-02	9.13E-02	1.09E-01	2.95E-03	4.89E-03	6.79E-03
13	5.48E-02	7.78E-02	9.81E-02	2.96E-03	2.73E-03	2.89E-03
14	5.55E-02	8.07E-02	1.03E-01	2.95E-03	2.69E-03	2.95E-03
15	5.77E-02	8.69E-02	1.02E-01	2.94E-03	3.63E-03	4.99E-03
16	5.84E-02	8.56E-02	1.03E-01	2.95E-03	4.22E-03	5.67E-03
17	5.79E-02	8.62E-02	1.01E-01	2.94E-03	3.32E-03	4.14E-03
18	5.79E-02	8.62E-02	1.04E-01	2.94E-03	3.21E-03	3.91E-03
19	5.79E-02	8.62E-02	1.04E-01	2.94E-03	3.21E-03	3.91E-03
20	5.79E-02	8.62E-02	1.04E-01	2.94E-03	3.21E-03	3.91E-03
21	5.79E-02	8.62E-02	1.04E-01	2.94E-03	3.21E-03	3.91E-03
22	5.79E-02	8.62E-02	1.04E-01	2.94E-03	3.21E-03	3.91E-03
23	5.79E-02	8.62E-02	1.04E-01	2.94E-03	3.21E-03	3.91E-03
24	5.79E-02	8.62E-02	1.04E-01	2.94E-03	3.21E-03	3.91E-03
25	5.79E-02	8.62E-02	1.04E-01	2.94E-03	3.21E-03	3.91E-03
26	5.71E-02	8.26E-02	1.04E-01	2.94E-03	2.85E-03	3.32E-03
27	6.07E-02	9.16E-02	9.70E-02	2.95E-03	5.02E-03	7.93E-03
28	5.66E-02	8.32E-02	1.01E-01	8.86E-06	6.85E-04	1.94E-03
29	5.75E-02	8.82E-02	1.09E-01	9.75E-03	9.41E-03	9.78E-03
30	5.70E-02	8.54E-02	1.01E-01	2.94E-03	3.32E-03	4.33E-03
31	5.69E-02	8.55E-02	1.02E-01	2.95E-03	3.30E-03	4.26E-03
32	1.38E-02	5.20E-02	7.33E-02	2.94E-03	2.70E-03	3.55E-03
33	1.04E-01	1.25E-01	1.35E-01	2.96E-03	3.98E-03	5.46E-03
34	5.78E-02	8.58E-02	9.63E-02	2.94E-03	3.31E-03	4.67E-03
35	5.78E-02	8.58E-02	9.63E-02	2.94E-03	3.31E-03	4.67E-03
36	5.76E-02	8.33E-02	9.66E-02	2.94E-03	3.23E-03	4.68E-03
37	5.51E-02	7.52E-02	9.14E-02	2.93E-03	2.59E-03	2.93E-03
38	6.09E-02	9.41E-02	1.10E-01	2.98E-03	4.32E-03	6.26E-03
39	5.78E-02	8.63E-02	1.08E-01	2.94E-03	3.32E-03	4.18E-03
40	5.67E-02	8.60E-02	9.59E-02	2.94E-03	3.35E-03	4.71E-03

Table 4-11. Estimated surface concentrations (ppb) of Ozone and H₂O₂ at 16:00L at 5 km, 25 km, and 50 km downwind of the major point source for the 41 test simulations.

Run	Ozone			H2O2		
	5 km	25 km	50 km	5 km	25 km	50 km
Baseline	5.57E-02	8.12E-02	1.04E-01	2.96E-03	3.04E-03	4.29E-03
1	5.39E-02	6.71E-02	8.24E-02	2.99E-03	2.92E-03	3.06E-03
2	5.85E-02	1.00E-01	1.43E-01	2.93E-03	3.99E-03	6.85E-03
3	5.53E-02	7.60E-02	9.63E-02	2.98E-03	3.10E-03	4.07E-03
4	5.39E-02	7.60E-02	1.07E-01	2.96E-03	2.81E-03	4.12E-03
5	5.51E-02	8.09E-02	1.02E-01	2.96E-03	3.04E-03	4.35E-03
6	5.58E-02	8.12E-02	1.06E-01	2.97E-03	3.04E-03	4.21E-03
7	5.63E-02	8.01E-02	1.04E-01	2.96E-03	3.00E-03	4.17E-03
8	5.51E-02	8.01E-02	1.09E-01	2.97E-03	2.93E-03	4.12E-03
9	5.64E-02	7.95E-02	1.04E-01	2.97E-03	3.10E-03	4.24E-03
10	5.71E-02	7.85E-02	9.92E-02	2.98E-03	3.22E-03	4.50E-03
11	5.56E-02	7.78E-02	1.02E-01	2.97E-03	2.76E-03	3.36E-03
12	5.75E-02	8.64E-02	1.11E-01	2.95E-03	4.01E-03	7.78E-03
13	5.49E-02	7.35E-02	9.66E-02	2.97E-03	2.72E-03	2.88E-03
14	5.44E-02	7.54E-02	1.01E-01	2.96E-03	2.70E-03	2.86E-03
15	5.56E-02	7.98E-02	1.02E-01	2.96E-03	3.26E-03	4.83E-03
16	5.57E-02	8.21E-02	1.07E-01	2.97E-03	3.56E-03	6.15E-03
17	5.52E-02	8.19E-02	1.06E-01	2.97E-03	3.31E-03	4.31E-03
18	5.52E-02	8.33E-02	1.03E-01	2.77E-03	5.20E-03	7.43E-03
19	5.52E-02	8.32E-02	1.01E-01	2.77E-03	5.20E-03	7.37E-03
20	5.58E-02	8.22E-02	1.06E-01	3.08E-03	1.03E-02	1.41E-02
21	5.59E-02	8.22E-02	1.07E-01	2.99E-03	3.16E-03	4.56E-03
22	5.59E-02	8.17E-02	1.06E-01	3.17E-03	1.22E-02	1.77E-02
23	5.52E-02	8.16E-02	1.04E-01	2.77E-03	3.79E-03	4.42E-03
24	5.51E-02	8.31E-02	1.08E-01	2.78E-03	2.38E-03	2.53E-03
25	5.51E-02	8.31E-02	1.08E-01	2.83E-03	1.95E-03	1.92E-03
26	5.55E-02	7.92E-02	1.03E-01	2.97E-03	2.80E-03	3.51E-03
27	5.76E-02	8.81E-02	9.80E-02	2.20E-03	6.73E-03	1.23E-02
28	5.48E-02	8.14E-02	1.08E-01	4.33E-05	2.94E-03	5.00E-03
29	5.56E-02	8.03E-02	1.13E-01	9.93E-03	1.08E-02	1.24E-02
30	5.56E-02	8.03E-02	1.07E-01	1.66E-03	2.89E-03	4.30E-03
31	5.65E-02	8.09E-02	1.06E-01	3.04E-03	4.66E-03	7.05E-03
32	1.20E-02	4.62E-02	8.37E-02	2.99E-03	3.80E-03	6.16E-03
33	1.01E-01	1.22E-01	1.36E-01	2.79E-03	6.41E-03	8.06E-03
34	5.56E-02	8.22E-02	1.08E-01	1.89E-03	4.84E-03	7.54E-03
35	5.48E-02	8.28E-02	1.08E-01	3.01E-03	5.37E-03	8.00E-03
36	5.59E-02	8.29E-02	1.08E-01	3.06E-03	6.34E-03	8.00E-03
37	5.39E-02	7.11E-02	9.56E-02	2.72E-03	3.65E-03	4.91E-03
38	5.71E-02	9.09E-02	1.18E-01	2.82E-03	7.06E-03	1.00E-02
39	5.57E-02	8.13E-02	1.06E-01	3.03E-03	5.09E-03	7.23E-03
40	5.51E-02	7.74E-02	1.04E-01	2.20E-03	4.20E-03	7.25E-03

Table 4-12. Estimated surface concentrations (ppb) of Ozone and H₂O₂ at 20:00L at 5 km, 25 km, and 50 km downwind of the major point source for the 41 test simulations.

Run	Ozone			H ₂ O ₂		
	5 km	25 km	50 km	5 km	25 km	50 km
Baseline	5.35E-02	5.36E-02	6.61E-02	3.00E-03	3.01E-03	2.94E-03
1	5.36E-02	5.28E-02	5.31E-02	3.00E-03	3.02E-03	3.01E-03
2	5.30E-02	6.13E-02	1.05E-01	3.01E-03	3.04E-03	4.58E-03
3	5.38E-02	5.40E-02	6.43E-02	3.00E-03	3.00E-03	3.02E-03
4	5.31E-02	5.20E-02	6.31E-02	3.00E-03	3.01E-03	2.91E-03
5	5.35E-02	5.35E-02	6.61E-02	3.00E-03	3.02E-03	2.94E-03
6	5.35E-02	5.36E-02	6.61E-02	3.00E-03	3.01E-03	2.94E-03
7	5.34E-02	5.35E-02	6.64E-02	3.00E-03	3.02E-03	2.94E-03
8	5.35E-02	5.30E-02	6.58E-02	3.00E-03	3.01E-03	2.88E-03
9	5.35E-02	5.36E-02	6.59E-02	3.00E-03	3.02E-03	2.98E-03
10	5.36E-02	5.39E-02	6.55E-02	3.00E-03	3.02E-03	3.03E-03
11	5.36E-02	5.35E-02	6.33E-02	3.00E-03	3.01E-03	2.87E-03
12	5.37E-02	5.37E-02	6.89E-02	3.00E-03	3.01E-03	3.20E-03
13	5.37E-02	5.32E-02	6.13E-02	3.00E-03	3.01E-03	2.88E-03
14	5.31E-02	5.29E-02	6.35E-02	3.00E-03	3.01E-03	2.84E-03
15	5.33E-02	5.31E-02	6.65E-02	3.00E-03	3.01E-03	3.02E-03
16	5.31E-02	5.34E-02	6.71E-02	3.00E-03	3.01E-03	3.09E-03
17	5.35E-02	5.36E-02	6.34E-02	3.00E-03	3.01E-03	2.98E-03
18	5.35E-02	5.31E-02	6.59E-02	3.00E-03	3.01E-03	3.86E-03
19	5.35E-02	5.34E-02	6.63E-02	3.00E-03	3.01E-03	4.05E-03
20	5.35E-02	5.33E-02	6.68E-02	3.00E-03	2.96E-03	6.46E-03
21	5.35E-02	5.40E-02	6.71E-02	3.00E-03	3.01E-03	2.97E-03
22	5.35E-02	5.37E-02	6.64E-02	3.00E-03	3.00E-03	7.45E-03
23	5.35E-02	5.33E-02	6.41E-02	3.00E-03	3.01E-03	3.25E-03
24	5.35E-02	5.33E-02	6.63E-02	3.00E-03	3.01E-03	3.02E-03
25	5.35E-02	5.34E-02	6.64E-02	3.00E-03	3.01E-03	2.94E-03
26	5.36E-02	5.32E-02	6.27E-02	3.00E-03	3.02E-03	3.44E-03
27	5.33E-02	5.38E-02	6.71E-02	3.00E-03	3.01E-03	3.86E-03
28	5.35E-02	5.29E-02	6.59E-02	5.07E-06	2.44E-05	1.44E-03
29	5.35E-02	5.40E-02	6.84E-02	1.00E-02	9.98E-03	1.03E-02
30	5.37E-02	5.34E-02	6.58E-02	3.00E-03	3.01E-03	3.01E-03
31	5.34E-02	5.34E-02	6.43E-02	3.00E-03	3.01E-03	3.76E-03
32	7.47E-03	8.98E-03	2.46E-02	3.00E-03	3.00E-03	3.18E-03
33	9.88E-02	9.87E-02	1.08E-01	3.01E-03	3.03E-03	4.52E-03
34	5.35E-02	5.33E-02	6.65E-02	3.00E-03	3.01E-03	3.87E-03
35	5.35E-02	5.34E-02	6.66E-02	3.00E-03	3.01E-03	4.07E-03
36	5.31E-02	5.38E-02	6.61E-02	3.00E-03	3.01E-03	4.51E-03
37	5.35E-02	5.35E-02	5.98E-02	3.00E-03	2.96E-03	3.15E-03
38	5.34E-02	5.36E-02	7.21E-02	3.01E-03	3.03E-03	5.33E-03
39	5.34E-02	5.34E-02	6.68E-02	3.00E-03	3.01E-03	4.15E-03
40	5.33E-02	5.32E-02	6.66E-02	3.00E-03	3.01E-03	3.97E-03

Table 4-13. Estimated surface concentrations (ppb) of HNO₃ and NH₃ at 12:00L at 5 km, 25 km, and 50 km downwind of the major point source for the 41 test simulations.

Run	HNO ₃			NH ₃		
	5 km	25 km	50 km	5 km	25 km	50 km
Baseline	3.19E-04	9.74E-04	1.33E-03	5.02E-03	4.59E-03	4.81E-03
1	2.68E-04	7.33E-04	9.61E-04	5.23E-03	4.83E-03	4.49E-03
2	5.71E-04	1.19E-03	1.68E-03	4.85E-03	4.56E-03	4.47E-03
3	1.94E-04	2.14E-04	1.40E-04	5.18E-03	4.37E-03	3.95E-03
4	5.77E-04	1.82E-03	2.35E-03	5.19E-03	5.14E-03	5.13E-03
5	3.26E-04	9.77E-04	1.13E-03	4.99E-03	4.36E-03	4.29E-03
6	3.19E-04	1.00E-03	1.22E-03	5.03E-03	4.51E-03	4.38E-03
7	3.19E-04	1.01E-03	1.13E-03	5.05E-03	4.55E-03	4.50E-03
8	3.63E-04	1.19E-03	1.32E-03	4.99E-03	4.45E-03	5.15E-03
9	3.00E-04	8.00E-04	1.16E-03	5.03E-03	4.88E-03	4.57E-03
10	2.35E-04	6.73E-04	8.53E-04	5.15E-03	4.67E-03	4.54E-03
11	2.19E-05	1.06E-05	1.81E-06	4.79E-03	3.75E-03	3.95E-03
12	7.93E-04	2.02E-03	2.53E-03	5.18E-03	5.10E-03	5.12E-03
13	1.74E-06	1.23E-06	8.08E-07	4.85E-03	4.10E-03	3.52E-03
14	3.67E-04	1.38E-03	2.04E-03	5.22E-03	5.17E-03	5.21E-03
15	9.22E-05	1.21E-04	1.34E-04	4.65E-03	4.06E-03	4.76E-03
16	3.01E-05	2.82E-05	3.00E-05	4.32E-03	3.24E-03	4.46E-03
17	3.21E-04	9.93E-04	1.16E-03	5.01E-03	4.46E-03	4.40E-03
18	3.21E-04	9.76E-04	1.24E-03	5.01E-03	4.69E-03	4.36E-03
19	3.21E-04	9.76E-04	1.24E-03	5.01E-03	4.69E-03	4.36E-03
20	3.21E-04	9.76E-04	1.24E-03	5.01E-03	4.69E-03	4.36E-03
21	3.21E-04	9.76E-04	1.24E-03	5.01E-03	4.69E-03	4.36E-03
22	3.21E-04	9.76E-04	1.24E-03	5.01E-03	4.69E-03	4.36E-03
23	3.21E-04	9.76E-04	1.24E-03	5.01E-03	4.69E-03	4.36E-03
24	3.21E-04	9.76E-04	1.24E-03	5.01E-03	4.69E-03	4.36E-03
25	3.21E-04	9.76E-04	1.24E-03	5.01E-03	4.69E-03	4.36E-03
26	2.09E-05	1.19E-05	7.37E-06	4.73E-03	3.89E-03	3.93E-03
27	7.92E-04	2.03E-03	2.09E-03	5.18E-03	5.08E-03	5.09E-03
28	3.10E-04	9.33E-04	1.15E-03	5.03E-03	4.53E-03	5.01E-03
29	3.74E-04	1.02E-03	1.33E-03	4.97E-03	4.70E-03	4.42E-03
30	5.12E-04	1.66E-03	2.01E-03	3.07E-04	2.35E-04	2.41E-04
31	1.11E-04	9.63E-05	1.03E-04	2.47E-02	2.35E-02	2.31E-02
32	2.02E-04	8.01E-04	9.66E-04	5.11E-03	4.59E-03	4.46E-03
33	4.34E-04	1.07E-03	1.31E-03	4.98E-03	4.46E-03	4.52E-03
34	3.19E-04	9.75E-04	1.07E-03	5.02E-03	4.58E-03	4.49E-03
35	3.19E-04	9.75E-04	1.07E-03	5.02E-03	4.58E-03	4.49E-03
36	0.00E+00	0.00E+00	0.00E+00	5.70E-03	5.70E-03	5.70E-03
37	3.24E-04	1.43E-03	1.92E-03	5.01E-03	4.11E-03	3.90E-03
38	3.27E-04	6.97E-04	8.43E-04	5.02E-03	4.70E-03	4.83E-03
39	3.19E-04	1.01E-03	1.32E-03	5.05E-03	4.56E-03	4.37E-03
40	3.26E-04	9.77E-04	1.05E-03	4.99E-03	4.36E-03	4.36E-03

Table 4-14. Estimated surface concentrations (ppb) of HNO₃ and NH₃ at 16:00L at 5 km, 25 km, and 50 km downwind of the major point source for the 41 test simulations.

Run	HNO ₃			NH ₃		
	5 km	25 km	50 km	5 km	25 km	50 km
Baseline	2.41E-04	8.97E-04	1.24E-03	5.09E-03	4.54E-03	4.26E-03
1	2.43E-04	5.80E-04	8.38E-04	5.21E-03	5.03E-03	4.84E-03
2	4.19E-04	1.25E-03	1.81E-03	4.96E-03	4.37E-03	4.49E-03
3	1.56E-04	1.81E-04	1.36E-04	5.09E-03	4.33E-03	4.15E-03
4	4.27E-04	1.62E-03	2.49E-03	5.21E-03	5.11E-03	5.07E-03
5	2.43E-04	8.82E-04	1.16E-03	5.07E-03	4.46E-03	4.53E-03
6	2.39E-04	9.06E-04	1.30E-03	5.12E-03	4.58E-03	4.38E-03
7	2.41E-04	8.90E-04	1.24E-03	5.12E-03	4.92E-03	5.14E-03
8	2.59E-04	1.01E-03	1.43E-03	5.09E-03	4.71E-03	4.37E-03
9	2.26E-04	7.55E-04	1.19E-03	5.12E-03	4.64E-03	4.33E-03
10	2.02E-04	6.44E-04	9.84E-04	5.11E-03	4.75E-03	4.65E-03
11	2.22E-05	6.36E-06	5.69E-06	4.85E-03	3.81E-03	3.84E-03
12	5.15E-04	1.81E-03	2.61E-03	5.22E-03	5.11E-03	5.07E-03
13	1.63E-06	1.02E-06	8.87E-07	4.89E-03	4.10E-03	3.50E-03
14	3.12E-04	1.21E-03	1.96E-03	5.23E-03	5.18E-03	5.15E-03
15	7.96E-05	1.12E-04	1.30E-04	4.81E-03	4.15E-03	3.83E-03
16	3.35E-05	2.74E-05	2.58E-05	4.72E-03	3.34E-03	3.82E-03
17	1.39E-04	4.03E-04	1.80E-04	4.96E-03	3.86E-03	4.26E-03
18	4.06E-05	2.94E-05	3.05E-05	4.12E-03	2.61E-03	1.14E-03
19	5.65E-05	4.12E-05	4.98E-05	4.11E-03	1.67E-03	1.30E-03
20	3.51E-05	3.01E-05	3.88E-05	4.14E-03	2.55E-03	1.84E-03
21	3.23E-05	3.13E-05	3.56E-05	4.15E-03	3.24E-03	1.87E-03
22	4.53E-05	4.43E-05	4.82E-05	4.10E-03	2.20E-03	1.99E-03
23	4.08E-05	3.78E-05	3.04E-05	4.15E-03	3.26E-03	9.62E-04
24	4.13E-05	2.88E-05	3.14E-05	4.27E-03	1.68E-03	1.92E-03
25	4.17E-05	2.88E-05	2.97E-05	4.39E-03	1.67E-03	1.89E-03
26	1.25E-06	1.03E-06	1.06E-06	4.14E-03	1.65E-03	1.80E-03
27	1.20E-04	9.90E-05	1.22E-04	2.21E-03	3.16E-03	1.28E-03
28	6.59E-05	4.08E-05	3.81E-05	4.19E-03	1.74E-03	3.14E-03
29	5.61E-05	6.22E-05	4.07E-05	4.54E-03	4.73E-03	2.08E-03
30	1.21E-04	1.17E-04	9.58E-05	2.19E-04	2.09E-04	1.71E-04
31	1.15E-05	1.49E-05	1.12E-05	2.40E-02	2.16E-02	2.22E-02
32	5.94E-05	4.06E-05	4.58E-05	4.63E-03	2.87E-03	1.41E-03
33	5.64E-05	4.02E-05	6.52E-05	4.04E-03	2.62E-03	4.69E-03
34	4.97E-05	4.48E-05	5.78E-05	2.43E-03	3.15E-03	1.80E-03
35	7.16E-05	4.22E-05	4.70E-05	5.01E-03	2.26E-03	1.55E-03
36	4.30E-18	0.00E+00	0.00E+00	8.56E-03	5.58E-03	5.63E-03
37	5.66E-05	4.29E-05	3.84E-05	4.14E-03	1.95E-03	2.95E-03
38	5.63E-05	4.08E-05	3.94E-05	4.08E-03	2.05E-03	3.38E-03
39	6.09E-05	5.69E-05	6.57E-05	4.77E-03	3.76E-03	4.73E-03
40	6.41E-05	5.89E-05	4.16E-05	3.81E-03	4.39E-03	9.25E-04

Table 4-15. Estimated surface concentrations (ppb) of HNO₃ and NH₃ at 20:00L at 5 km, 25 km, and 50 km downwind of the major point source for the 41 test simulations.

Run	HNO ₃			NH ₃		
	5 km	25 km	50 km	5 km	25 km	50 km
Baseline	1.76E-04	2.18E-04	8.31E-04	5.16E-03	5.18E-03	4.63E-03
1	2.05E-04	2.56E-04	2.54E-04	5.24E-03	5.12E-03	5.03E-03
2	2.27E-04	6.24E-04	1.61E-03	5.15E-03	5.08E-03	4.76E-03
3	1.48E-04	1.82E-04	9.68E-05	5.14E-03	5.16E-03	4.81E-03
4	3.16E-04	4.47E-04	1.33E-03	5.24E-03	5.23E-03	5.19E-03
5	1.75E-04	2.23E-04	8.25E-04	5.16E-03	5.17E-03	4.59E-03
6	1.74E-04	2.18E-04	8.31E-04	5.16E-03	5.18E-03	4.66E-03
7	1.73E-04	2.26E-04	8.28E-04	5.15E-03	5.17E-03	4.67E-03
8	1.79E-04	2.36E-04	9.31E-04	5.15E-03	5.14E-03	4.58E-03
9	1.61E-04	2.29E-04	7.38E-04	5.16E-03	5.14E-03	4.69E-03
10	1.50E-04	2.27E-04	6.70E-04	5.16E-03	5.12E-03	4.73E-03
11	2.15E-05	2.31E-05	4.85E-06	4.94E-03	4.87E-03	3.98E-03
12	2.60E-04	4.26E-04	1.55E-03	5.25E-03	5.25E-03	5.19E-03
13	1.75E-06	1.63E-06	1.37E-06	4.98E-03	4.89E-03	4.38E-03
14	2.23E-04	3.32E-04	1.18E-03	5.24E-03	5.24E-03	5.21E-03
15	8.64E-05	1.06E-04	1.00E-04	5.00E-03	4.82E-03	3.92E-03
16	3.01E-05	4.88E-05	2.98E-05	4.76E-03	4.75E-03	3.35E-03
17	1.75E-04	2.11E-04	6.69E-04	5.16E-03	5.16E-03	4.84E-03
18	1.75E-04	2.04E-04	5.88E-04	5.16E-03	5.13E-03	4.47E-03
19	1.72E-04	2.08E-04	6.04E-04	5.15E-03	5.15E-03	4.36E-03
20	1.70E-04	2.34E-04	5.86E-04	5.15E-03	4.91E-03	5.08E-03
21	1.70E-04	2.44E-04	6.13E-04	5.15E-03	5.23E-03	3.73E-03
22	1.72E-04	2.48E-04	6.21E-04	5.15E-03	5.07E-03	3.37E-03
23	1.73E-04	2.11E-04	4.75E-04	5.15E-03	5.13E-03	5.03E-03
24	1.73E-04	2.06E-04	5.58E-04	5.15E-03	5.14E-03	3.88E-03
25	1.70E-04	2.06E-04	4.91E-04	5.15E-03	5.14E-03	3.94E-03
26	3.21E-05	1.44E-04	4.57E-04	5.00E-03	4.99E-03	4.02E-03
27	2.79E-04	3.54E-04	1.40E-03	5.25E-03	5.25E-03	5.74E-03
28	1.71E-04	2.33E-04	5.83E-04	5.15E-03	5.11E-03	4.36E-03
29	1.71E-04	2.08E-04	5.69E-04	5.15E-03	5.23E-03	4.95E-03
30	2.37E-04	3.40E-04	1.74E-03	3.39E-04	3.42E-04	1.34E-04
31	9.37E-05	1.51E-04	1.08E-04	2.48E-02	2.49E-02	2.48E-02
32	1.49E-04	1.84E-04	4.58E-04	5.17E-03	5.19E-03	4.64E-03
33	2.12E-04	2.69E-04	6.58E-04	5.11E-03	5.07E-03	4.96E-03
34	1.70E-04	2.40E-04	6.24E-04	5.15E-03	5.12E-03	3.83E-03
35	1.70E-04	2.08E-04	6.12E-04	5.15E-03	5.15E-03	3.95E-03
36	0.00E+00	2.38E-10	5.10E-18	5.70E-03	6.11E-03	6.62E-03
37	1.71E-04	2.32E-04	5.56E-04	5.16E-03	4.94E-03	3.94E-03
38	1.71E-04	2.67E-04	6.04E-04	5.15E-03	4.97E-03	3.90E-03
39	1.71E-04	2.09E-04	8.25E-04	5.15E-03	5.15E-03	4.39E-03
40	1.71E-04	2.40E-04	5.49E-04	5.15E-03	5.13E-03	4.45E-03

Table 4-16. Estimated surface concentrations ($\mu\text{g}/\text{m}^3$) of sulfate aerosol particle at 12:00L at 5 km, 25 km, and 50 km downwind of the major point source for the 41 test simulations.

Run	Sulfate		
	5 km	25 km	50 km
Baseline	1.06E+00	1.18E+00	1.19E+00
1	1.02E+00	1.09E+00	1.13E+00
2	1.16E+00	1.25E+00	1.20E+00
3	1.02E+00	1.09E+00	1.13E+00
4	1.10E+00	1.31E+00	1.32E+00
5	1.12E+00	1.36E+00	1.35E+00
6	1.03E+00	1.11E+00	1.12E+00
7	1.01E+00	1.03E+00	1.04E+00
8	1.05E+00	1.18E+00	1.19E+00
9	1.08E+00	1.17E+00	1.18E+00
10	1.08E+00	1.18E+00	1.18E+00
11	1.04E+00	1.13E+00	1.13E+00
12	1.12E+00	1.27E+00	1.24E+00
13	1.04E+00	1.12E+00	1.15E+00
14	1.04E+00	1.13E+00	1.16E+00
15	1.08E+00	1.19E+00	1.19E+00
16	1.10E+00	1.23E+00	1.22E+00
17	1.06E+00	1.19E+00	1.19E+00
18	1.06E+00	1.18E+00	1.18E+00
19	1.06E+00	1.18E+00	1.18E+00
20	1.06E+00	1.18E+00	1.18E+00
21	1.06E+00	1.18E+00	1.18E+00
22	1.06E+00	1.18E+00	1.18E+00
23	1.06E+00	1.18E+00	1.18E+00
24	1.06E+00	1.18E+00	1.18E+00
25	1.06E+00	1.18E+00	1.18E+00
26	1.04E+00	1.12E+00	1.14E+00
27	1.12E+00	1.27E+00	1.25E+00
28	1.06E+00	1.17E+00	1.19E+00
29	1.08E+00	1.20E+00	1.21E+00
30	1.06E+00	1.19E+00	1.19E+00
31	1.05E+00	1.21E+00	1.24E+00
32	1.04E+00	1.19E+00	1.21E+00
33	1.09E+00	1.19E+00	1.20E+00
34	1.06E+00	1.19E+00	1.19E+00
35	1.06E+00	1.19E+00	1.19E+00
36	1.01E+00	1.13E+00	1.15E+00
37	1.06E+00	1.29E+00	1.34E+00
38	1.06E+00	1.12E+00	1.11E+00
39	1.01E+00	1.03E+00	1.03E+00
40	1.12E+00	1.36E+00	1.35E+00

Table 4-17. Estimated surface concentrations ($\mu\text{g}/\text{m}^3$) of sulfate aerosol particle at 14:00L at 5 km, 25 km, and 50 km downwind of the major point source for the 41 test simulations.

Run	Sulfate		
	5 km	25 km	50 km
Baseline	1.06E+00	1.20E+00	1.23E+00
1	1.02E+00	1.08E+00	1.11E+00
2	1.14E+00	1.31E+00	1.31E+00
3	1.02E+00	1.09E+00	1.14E+00
4	1.11E+00	1.33E+00	1.46E+00
5	1.12E+00	1.37E+00	1.43E+00
6	1.03E+00	1.11E+00	1.14E+00
7	1.01E+00	1.02E+00	1.04E+00
8	1.05E+00	1.16E+00	1.25E+00
9	1.07E+00	1.19E+00	1.22E+00
10	1.08E+00	1.19E+00	1.22E+00
11	1.04E+00	1.14E+00	1.16E+00
12	1.11E+00	1.28E+00	1.30E+00
13	1.03E+00	1.12E+00	1.18E+00
14	1.03E+00	1.14E+00	1.19E+00
15	1.07E+00	1.22E+00	1.24E+00
16	1.09E+00	1.23E+00	1.27E+00
17	1.06E+00	1.20E+00	1.24E+00
18	1.06E+00	1.20E+00	1.23E+00
19	1.06E+00	1.20E+00	1.23E+00
20	1.06E+00	1.20E+00	1.23E+00
21	1.06E+00	1.20E+00	1.23E+00
22	1.06E+00	1.20E+00	1.23E+00
23	1.06E+00	1.20E+00	1.23E+00
24	1.06E+00	1.20E+00	1.23E+00
25	1.06E+00	1.20E+00	1.23E+00
26	1.04E+00	1.15E+00	1.16E+00
27	1.11E+00	1.29E+00	1.30E+00
28	1.05E+00	1.19E+00	1.21E+00
29	1.08E+00	1.20E+00	1.25E+00
30	1.06E+00	1.21E+00	1.24E+00
31	1.05E+00	1.21E+00	1.26E+00
32	1.04E+00	1.20E+00	1.25E+00
33	1.08E+00	1.20E+00	1.23E+00
34	1.06E+00	1.19E+00	1.24E+00
35	1.06E+00	1.19E+00	1.24E+00
36	1.06E+00	1.10E+00	1.09E+00
37	1.06E+00	1.30E+00	1.40E+00
38	1.06E+00	1.12E+00	1.13E+00
39	1.01E+00	1.02E+00	1.07E+00
40	1.12E+00	1.38E+00	1.43E+00

Table 4-18. Estimated surface concentrations ($\mu\text{g}/\text{m}^3$) of sulfate aerosol particle at 16:00L at 5 km, 25 km, and 50 km downwind of the major point source for the 41 test simulations.

Run	Sulfate		
	5 km	25 km	50 km
Baseline	1.03E+00	1.16E+00	1.23E+00
1	1.01E+00	1.06E+00	1.10E+00
2	1.10E+00	1.33E+00	1.36E+00
3	1.02E+00	1.08E+00	1.12E+00
4	1.06E+00	1.26E+00	1.41E+00
5	1.07E+00	1.31E+00	1.43E+00
6	1.02E+00	1.09E+00	1.14E+00
7	1.00E+00	1.02E+00	1.04E+00
8	1.03E+00	1.14E+00	1.22E+00
9	1.04E+00	1.16E+00	1.22E+00
10	1.05E+00	1.15E+00	1.22E+00
11	1.02E+00	1.12E+00	1.18E+00
12	1.06E+00	1.22E+00	1.32E+00
13	1.02E+00	1.08E+00	1.18E+00
14	1.02E+00	1.11E+00	1.18E+00
15	1.04E+00	1.17E+00	1.23E+00
16	1.05E+00	1.20E+00	1.27E+00
17	1.04E+00	1.18E+00	1.22E+00
18	1.60E+01	8.18E+00	6.41E+00
19	1.60E+01	7.92E+00	6.03E+00
20	1.98E+01	7.92E+00	6.25E+00
21	1.66E+01	8.44E+00	6.43E+00
22	1.75E+01	7.83E+00	6.09E+00
23	1.54E+01	7.24E+00	5.87E+00
24	1.37E+01	4.52E+00	3.70E+00
25	1.34E+01	4.22E+00	3.56E+00
26	1.57E+01	8.15E+00	6.13E+00
27	1.12E+01	6.99E+00	5.71E+00
28	1.54E+01	7.83E+00	6.21E+00
29	1.60E+01	8.17E+00	5.68E+00
30	8.70E+00	6.80E+00	5.44E+00
31	1.67E+01	5.38E+00	9.32E+00
32	1.58E+01	8.21E+00	6.30E+00
33	1.60E+01	7.81E+00	5.88E+00
34	1.18E+01	7.84E+00	5.84E+00
35	1.61E+01	7.85E+00	5.91E+00
36	1.70E+01	8.06E+00	5.97E+00
37	1.60E+01	8.96E+00	6.23E+00
38	1.60E+01	8.23E+00	6.08E+00
39	2.27E+00	2.53E+00	2.40E+00
40	2.47E+01	1.38E+01	9.56E+00

Table 4-19. Estimated surface concentrations ($\mu\text{g}/\text{m}^3$) of sulfate aerosol particle at 18:00L at 5 km, 25 km, and 50 km downwind of the major point source for the 41 test simulations.

Run	Sulfate		
	5 km	25 km	50 km
Baseline	1.03E+00	1.16E+00	1.23E+00
1	1.01E+00	1.06E+00	1.10E+00
2	1.10E+00	1.33E+00	1.36E+00
3	1.02E+00	1.08E+00	1.12E+00
4	1.06E+00	1.26E+00	1.41E+00
5	1.07E+00	1.31E+00	1.43E+00
6	1.02E+00	1.09E+00	1.14E+00
7	1.00E+00	1.02E+00	1.04E+00
8	1.03E+00	1.14E+00	1.22E+00
9	1.04E+00	1.16E+00	1.22E+00
10	1.05E+00	1.15E+00	1.22E+00
11	1.02E+00	1.12E+00	1.18E+00
12	1.06E+00	1.22E+00	1.32E+00
13	1.02E+00	1.08E+00	1.18E+00
14	1.02E+00	1.11E+00	1.18E+00
15	1.04E+00	1.17E+00	1.23E+00
16	1.05E+00	1.20E+00	1.27E+00
17	1.04E+00	1.18E+00	1.22E+00
18	1.60E+01	8.18E+00	6.41E+00
19	1.60E+01	7.92E+00	6.03E+00
20	1.98E+01	7.92E+00	6.25E+00
21	1.66E+01	8.44E+00	6.43E+00
22	1.75E+01	7.83E+00	6.09E+00
23	1.54E+01	7.24E+00	5.87E+00
24	1.37E+01	4.52E+00	3.70E+00
25	1.34E+01	4.22E+00	3.56E+00
26	1.57E+01	8.15E+00	6.13E+00
27	1.12E+01	6.99E+00	5.71E+00
28	1.54E+01	7.83E+00	6.21E+00
29	1.60E+01	8.17E+00	5.68E+00
30	8.70E+00	6.80E+00	5.44E+00
31	1.67E+01	5.38E+00	9.32E+00
32	1.58E+01	8.21E+00	6.30E+00
33	1.60E+01	7.81E+00	5.88E+00
34	1.18E+01	7.84E+00	5.84E+00
35	1.61E+01	7.85E+00	5.91E+00
36	1.70E+01	8.06E+00	5.97E+00
37	1.60E+01	8.96E+00	6.23E+00
38	1.60E+01	8.23E+00	6.08E+00
39	2.27E+00	2.53E+00	2.40E+00
40	2.47E+01	1.38E+01	9.56E+00

Table 4-20. Estimated surface concentrations ($\mu\text{g}/\text{m}^3$) of sulfate aerosol particle at 20:00L at 5 km, 25 km, and 50 km downwind of the major point source for the 41 test simulations.

Run	Sulfate		
	5 km	25 km	50 km
Baseline	1.00E+00	1.01E+00	1.07E+00
1	1.00E+00	1.00E+00	1.01E+00
2	1.01E+00	1.09E+00	1.30E+00
3	1.00E+00	1.01E+00	1.04E+00
4	1.01E+00	1.02E+00	1.12E+00
5	1.01E+00	1.02E+00	1.14E+00
6	1.00E+00	1.01E+00	1.04E+00
7	1.00E+00	1.00E+00	1.01E+00
8	1.00E+00	1.01E+00	1.07E+00
9	1.00E+00	1.01E+00	1.08E+00
10	1.00E+00	1.01E+00	1.08E+00
11	1.00E+00	1.01E+00	1.01E+00
12	1.00E+00	1.01E+00	1.10E+00
13	1.00E+00	1.01E+00	1.04E+00
14	1.00E+00	1.01E+00	1.06E+00
15	1.00E+00	1.01E+00	1.07E+00
16	1.00E+00	1.01E+00	1.09E+00
17	1.00E+00	1.01E+00	1.06E+00
18	1.00E+00	2.70E+00	5.97E+00
19	1.00E+00	2.69E+00	5.68E+00
20	1.00E+00	4.52E+00	6.32E+00
21	1.00E+00	4.51E+00	5.89E+00
22	1.00E+00	6.98E+00	7.21E+00
23	1.00E+00	2.66E+00	5.42E+00
24	1.00E+00	2.53E+00	2.60E+00
25	1.00E+00	2.27E+00	2.06E+00
26	1.00E+00	2.84E+00	6.85E+00
27	1.00E+00	2.03E+00	5.28E+00
28	1.00E+00	2.64E+00	5.68E+00
29	1.00E+00	2.85E+00	5.86E+00
30	1.00E+00	1.73E+00	5.07E+00
31	1.01E+00	3.34E+00	6.59E+00
32	1.00E+00	2.71E+00	6.61E+00
33	1.01E+00	2.68E+00	5.95E+00
34	1.00E+00	2.01E+00	5.52E+00
35	1.00E+00	2.80E+00	5.83E+00
36	9.13E-01	3.10E+00	6.14E+00
37	1.00E+00	2.70E+00	6.17E+00
38	1.00E+00	2.69E+00	5.69E+00
39	1.00E+00	1.11E+00	2.38E+00
40	1.01E+00	3.42E+00	9.30E+00

Table 4-21. Estimated surface concentrations ($\mu\text{g}/\text{m}^3$) of nitrate and ammonium aerosol particles at 12:00L at 5 km, 25 km, and 50 km downwind of the major point source for the 41 test simulations.

Run	Nitrate			Ammonium		
	5 km	25 km	50 km	5 km	25 km	50 km
Baseline	4.54E-01	1.65E+00	2.52E+00	4.99E-01	9.00E-01	1.16E+00
1	6.81E-03	8.90E-01	1.67E+00	3.49E-01	6.37E-01	8.84E-01
2	8.07E-01	2.18E+00	3.34E+00	6.36E-01	1.08E+00	1.40E+00
3	3.85E-01	2.51E+00	4.19E+00	4.64E-01	1.14E+00	1.66E+00
4	3.97E-03	1.96E-02	2.61E-02	3.80E-01	4.61E-01	4.66E-01
5	4.52E-01	1.71E+00	2.01E+00	5.20E-01	9.80E-01	1.07E+00
6	4.53E-01	1.65E+00	2.09E+00	4.87E-01	8.70E-01	1.00E+00
7	4.53E-01	1.64E+00	1.88E+00	4.75E-01	8.35E-01	9.08E-01
8	5.31E-01	2.10E+00	2.36E+00	5.16E-01	1.03E+00	1.10E+00
9	4.01E-01	1.36E+00	2.04E+00	4.90E-01	8.03E-01	1.01E+00
10	3.01E-01	1.14E+00	1.44E+00	4.60E-01	7.49E-01	8.39E-01
11	1.12E+00	3.86E+00	5.60E+00	7.42E-01	1.61E+00	2.18E+00
12	1.79E-02	5.39E-02	6.63E-02	3.88E-01	4.50E-01	4.45E-01
13	8.55E-01	3.31E+00	4.79E+00	6.37E-01	1.38E+00	1.83E+00
14	0.00E+00	5.68E-11	7.76E-08	3.53E-01	3.89E-01	3.98E-01
15	1.29E+00	4.06E+00	5.00E+00	7.75E-01	1.67E+00	1.98E+00
16	1.95E+00	4.74E+00	6.36E+00	1.03E+00	1.91E+00	2.42E+00
17	4.64E-01	1.68E+00	2.06E+00	5.01E-01	9.08E-01	1.01E+00
18	4.64E-01	1.68E+00	2.19E+00	5.01E-01	9.08E-01	1.06E+00
19	4.64E-01	1.68E+00	2.19E+00	5.01E-01	9.08E-01	1.06E+00
20	4.64E-01	1.68E+00	2.19E+00	5.01E-01	9.08E-01	1.06E+00
21	4.64E-01	1.68E+00	2.19E+00	5.01E-01	9.08E-01	1.06E+00
22	4.64E-01	1.68E+00	2.19E+00	5.01E-01	9.08E-01	1.06E+00
23	4.64E-01	1.68E+00	2.19E+00	5.01E-01	9.08E-01	1.06E+00
24	4.64E-01	1.68E+00	2.19E+00	5.01E-01	9.08E-01	1.06E+00
25	4.64E-01	1.68E+00	2.19E+00	5.01E-01	9.08E-01	1.06E+00
26	1.10E+00	3.85E+00	5.54E+00	7.28E-01	1.61E+00	2.17E+00
27	1.80E-02	5.21E-02	5.42E-02	3.88E-01	4.54E-01	4.46E-01
28	4.31E-01	1.55E+00	2.14E+00	4.89E-01	8.64E-01	1.04E+00
29	5.46E-01	1.78E+00	2.43E+00	5.36E-01	9.43E-01	1.14E+00
30	1.77E-02	4.86E-02	6.17E-02	3.65E-01	4.22E-01	4.23E-01
31	1.17E+00	3.86E+00	5.00E+00	7.18E-01	1.58E+00	1.93E+00
32	2.49E-01	1.34E+00	1.66E+00	4.31E-01	8.12E-01	9.06E-01
33	6.29E-01	1.85E+00	2.41E+00	5.60E-01	9.64E-01	1.12E+00
34	4.54E-01	1.66E+00	1.84E+00	4.99E-01	9.02E-01	9.53E-01
35	4.54E-01	1.66E+00	1.84E+00	4.99E-01	9.02E-01	9.53E-01
36	1.26E+00	3.69E+00	4.45E+00	6.61E-07	5.95E-07	5.34E-07
37	4.62E-01	2.67E+00	4.20E+00	5.02E-01	1.23E+00	1.70E+00
38	4.64E-01	1.15E+00	1.45E+00	5.01E-01	7.28E-01	8.11E-01
39	4.53E-01	1.64E+00	2.30E+00	4.75E-01	8.33E-01	1.03E+00
40	4.53E-01	1.71E+00	1.87E+00	5.21E-01	9.81E-01	1.02E+00

Table 4-22. Estimated surface concentrations ($\mu\text{g}/\text{m}^3$) of nitrate and ammonium aerosol particles at 14:00L at 5 km, 25 km, and 50 km downwind of the major point source for the 41 test simulations.

Run	Nitrate			Ammonium		
	5 km	25 km	50 km	5 km	25 km	50 km
Baseline	4.38E-01	1.64E+00	2.53E+00	4.93E-01	9.01E-01	1.18E+00
1	2.68E-02	7.75E-01	1.59E+00	3.54E-01	6.01E-01	8.55E-01
2	7.29E-01	2.67E+00	3.97E+00	6.10E-01	1.24E+00	1.62E+00
3	3.78E-01	2.16E+00	4.24E+00	4.62E-01	1.02E+00	1.67E+00
4	3.53E-03	2.52E-02	3.47E-02	3.81E-01	4.72E-01	5.21E-01
5	4.41E-01	1.76E+00	2.30E+00	5.15E-01	9.96E-01	1.18E+00
6	4.42E-01	1.55E+00	2.43E+00	4.86E-01	8.38E-01	1.11E+00
7	4.53E-01	1.51E+00	2.29E+00	4.78E-01	7.92E-01	1.03E+00
8	4.99E-01	1.85E+00	2.94E+00	5.08E-01	9.44E-01	1.28E+00
9	3.83E-01	1.33E+00	2.40E+00	4.81E-01	8.04E-01	1.13E+00
10	2.95E-01	1.17E+00	1.52E+00	4.56E-01	7.60E-01	8.76E-01
11	1.01E+00	3.54E+00	5.88E+00	6.99E-01	1.52E+00	2.26E+00
12	1.75E-02	5.36E-02	7.17E-02	3.86E-01	4.60E-01	4.70E-01
13	8.39E-01	3.63E+00	5.09E+00	6.29E-01	1.49E+00	1.94E+00
14	1.05E-13	3.21E-22	1.27E-06	3.52E-01	3.92E-01	4.10E-01
15	1.22E+00	3.89E+00	5.47E+00	7.53E-01	1.61E+00	2.12E+00
16	1.86E+00	4.68E+00	6.85E+00	9.97E-01	1.90E+00	2.62E+00
17	4.39E-01	1.61E+00	2.61E+00	4.92E-01	8.91E-01	1.20E+00
18	4.40E-01	1.71E+00	2.31E+00	4.92E-01	9.18E-01	1.10E+00
19	4.40E-01	1.71E+00	2.31E+00	4.92E-01	9.18E-01	1.10E+00
20	4.40E-01	1.71E+00	2.31E+00	4.92E-01	9.18E-01	1.10E+00
21	4.40E-01	1.71E+00	2.31E+00	4.92E-01	9.18E-01	1.10E+00
22	4.40E-01	1.71E+00	2.31E+00	4.92E-01	9.18E-01	1.10E+00
23	4.40E-01	1.71E+00	2.31E+00	4.92E-01	9.18E-01	1.10E+00
24	4.40E-01	1.71E+00	2.31E+00	4.92E-01	9.18E-01	1.10E+00
25	4.40E-01	1.71E+00	2.31E+00	4.92E-01	9.18E-01	1.10E+00
26	9.97E-01	3.88E+00	5.86E+00	7.01E-01	1.60E+00	2.25E+00
27	1.78E-02	5.25E-02	5.57E-02	3.85E-01	4.64E-01	4.66E-01
28	4.03E-01	1.62E+00	2.31E+00	4.80E-01	8.88E-01	1.10E+00
29	5.23E-01	1.57E+00	2.71E+00	5.23E-01	8.78E-01	1.23E+00
30	1.63E-02	5.33E-02	7.64E-02	3.64E-01	4.28E-01	4.46E-01
31	1.22E+00	4.10E+00	5.28E+00	7.32E-01	1.66E+00	2.01E+00
32	2.39E-01	1.36E+00	2.30E+00	4.27E-01	8.16E-01	1.12E+00
33	6.06E-01	1.93E+00	2.79E+00	5.50E-01	9.84E-01	1.25E+00
34	4.38E-01	1.62E+00	2.45E+00	4.93E-01	8.90E-01	1.15E+00
35	4.38E-01	1.62E+00	2.45E+00	4.93E-01	8.90E-01	1.15E+00
36	1.08E+00	3.81E+00	5.51E+00	3.95E-06	9.44E-07	6.42E-07
37	4.31E-01	2.71E+00	4.33E+00	4.89E-01	1.25E+00	1.76E+00
38	4.45E-01	1.21E+00	1.55E+00	4.93E-01	7.46E-01	8.47E-01
39	4.51E-01	1.57E+00	2.37E+00	4.78E-01	8.15E-01	1.06E+00
40	4.39E-01	1.79E+00	2.02E+00	5.13E-01	1.01E+00	1.09E+00

Table 4-23. Estimated surface concentrations ($\mu\text{g}/\text{m}^3$) of nitrate and ammonium aerosol particles 16:00L at 5 km, 25 km, and 50 km downwind of the major point source for the 41 test simulations.

Run	Nitrate			Ammonium		
	5 km	25 km	50 km	5 km	25 km	50 km
Baseline	3.01E-01	1.50E+00	2.18E+00	4.43E-01	8.45E-01	1.06E+00
1	4.66E-02	6.07E-01	1.41E+00	3.59E-01	5.42E-01	7.95E-01
2	5.59E-01	2.33E+00	4.18E+00	5.43E-01	1.15E+00	1.71E+00
3	3.36E-01	2.26E+00	3.76E+00	4.48E-01	1.06E+00	1.51E+00
4	2.34E-03	3.43E-04	1.79E-02	3.63E-01	4.36E-01	5.01E-01
5	3.16E-01	1.53E+00	2.18E+00	4.60E-01	9.04E-01	1.13E+00
6	2.87E-01	1.48E+00	2.30E+00	4.33E-01	8.14E-01	1.06E+00
7	3.14E-01	1.41E+00	2.15E+00	4.33E-01	7.69E-01	9.85E-01
8	3.51E-01	1.75E+00	2.69E+00	4.53E-01	9.09E-01	1.22E+00
9	2.73E-01	1.26E+00	2.08E+00	4.36E-01	7.71E-01	1.03E+00
10	2.40E-01	1.10E+00	1.73E+00	4.33E-01	7.24E-01	9.33E-01
11	8.63E-01	3.43E+00	5.29E+00	6.51E-01	1.46E+00	2.07E+00
12	1.18E-02	4.73E-02	6.89E-02	3.65E-01	4.34E-01	4.73E-01
13	7.66E-01	2.90E+00	4.60E+00	6.09E-01	1.26E+00	1.78E+00
14	0.00E+00	1.70E-10	0.00E+00	3.49E-01	3.81E-01	4.07E-01
15	9.42E-01	3.35E+00	4.86E+00	6.57E-01	1.44E+00	1.93E+00
16	1.44E+00	4.46E+00	6.78E+00	8.69E-01	1.82E+00	2.57E+00
17	6.66E-01	3.18E+00	5.82E+00	5.68E-01	1.37E+00	2.24E+00
18	1.46E+00	5.56E+00	6.54E+00	6.47E+00	4.80E+00	4.43E+00
19	1.63E+00	5.33E+00	6.45E+00	6.54E+00	4.62E+00	4.25E+00
20	1.53E+00	5.19E+00	6.96E+00	7.93E+00	4.58E+00	4.49E+00
21	1.49E+00	5.15E+00	6.86E+00	6.75E+00	4.79E+00	4.53E+00
22	1.70E+00	5.09E+00	6.82E+00	7.13E+00	4.50E+00	4.36E+00
23	1.43E+00	4.96E+00	5.87E+00	6.27E+00	4.30E+00	4.02E+00
24	1.32E+00	3.06E+00	4.17E+00	5.60E+00	2.63E+00	2.66E+00
25	1.31E+00	2.87E+00	3.88E+00	5.46E+00	2.46E+00	2.54E+00
26	8.48E-01	3.82E+00	5.70E+00	6.35E+00	4.37E+00	4.25E+00
27	2.32E+00	6.16E+00	6.11E+00	4.87E+00	4.51E+00	4.00E+00
28	1.41E+00	5.04E+00	7.65E+00	6.25E+00	4.50E+00	4.70E+00
29	1.70E+00	5.34E+00	7.26E+00	6.59E+00	4.76E+00	4.38E+00
30	2.52E+00	6.29E+00	7.74E+00	1.35E+00	1.83E+00	1.66E+00
31	1.19E+00	4.74E+00	6.86E+00	6.80E+00	4.53E+00	6.04E+00
32	1.27E+00	4.53E+00	6.24E+00	6.37E+00	4.51E+00	4.32E+00
33	1.93E+00	5.87E+00	6.83E+00	6.63E+00	4.77E+00	4.30E+00
34	1.68E+00	5.41E+00	7.00E+00	4.97E+00	4.66E+00	4.35E+00
35	1.43E+00	5.24E+00	7.06E+00	6.51E+00	4.60E+00	4.40E+00
36	9.88E-01	3.97E+00	5.76E+00	6.48E-01	1.04E-01	1.11E-01
37	1.63E+00	6.68E+00	1.07E+01	6.54E+00	5.44E+00	5.59E+00
38	1.64E+00	4.28E+00	5.96E+00	6.54E+00	4.47E+00	4.19E+00
39	1.53E+00	5.00E+00	6.79E+00	1.35E+00	2.52E+00	2.99E+00
40	1.48E+00	5.27E+00	6.90E+00	9.69E+00	6.89E+00	5.75E+00

Table 4-24. Estimated surface concentrations ($\mu\text{g}/\text{m}^3$) of nitrate and ammonium aerosol particles at 18:00L at 5 km, 25 km, and 50 km downwind of the major point source for the 41 test simulations.

Run	Nitrate			Ammonium		
	5 km	25 km	50 km	5 km	25 km	50 km
Baseline	2.19E-01	9.39E-01	1.87E+00	4.11E-01	6.45E-01	9.52E-01
1	3.56E-02	3.26E-01	9.27E-01	3.52E-01	4.47E-01	6.36E-01
2	2.74E-01	1.74E+00	3.98E+00	4.34E-01	9.45E-01	1.65E+00
3	2.75E-01	1.47E+00	2.81E+00	4.29E-01	8.05E-01	1.23E+00
4	2.27E-03	2.42E-03	3.97E-02	3.49E-01	3.83E-01	4.60E-01
5	2.20E-01	9.53E-01	1.77E+00	4.13E-01	6.75E-01	9.81E-01
6	2.16E-01	9.35E-01	1.78E+00	4.08E-01	6.36E-01	9.07E-01
7	2.28E-01	9.35E-01	1.95E+00	4.08E-01	6.24E-01	9.30E-01
8	2.32E-01	1.06E+00	2.17E+00	4.13E-01	6.83E-01	1.04E+00
9	2.10E-01	8.65E-01	1.52E+00	4.09E-01	6.26E-01	8.43E-01
10	2.05E-01	7.65E-01	1.45E+00	4.07E-01	6.01E-01	8.31E-01
11	7.21E-01	2.06E+00	4.01E+00	6.07E-01	1.05E+00	1.63E+00
12	8.21E-03	3.61E-02	5.78E-02	3.48E-01	3.89E-01	4.35E-01
13	6.42E-01	1.76E+00	4.01E+00	5.70E-01	9.08E-01	1.60E+00
14	0.00E+00	2.94E-09	0.00E+00	3.44E-01	3.60E-01	3.91E-01
15	6.64E-01	2.34E+00	3.89E+00	5.68E-01	1.10E+00	1.60E+00
16	9.99E-01	3.05E+00	5.20E+00	7.15E-01	1.35E+00	2.08E+00
17	2.41E-01	7.54E-01	2.03E+00	4.16E-01	5.85E-01	1.01E+00
18	3.18E-01	2.01E+00	4.25E+00	3.19E+00	3.64E+00	3.90E+00
19	7.34E-01	2.75E+00	5.14E+00	3.38E+00	3.84E+00	4.02E+00
20	9.60E-01	2.72E+00	5.47E+00	6.39E+00	4.17E+00	4.68E+00
21	9.50E-01	2.66E+00	5.26E+00	6.37E+00	3.92E+00	4.36E+00
22	1.05E+00	3.02E+00	5.25E+00	6.47E+00	4.31E+00	5.43E+00
23	7.46E-01	2.10E+00	4.81E+00	3.40E+00	3.47E+00	3.42E+00
24	7.53E-01	1.66E+00	1.90E+00	3.31E+00	2.21E+00	1.55E+00
25	6.81E-01	1.38E+00	1.71E+00	2.86E+00	1.76E+00	1.42E+00
26	6.32E-01	2.14E+00	4.44E+00	4.88E+00	3.72E+00	4.08E+00
27	1.29E-01	1.23E+00	2.29E+00	2.13E+00	3.21E+00	3.05E+00
28	7.06E-01	2.62E+00	5.18E+00	3.23E+00	3.79E+00	4.06E+00
29	9.57E-01	3.07E+00	6.47E+00	3.95E+00	3.99E+00	4.86E+00
30	3.37E-02	3.46E-02	1.81E+00	1.26E+00	1.73E+00	2.04E+00
31	9.34E-01	2.00E+00	5.37E+00	5.72E+00	3.94E+00	5.29E+00
32	6.84E-01	2.13E+00	5.12E+00	3.47E+00	4.51E+00	4.37E+00
33	8.07E-01	3.27E+00	6.91E+00	3.40E+00	4.01E+00	4.80E+00
34	6.74E-01	2.87E+00	5.94E+00	2.02E+00	3.71E+00	4.55E+00
35	7.84E-01	2.76E+00	5.79E+00	3.66E+00	3.91E+00	4.41E+00
36	6.05E-01	2.40E+00	4.29E+00	2.89E-01	2.03E-05	8.49E-03
37	7.22E-01	2.67E+00	7.85E+00	3.46E+00	4.04E+00	5.25E+00
38	7.88E-01	2.54E+00	4.40E+00	3.42E+00	3.73E+00	4.00E+00
39	5.24E-01	2.51E+00	5.48E+00	6.45E-01	1.86E+00	3.05E+00
40	7.22E-01	2.84E+00	6.14E+00	4.16E+00	5.89E+00	5.93E+00

Table 4-25. Estimated surface concentrations ($\mu\text{g}/\text{m}^3$) of nitrate and ammonium aerosol particles at 20:00L at 5 km, 25 km, and 50 km downwind of the major point source for the 41 test simulations.

Run	Nitrate			Ammonium		
	5 km	25 km	50 km	5 km	25 km	50 km
Baseline	2.14E-01	4.01E-01	1.37E+00	4.06E-01	4.64E-01	7.82E-01
1	1.21E-02	2.78E-01	4.76E-01	3.45E-01	4.23E-01	4.90E-01
2	2.53E-01	1.04E+00	3.43E+00	4.19E-01	6.82E-01	1.46E+00
3	2.36E-01	7.71E-01	2.74E+00	4.16E-01	5.85E-01	1.21E+00
4	3.64E-03	3.44E-03	8.34E-04	3.43E-01	3.47E-01	3.83E-01
5	2.27E-01	4.14E-01	1.38E+00	4.09E-01	4.70E-01	8.03E-01
6	2.28E-01	4.01E-01	1.36E+00	4.08E-01	4.63E-01	7.61E-01
7	2.27E-01	4.22E-01	1.37E+00	4.08E-01	4.70E-01	7.51E-01
8	2.30E-01	4.44E-01	1.56E+00	4.11E-01	4.77E-01	8.22E-01
9	2.13E-01	4.34E-01	1.25E+00	4.05E-01	4.75E-01	7.36E-01
10	1.94E-01	4.25E-01	1.15E+00	3.99E-01	4.73E-01	7.10E-01
11	6.91E-01	1.35E+00	2.99E+00	5.98E-01	8.69E-01	1.32E+00
12	8.00E-03	1.52E-02	4.08E-02	3.42E-01	3.49E-01	3.85E-01
13	5.61E-01	8.24E-01	2.25E+00	5.44E-01	6.27E-01	1.05E+00
14	0.00E+00	9.06E-15	2.41E-12	3.42E-01	3.44E-01	3.61E-01
15	8.22E-01	1.45E+00	3.37E+00	6.16E-01	8.25E-01	1.41E+00
16	1.10E+00	1.68E+00	4.44E+00	7.35E-01	9.56E-01	1.80E+00
17	2.25E-01	3.80E-01	1.17E+00	4.08E-01	4.57E-01	7.13E-01
18	2.25E-01	3.67E-01	2.32E+00	4.08E-01	1.09E+00	2.91E+00
19	2.43E-01	4.89E-01	2.47E+00	4.14E-01	1.12E+00	2.83E+00
20	2.46E-01	5.83E-01	2.43E+00	4.15E-01	1.84E+00	3.05E+00
21	2.46E-01	6.44E-01	2.43E+00	4.15E-01	1.86E+00	2.89E+00
22	2.43E-01	6.26E-01	2.37E+00	4.14E-01	2.77E+00	3.37E+00
23	2.36E-01	4.79E-01	1.97E+00	4.13E-01	1.11E+00	2.58E+00
24	2.36E-01	4.97E-01	1.34E+00	4.13E-01	1.06E+00	1.34E+00
25	2.46E-01	4.74E-01	1.12E+00	4.15E-01	9.62E-01	1.07E+00
26	5.00E-01	5.24E-01	1.75E+00	5.20E-01	1.21E+00	3.16E+00
27	8.65E-03	1.67E-02	2.57E-01	3.41E-01	7.28E-01	2.02E+00
28	2.43E-01	5.39E-01	2.41E+00	4.14E-01	1.11E+00	2.81E+00
29	2.45E-01	5.30E-01	2.61E+00	4.14E-01	1.20E+00	2.94E+00
30	1.12E-02	2.04E-02	3.45E-02	3.42E-01	6.14E-01	1.84E+00
31	1.13E+00	1.88E+00	4.15E+00	6.97E-01	1.82E+00	3.77E+00
32	1.64E-01	4.30E-01	1.59E+00	3.91E-01	1.11E+00	2.93E+00
33	2.98E-01	6.93E-01	2.95E+00	4.33E-01	1.18E+00	3.09E+00
34	2.45E-01	5.50E-01	2.39E+00	4.13E-01	8.84E-01	2.74E+00
35	2.45E-01	4.98E-01	2.47E+00	4.13E-01	1.17E+00	2.88E+00
36	6.46E-01	7.14E-01	3.08E+00	6.73E-08	8.17E-05	1.93E-06
37	2.39E-01	4.48E-01	2.34E+00	4.12E-01	1.11E+00	2.98E+00
38	2.33E-01	6.09E-01	2.35E+00	4.12E-01	1.16E+00	2.80E+00
39	2.33E-01	4.73E-01	1.94E+00	4.13E-01	5.21E-01	1.43E+00
40	2.33E-01	5.26E-01	2.60E+00	4.14E-01	1.41E+00	4.22E+00

4.4.1 Sensitivity Results Without Clouds

Examination of the SO₂ concentrations at the specified times and distances downwind illustrates the effects of the first seven sensitivity runs. Doubling the wind speed (Run 1) decreases the surface SO₂ concentration by about 17 percent at 5 km; halving the wind speed (Run 2) increases the surface SO₂ concentration by about 14 percent at 5 km. Perturbations in the wind speed have smaller (almost negligible) effects farther downwind. These effects are directionally correct but less than linear due to the fact that SCICHEM uses a minimum allowable turbulence level, which is provided as a model input in variable (UU_CALM), that is used under light wind conditions. It has no effect close to the source, but farther downwind, it enhances the dispersion, and is accounting for light wind meander effects. If UU_CALM is set to zero, the behavior will be directly linear, however, for the test cases, UU_CALM was set to the default value of 0.25 m²/s².

The effects of doubling and halving the mixing height (Runs 3 and 4, respectively) are quite linear at 25 and 50 km from the source, while closer to the source (at 5km) the effects are enhanced. For example, a 50 percent reduction in the mixing height results in a 210 percent increase in the SO₂ concentration at 5 km and 110 percent increases at 25 and 50 km. Likewise, increasing the mixing height from 800 to 1600 meters reduces the SO₂ concentration by 66, 47, and 47 percent at 5, 25, and 50 km downwind, respectively. The model's responses to changes in the mixing heights were directionally correct and quantitatively consistent with expectations.

Doubling and halving the SO₂ emissions rate from the single source (Runs 5 and 6, respectively) results in surface SO₂ concentrations that are nearly double and half the baseline case concentration, respectively, at 5 km downwind of the source. Farther downwind, the effects are virtually linear if one considers the 0.1 ppb background. For example, at 50 km the noon surface concentration decreases from 1.0 to 0.54 ppb when the emissions are reduced by 50 percent. This corresponds to a 54 percent reduction in the concentration in excess of the background. The model also responds as expected for the case with zero SO₂ emissions (Run 7).

The results for nitrogen species and ozone are more informative than those for SO₂ for sensitivity Runs 8-16. The simulations with zero, half, and double the NO_x emission rate (Runs 8-10) do not consistently show the expected trends of NO and NO₂ concentrations increasing with increasing emissions and ozone concentrations decreasing in the near-field and increasing in the far-field as NO_x emissions increase. Table 4-26 lists the estimated noontime concentrations at 25 and 50 km downwind for NO, NO₂, ozone, nitric acid, and particulate nitrate. The model estimates at 25 km are mutually consistent and directionally correct for species other than PAN and NO_x. The ozone, nitric acid, and particulate nitrate increase with increasing NO_x emissions as expected, but the NO, NO₂ and PAN do not consistently increase with emissions. NO₂ concentrations remain below the 2 ppb background level for both distances shown. At 50 km downwind, the results are less consistent. The NO_x concentrations do not appear to be correlated to the NO_x emission rates. Ozone, PAN, HNO₃ and particulate nitrate increase with increasing NO_x except for the 40 g/s results.

Table 4-26. Noontime concentrations with different NO_x emission rates.

Distance (km)	Species	Concentrations with Different NO _x Emission Rates			
		0 gm/sec	10 gm/sec	20 gm/sec	40 gm/sec
25	NO (ppb)	0.242	0.511	0.418	0.575
	NO ₂ (ppb)	0.365	0.962	0.417	0.521
	Ozone (ppb)	81.1	82.3	85.8	87.2
	PAN (ppb)	1.60	1.50	1.77	1.80
	HNO ₃ (ppb)	0.673	0.80	0.974	1.19
	NO ₃ ⁻ (µg/m ³)	1.14	1.36	1.65	2.10
50	NO (ppb)	0.029	0.501	0.357	0.279
	NO ₂ (ppb)	0.576	0.462	0.333	1.63
	Ozone (ppb)	92.0	102.4	109.4	99.9
	PAN (ppb)	2.92	3.13	3.74	3.08
	HNO ₃ (ppb)	0.853	1.16	1.33	1.32
	NO ₃ ⁻ (µg/m ³)	1.44	2.04	2.52	2.36

Figure 4-10 shows the downwind centerline surface concentrations of these species. It can be seen that the NO_x concentrations in the near field increase with emissions;

however, the NO_x concentration estimates converge farther downwind. Unfortunately, the results have some unexpected oscillations. Given the inputs and options selected for this particular test problem, we find that the results are difficult to interpret because the model seems to make nearly as much ozone from the background NO₂ entrained into the plume than from the NO_x emissions emitted from the source. With zero NO_x emissions, the ozone increases from 54 to 92 ppb by noontime in the SO₂/background air plume, whereas in the SO₂/NO_x/background air plume, the ozone increases from 54 to 100 with 40 gm/sec of NO_x emissions and from 54 to 109 with 20 gm/sec of NO_x emissions. While these results could be due to the conditions selected for the test problem, the selected test case is not atypical and the results illustrate the model's insensitivity to NO_x emission changes under these circumstances and possibly exaggerated ozone production with zero or low NO_x emissions. These results may be due to the VOC/NO_x ratios for these simulations. Additional testing should be performed for cases with a range of background VOCs and larger NO_x emissions to test this hypothesis.

Tests with variations in ambient temperature and relative humidity were made to assess whether the model's estimates for ozone, nitric acid, ammonia, and ammonium nitrate aerosol responded as expected. Generally, gas-phase oxidation rates increase with temperature, resulting in faster production of ozone and nitric acid. The gas-phase chemistry is only sensitive to absolute humidity at extremely low humidity levels. The gas-particle partitioning of the nitric acid/ammonia/ammonium nitrate system is sensitive to temperature, with low temperatures favoring ammonium nitrate and high temperatures favoring nitric acid and ammonia. Similarly, the particle phase is favored under humid conditions while the gas phase is favored under dry conditions. The ozone results for cases with -10, 5, 20, and 35°C temperatures are consistent since they show, for example, that the hour 16 ozone concentration at 50 km increases from 97 to 111 ppb as the temperature increases. The results with 10, 50, 70, and 95 percent relative humidity at 20°C show that ozone concentrations at 50 km at hour 16 are 101, 104, 102, and 107 ppb., While the extremes are directionally correct, it is not clear why the model estimates only 102 ppb at 70 percent relative humidity when it estimates 104 and 107 ppb at 50 percent and 95 percent relative humidity. This is a small unexpected response that may also be related to the oscillations noted above.

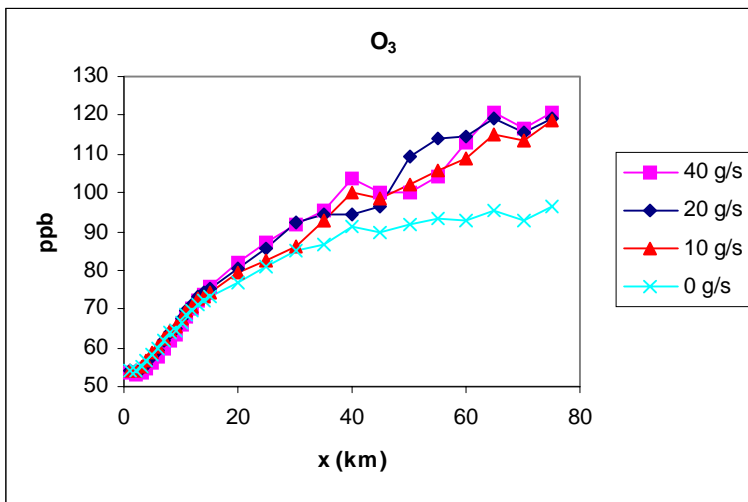
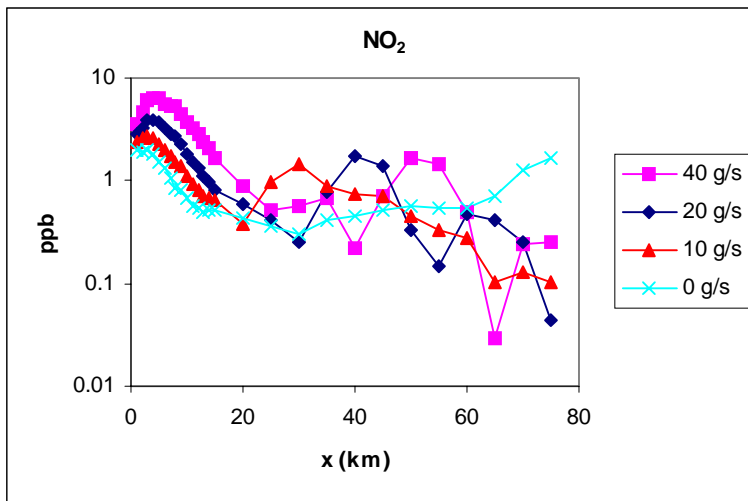
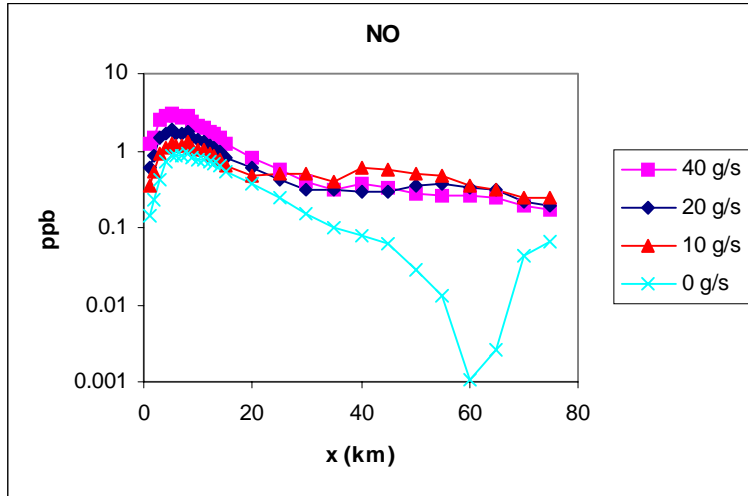


Figure 4-10. Downwind surface concentrations of NO_x, ozone, PAN, HNO₃ and aerosol nitrate for NO_x emissions

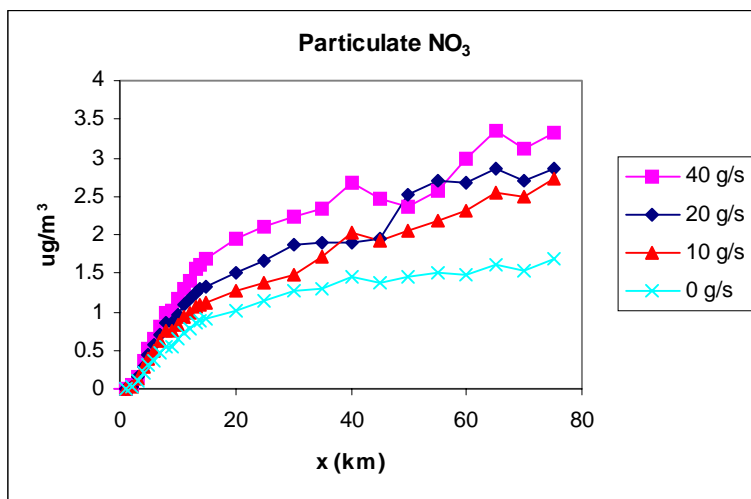
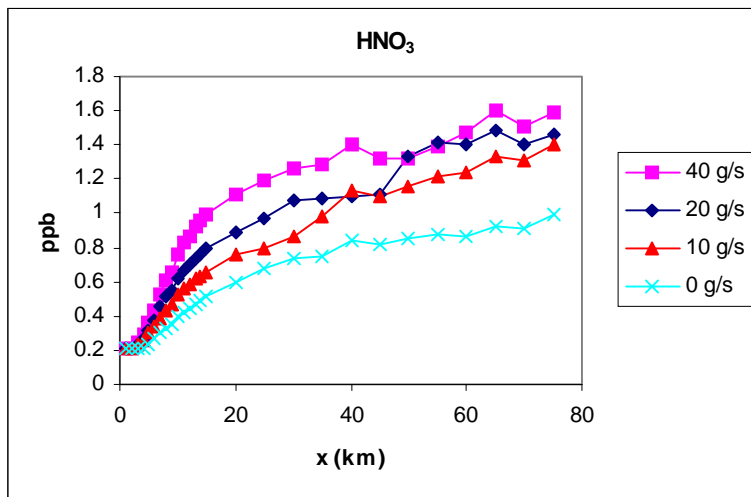
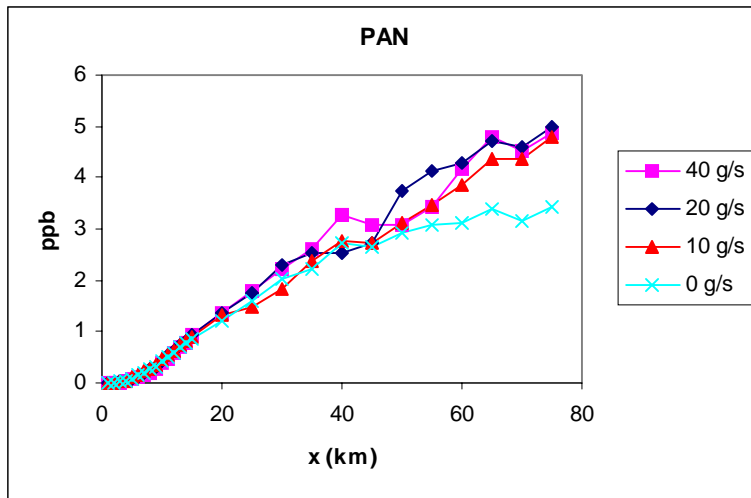


Figure 4-10. Results of varying NO_x emissions (continued)

The effects of variations in ambient temperature and relative humidity on estimated nitric acid vapor and particulate nitrate concentrations are summarized in Table 4-27 for noontime at 25 km downwind. The results show that particulate nitrate concentrations decrease with increasing temperature and the nitric acid concentrations increase with temperature. Table 4-27 also shows that when relative humidity is increased for a fixed temperature (base case and runs 14, 15, and 16), more of the total nitrate goes into the particle phase. These responses are directionally correct, and are consistent with the responses predicted by the SCAPE2 aerosol equilibrium module incorporated in SCICHEM.

Table 4-27. Noontime concentrations 25 km downwind with different temperature and relative humidity.

Run	Temperature (°C)	Relative Humidity (%)	HNO ₃ at 25 km (ppb)	NO ₃ at 25 km (µg/m ³)
13	-10	50	0.0	3.31
11	5	50	0.01	3.86
14	20	10	1.38	0.0
Base	20	50	0.97	1.65
15	20	70	0.12	4.06
16	20	95	0.03	4.74
12	35	50	2.02	0.05

4.4.2 Sensitivity Results With Clouds

The sensitivity simulations with clouds are most appropriately evaluated through examination of the simulated sulfate and nitrate aerosol concentrations during and after the clouds. The hour 16 concentrations of sulfate and nitrate at 5 and 25 km downwind of the source are shown in Table 4-28. At hour 16, the clouds and aqueous-phase chemistry have had 1 to 1.5 hours to influence the concentrations, so the effects are quite evident.

Table 4-28. Sulfate and Nitrate Aerosol Concentrations for Sensitivity Cases.

Run	Conditions	SO ₄ (µg/m ³)		NO ₃ (µg/m ³)	
		5km	25 km	5 km	25 km
19	Aqueous-chemistry baseline	16.00	7.92	1.63	5.33
17	Only 1 hr of clouds (hour 15-16)	1.04	1.18	0.67	3.18
18	Only 2 hrs of clouds (hour 15-17)	16.00	8.18	1.46	5.56
20	LWC=0.3	19.80	7.92	1.53	5.19
22	LWC=0.4	17.50	7.83	1.70	5.09
21	Run 20 with aqueous-phase free radical chemistry disabled	16.60	8.44	1.49	5.15
23	Precipitation = 1 mm/hr	15.40	7.24	1.43	4.96
24	Precipitation = 5 mm/hr	13.70	4.52	1.32	3.06
25	Precipitation = 10 mm/hr	13.40	4.22	1.31	2.87
26	Low temperature (278.15 K)	15.70	8.15	0.85	3.82
27	High temperature (308.15 K)	11.20	6.99	2.32	6.16
28	Low H ₂ O ₂ (1 ppt)	15.40	7.83	1.41	5.04
29	High H ₂ O ₂ (10 ppb)	16.00	8.17	1.70	5.34
30	Low NH ₃ (0.1 ppb)	8.70	6.80	2.52	6.29
31	High NH ₃ (25 ppb)	16.70	5.38	1.19	4.74
32	Low Ozone (10 ppb)	15.80	8.21	1.27	4.53
33	High Ozone (100 ppb)	16.00	7.81	1.93	5.87
34	Low CRUS (0.1 µg/m ³)	11.80	7.84	1.68	5.41
35	High CRUS (100.00 µg/m ³)	16.10	7.85	1.43	5.24
36	High NAACL (5 µg/m ³)	17.00	8.06	0.99	3.97
37	Low VOCs (10 ppbC)	16.00	8.96	1.63	6.68
38	High VOCs (300 ppbC)	16.00	8.23	1.64	4.28
39	Zero SO ₂ emissions	2.27	2.53	1.53	5.00
40	Double SO ₂ emissions	24.70	13.80	1.48	5.27

Sensitivity cases 17 and 18 have the clouds present for 1 hour and 2 hours rather than 3 hours. With the short duration cloud (1-hr), the concentrations near the source (5 km) and at 25 km downwind are quite similar to the no cloud case. Detailed inspection shows that a bulge in sulfate occurs in between these downwind distances. The results at hour 16 for the simulation with clouds from hours 15-17 indicates sulfate and nitrate concentration estimates are very similar to the 3-hr duration baseline run. After hour 17, the sulfate and nitrate production decrease significantly in the case where the cloud evaporates compared to the baseline case where production continues. These results are directionally and quantitatively consistent with expectations for a short cloud duration.

Runs 20, 21 and 22 incorporate higher liquid water content (0.3 and 0.4 g/cm³) than the base case (0.1 g/cm³). Initially, Run 22 was attempted with a liquid water content of 0.6 g/cm³, but the aqueous-phase module did not execute properly when the aqueous-phase chemistry solver failed to converge. The 0.6 g/cm³ case was later re-ran with the aqueous free-radical chemistry disabled and the solver was able to converge in that case, suggesting that the radical chemistry was the reason for the non-convergence. Increased liquid water is likely to reduce the droplet acidity and increase sulfate production. The expected effects on nitrate are small. The results show higher sulfate concentrations at 5 and 25 km with both higher liquid water contents. For nitrate, increasing the liquid water content is estimated to reduce concentrations (at 25 km) by small amounts which is quite plausible. Run 21 is the same as Run 20, except that the aqueous-phase free radical chemistry has been disabled. Compared to Run 20, the sulfate concentration is lower near the source, which is expected and slightly higher farther downwind, which is not implausible. The nitrate concentrations for Run 21 are lower for both downwind distances, which follows expectations.

Runs 23-25 simulate precipitating clouds. The precipitation rates are 1, 5, and 10 mm/hr for hours 15-18. Precipitation is expected to remove SO₂, HNO₃, NH₃, and sulfate, nitrate, and ammonium aerosol particles. The effects of precipitation in the simulations are clearly evident after only one hour. At hour 16, the sulfate and nitrate concentrations 25 km downwind are 7, 43, and 47 percent lower with 1, 5, and 10 mm/hr precipitation rates than in the aqueous-chemistry base case. The effects on other species and the effects on sulfate and nitrate at later times in the simulation are consistent with expectations for precipitation scavenging.

The effects of higher ambient temperatures with clouds are simulated in Runs 26 and 27. The temperatures were perturbed throughout the simulations, not just during the period with clouds. The simulation (Run 26) with a lower temperature (5°C) could not execute successfully in the aqueous-phase module unless the free radical chemistry was disabled, due to the stiffness of the equations. When the simulation was performed with out aqueous-phase free radical chemistry, the results are as expected. For the lower temperature, the sulfate concentrations are slightly lower closer to the source and higher

farther downwind, but the differences are not large. The nitrate concentrations are significantly lower than the base case since the photochemistry and nitric acid production from NO_x have proceeded at a much slower rate at the lower temperature. For the higher temperature case (Run 27), the sulfate concentrations after an hour of clouds are significantly lower at 35°C than 20°C ., which is quite plausible. The nitrate concentrations are noticeably higher in the cloud with higher temperature. This is consistent with the higher nitric acid production expected at the higher temperature. In summary, the model appears to respond in a reasonable manner to variations in temperature.

Hydrogen peroxide is a particularly effective oxidant for dissolved SO_2 . The sensitivity of the model to variations in this input was simulated in Runs 28 and 29, where 0.001 and 10 ppb of H_2O_2 were used. Even with zero initial and background H_2O_2 concentration, the gas-phase chemistry produces significant H_2O_2 concentrations before the clouds are introduced at hour 15 which reduces the effects of this parameter variation. The baseline case actually has excess H_2O_2 , so increasing the initial and background concentration to 10 ppb (Run 29) has little effect; it produces slightly higher sulfate farther downwind. Reducing the initial and background H_2O_2 concentration to almost zero (Run 28) slightly reduces sulfate 5 km downwind as well as farther downwind. These results are directionally correct and quantitatively plausible; however, the simplistic low NO_x gas-phase free-radical chemistry in the Carbon Bond IV mechanism probably overestimates H_2O_2 production in these simulations. The RADM-II and SAPRC98 gas-phase chemical mechanisms are likely to simulate H_2O_2 concentrations more accurately than the CB-IV mechanism, although all of the mechanisms are untested for this species.

Runs 30 and 31 simulate the effects of lower and higher background ammonia concentrations. As the baseline results indicate, the standard simulations have sufficient ammonia to form ammonium sulfate and ammonium nitrate at 20°C prior to formation of the cloud. The excess ammonia then serves to buffer the acidity of the cloudwater, which promotes efficient oxidation of dissolved SO_2 . The SCICHEM model estimates of sulfate concentration with 0.1 and 25 ppb of background ammonia are 46 percent lower and 4 percent higher than in the baseline case 5km downwind of the source. Farther

downwind, the effects of reduced ammonia are quite evident: the estimated sulfate levels are 14 percent lower than the baseline results at 25 km in the low ammonia case which is reasonable. However, the results for sulfate at 25 km with high ammonia and the results for nitrate are problematic. Our expectation for sulfate 25 km downwind of the source in a high ammonia background is that the sulfate should be equal to or greater than the baseline case. As Table 4-28 shows, sulfate and aerosol nitrate are estimated to decrease with a high background ammonia level which is directionally incorrect. We subsequently conducted simulations with the stand-alone aqueous chemistry module for high ammonia concentrations. The results from these studies show that the module has trouble integrating the chemistry at high ammonia concentrations and is unable to maintain sulfur mass balance. This suggests that the anomalous results found in the SCICHEM simulations for the high ammonia simulation may be due to inherent limitations in the aqueous-phase chemistry module for high pH conditions.

The effects of variations in the background ozone concentrations were simulated in sensitivity Runs 32 and 33. Lowering the background ozone slows down the photochemistry and reduces the gas-phase oxidation rates of SO₂ and NO_x, which also reduces the production of sulfuric acid, nitric acid, hydrogen peroxide, and ozone. Higher ozone levels have the opposite effects. The results for these sensitivity simulations show that varying the background ozone levels has only a small effect on sulfate estimates in the cloud, but does affect nitrate before, during, and after the cloud. Compared to the baseline aqueous-phase case, nitrate aerosol levels were 15 to 22 percent lower with the 10 ppb background ozone levels, and 10 to 20 percent higher with the 100 ppb ozone level during the cloud event. These results are directionally correct and quantitatively consistent with our expectations.

The aqueous-phase chemistry module estimates the iron and manganese aerosol concentrations from the total concentration of crustal material. Iron and manganese catalyze the oxidation of dissolved SO₂ and are particularly effective at moderate and high pHs. Simulations were made with 0.1 and 100 µg/m³ of crustal material to explore the sensitivity to this input. The results show that removing the crustal material in the background air decreases sulfate significantly near the source, but does not have much

effect on sulfate farther downwind. For example, the hour 16 sulfate at 5 km downwind of the source is reduced from 16 to 11.8 $\mu\text{g}/\text{m}^3$, while the sulfate 25 km downwind is reduced slightly when the crustal aerosol concentration is reduced from 10 to 0.1 $\mu\text{g}/\text{m}^3$. Increasing the background crustal material is estimated to have small effects on sulfate. The changes in nitrate with background crustal aerosol concentrations are also small. Overall, the SCICHEM model responded in a rational manner to changes in the crustal concentration inputs.

A simulation with elevated background sodium chloride concentrations (Run 36) was made. The results show higher sulfate levels in the near-field, and lower nitrate aerosol levels in both the near- and far-field. It makes sense for chloride to accelerate sulfate formation. It is not clear why the aerosol nitrate in the cloud decreased 30 percent. This result deserves further investigation because it was unexpected.

Runs 37 and 38 were conducted to investigate the effects of variations in background VOC concentrations (of 10 and 300 ppbC) on concentrations of other species downwind of the source. The VOC effects on estimated sulfate levels are quite small; however, under these VOC rich conditions, a considerable amount of NO_x is converted to less-soluble organic nitrate (e.g., PAN) rather than highly-soluble inorganic nitrate. As a result, the model estimates lower aerosol nitrate concentration at 50 km during the cloud event with the high VOC inputs. The result with lower VOC levels produced higher sulfate and nitrate levels than the baseline results. These responses are consistent with expectations.

Lastly, two simulations were made to explore the effects of varying the SO_2 emission rates in simulations with clouds. Runs 39 and 40 have zero and double the baseline SO_2 emissions rates, respectively. Recall that there was essentially no sulfate production in the zero SO_2 emissions case without clouds (Run 7). With clouds and without SO_2 emissions, the model produces about 1.5 $\mu\text{g}/\text{m}^3$ above the 1 $\mu\text{g}/\text{m}^3$ background sulfate concentration which is too much, given that the background SO_2 concentration is only 0.1 ppb. The model should not have produced more than 0.4 $\mu\text{g}/\text{m}^3$ of sulfate in this case. The artificial source of aerosol sulfate in the simulation needs to be identified and

corrected. The simulation with double the SO₂ emissions produced about 50 to 70 percent higher sulfate than the baseline case during the cloud event. The estimated nitrate levels were not significantly affected by the increased SO₂ emissions. This response is consistent with the expectation that aqueous conversion of dissolved SO₂ should be less efficient in plumes with higher SO₂ concentrations.

5. SUMMARY AND RECOMMENDATIONS

5.1. Summary of Model Testing

The SCICHEM model was exercised for forty case studies to test the newly added aerosol and aqueous-phase chemistry modules. The model's response and sensitivity to changes in model inputs were evaluated for hypothetical conditions involving a single elevated point source emitting SO₂ and NO_x under relatively constant meteorological conditions. The model's performance was evaluated on a qualitative and semi-quantitative basis. This entailed assessing whether the model's responses were directionally correct and were plausible in magnitude. No comparisons against observed data were made in the evaluation.

Plausible baseline case simulations were established without and with afternoon clouds. The model's responses to most of the input parameter variations were entirely consistent with scientific expectations. For cases without clouds, variations in wind speeds, mixing heights, temperatures, relative humidities, and SO₂ emission rates produced results that were directionally correct and quantitatively consistent with physical and chemical expectations. Similarly, for cases with afternoon clouds, the model produced plausible responses to changes in cloud duration, liquid water content, precipitation, background H₂O₂, background ozone, background VOCs, and background crustal aerosol concentrations.

However, model results for some of the case studies were anomalous. For the cases without clouds, variations in the point source NO_x emission rates yielded some unexpected results. Simulations with zero NO_x emissions indicate that the model produces almost as much ozone from the background NO₂ (2 ppb) than cases with a NO_x source. These results could be due to SCICHEM's treatment of the interaction of the plume with the background air. It may be inappropriate to apply the model with constant ("unstepped") background concentrations for highly reactive species (as was done for these tests). These results may also be due to the VOC/NO_x ratios in these simulations.

Additional simulations with a range of VOC background concentrations will be required to test this hypothesis.

The test cases involving the varying NO_x emission rates also indicated that concentrations can oscillate downwind of the source. This is an undesirable result which needs more analysis. Further testing is required to determine the source of the oscillations.

Additional unexpected responses were also identified in some of the model tests with clouds. These involved variations in background ammonia, background sodium chloride, and SO₂ emission rates:

- A cloud simulation with a high ammonia background concentration (25 ppb) produced less ammonium sulfate and nitrate in the afternoon than the baseline case with a 5 ppb ammonia background. It should have produced the same or higher levels of both species. We subsequently conducted simulations with the stand-alone aqueous chemistry module for high ammonia concentrations. The results from these studies show that the module has trouble integrating the chemistry at high ammonia concentrations and is unable to maintain sulfur mass balance. This suggests that the anomalous results found in the SCICHEM simulations for the high ammonia simulation may be due to inherent limitations in the aqueous-phase chemistry module for high pH conditions.
- A simulation with a high background concentration (5 µg/m³) of sodium chloride also produced lower nitrate estimates in the afternoon than the baseline case that had 0.1 µg/m³ of sea salt. This input perturbation was not expected to materially alter the estimated nitrate levels.
- Lastly, while a cloud simulation with increased SO₂ emissions showed a plausible response, a simulation with zero SO₂ emissions produced higher than expected sulfate aerosol particle concentrations. The model predicted sulfate concentrations that are 1.5 µg/m³ above the background level whereas the expected value (from conversion of the 0.1 ppb background SO₂ to sulfate) should not have been more than about 0.4

$\mu\text{g}/\text{m}^3$. This result bears some similarity to the high ozone production rates found in the dry case with zero NO_x emissions and may be related to the model's treatment of plume interaction with the background air. Alternately, this response might be caused by poor conservation of mass in the aqueous-phase chemistry module, particularly at low concentrations.

As discussed in the following section, it is necessary to perform further testing to determine the reasons for some of these unexpected results.

5.1. Recommendations

While SCICHEM with aerosol thermodynamics and aqueous chemistry appears to respond correctly for most of the tests that were conducted, it is necessary to perform a more detailed investigation and analysis of some of the case studies for which the model produced unexpected results. Such a detailed analysis was not possible within the scope of this brief study, but is essential if the model is to be widely used and evaluated against observations. In addition, there were two test cases that did not execute because the aqueous-phase chemistry module solver failed. They were a case with $0.6 \text{ g}/\text{m}^3$ cloud liquid water content (results not presented) and the low background temperature case (Run 26). Both cases were run successfully with the aqueous free-radical chemistry disabled, suggesting that the radical chemistry was the reason for the non-convergence. Further testing of the aqueous-phase chemistry module in a stand-alone mode using the input conditions that caused SCICHEM to fail will be required to understand and rectify the problem. Additionally, testing of SCICHEM should be extended to include more complex meteorological conditions, as well as comparison with actual data sets.

These analyses and testing may point to the need, among other things, to improve the current treatment in SCICHEM of ambient concentrations of reactive species, as well as address the issue of whether the plume perturbations should be advanced instead of the total plume concentrations. SCICHEM currently advances the total concentration in the plume, including the ambient. Therefore, when zero emissions are released, the ambient conditions will be reacted in the path of the plume. This was chosen as the approach

since other reactive plume models, such as ROME, also take this approach. However, for a puff model, it may be more appropriate to step the perturbation concentrations, while still taking into account the interaction with the ambient concentrations. For example, the rate of a nonlinear reaction for the total concentration is as follows:

$$R_T = k(A_P + A_B)(B_P + B_B)$$

where A_P and B_P are the plume concentrations of the reactants and A_B and B_B are the corresponding background concentrations. The rate of change of the ambient is $k A_B B_B$. In order to avoid advancing the ambient in the path of the plume, the rate of change of the perturbation concentrations would then be as follows:

$$R_P = k(A_P B_P + A_B B_P + A_P B_B)$$

The perturbation concentrations can be stepped using R_P as the rate of change. This would give the consistent result that with no emissions, the plume has no impact and the ambient concentrations will be the result of the simulation. This is an issue that needs further consideration.

There are several other areas for future development and improvement of SCICHEM. These improvements are necessary for SCICHEM to be accepted by the scientific and regulatory communities (after appropriate validation and review) as a tool that can be used to address air quality issues such as $PM_{2.5}$, visibility, and regional haze. Most of these improvements are directly relevant and natural sequels to the study described here. For example, the aqueous-phase chemistry module implemented in this study is a bulk aqueous-phase chemistry module. There is some evidence (Strader et al., 1998) that using a bulk module may result in underestimation of aqueous-phase SO_2 to sulfate chemical transformation rates under certain conditions. As the next step in the improvement of SCICHEM, the two-section aqueous-phase chemistry module described by Strader et al. (1998) could be incorporated into SCICHEM. Similarly, an aerosol equilibrium module has been implemented in this study, but there is no treatment of aerosol particle size distribution and dynamics or secondary organic aerosol formation. Modules that treat these processes exist or are currently under development and should be

available for future incorporation into SCICHEM. Note that the foundation for incorporation of multiple droplet sizes for aqueous-phase chemistry and multiple particle sizes for aerosol particles has already been laid in the current study, but has not been activated since the size-resolved modules are not yet implemented. This will facilitate the implementation of size-resolved aqueous-phase chemistry and aerosol modules in the future.

Another area for future investigation involves the gas-phase mechanism used in SCICHEM simulations. For the study described here, we tested SCICHEM using the CB-IV mechanism for gas-phase chemistry. The CB-IV mechanism was designed and optimized to estimate ozone concentrations. It often produces much higher hydrogen peroxide levels than other mechanisms and does not include species required by aqueous-phase chemistry modules, such as higher peroxides or organic acids, that are included in other mechanisms. The SAPRC98 and RADM-II chemical mechanisms were designed to be coupled with aqueous-phase chemistry models and provide a more refined treatment of radical reactions under low NO_x conditions. In future applications involving aqueous-phase chemistry, it would be advantageous to use the SAPRC98 or RADM-II chemical mechanisms. This would be particularly important for simulations with major point source emissions in pristine environments where the gas-phase production of oxidants in the background air may influence subsequent SO₂ oxidation rates in clouds. Note that gas-phase chemistry mechanisms may be freely switched in SCICHEM, but there are certain dependencies between the species in the mechanism and the species used in certain modules, such as the staged-chemistry module and the newly incorporated aerosol equilibrium and aqueous-phase chemistry module. For the most part, these dependencies should not be a restriction since many of the species in different gas-phase chemical mechanisms are identical. However, some small effort may be required to develop an interface that reads a switch (in the IMC file) naming the mechanism used (e.g., CB-IV or SAPRC98), and sets up the correct species names depending on the mechanism.

One component of SCICHEM that definitely requires improvement is the treatment of dry deposition for gases. Currently, the deposition velocities of the gas-phase species are specified in the IMC file and the same fixed values are used throughout the simulation.

This approach is not realistic, since it does not take into account the time of day, atmospheric conditions, or surface types, all of which influence the rate at which material is dry deposited. Most of the currently available air quality models take these factors into account and calculate resistances for the various pathways leading to dry deposition of pollutants are calculated and combined to estimate dry deposition velocities. It should be straightforward to incorporate similar algorithms in SCICHEM.

Additional improvements that can be added to the model include reflecting the cloud cover in the photolysis rates that are calculated. In addition, alternative ways of providing cloud liquid water content may be desirable. For example, to specify three-dimensional cloud cover, a profile type or gridded type meteorological input file must be provided by the user. It would be useful to allow the user to specify all cloud information on a surface type file by also specifying cloud top and cloud bottom. This would allow the user to run simple test cases specifying a layer of clouds without having to construct the necessary profile or gridded files.

A final area of improvement that deserves consideration is the source specification. It would be useful to specify an area source term that can be used to represent urban areas. SCICHEM currently does not allow the user to specify an area source type. In addition, it would be helpful to add the capability to simulate stacks that are close together more efficiently, either by combining the sources internally or by allowing the interaction of “static puffs”, which are used to represent the early portion of the plume and increase computation time. Currently, static puffs can only be used for sources that do not interact.

6. REFERENCES

- Ansari, A.S. and S.N. Pandis, 1999. An analysis of four models predicting the partitioning of semi-volatile inorganic aerosol components, *Aerosol Sci. Technol.*, in press.
- Binkowski, F.S. and U. Shankar, 1995. The regional particulate matter model, 1: Model description and preliminary results, *J. Geophys. Res.*, **100**, 26,191-26,209.
- Clegg, S.L., P. Brimblecombe, and A.S. Wexler, 1998a. A thermodynamic model of the system $\text{H}^+ - \text{NH}_4^+ - \text{Na}^+ - \text{SO}_4^{2-} - \text{NO}_3^- - \text{Cl}^- - \text{H}_2\text{O}$ at tropospheric temperatures, *J. Phys. Chem.*, **102**, 2137-2154.
- Clegg, S.L., P. Brimblecombe, and A.S. Wexler, 1998b. A thermodynamic model of the system $\text{H}^+ - \text{NH}_4^+ - \text{Na}^+ - \text{SO}_4^{2-} - \text{NO}_3^- - \text{Cl}^- - \text{H}_2\text{O}$ at 298.15 K, *J. Phys. Chem.*, **102**, 2155-2171.
- Gabruk, R.S., R.I. Sykes, C. Seigneur, P. Pai, P. Gillespie, R.W. Bergstrom, and P. Saxena, 1999. Evaluation of the Reactive and Optics Model of Emissions (ROME), *Atmos. Environ.*, **33**, 383-399.
- Godden, D. and F. Lurmann, 1983. Development of the PLMSTAR Model and Its Application to Ozone Episode Conditions in the South Coast Air Basin. Southern California Edison Co., Rosemead, CA.
- Jacob D.J., 1986. Chemistry of OH in remote clouds and its role in the production of formic acid and proxymonosulfate. *J. Geophys. Res.* **91**, 9807-9826.
- Jacobson, M.Z., 1999. Studying the effects of calcium and magnesium on size-distributed nitrate and ammonium with EQUISOLV II, *Atmos. Environ.*, **33**, 3635-3649.
- Jayson G.G., Parsons B.J., and Swallow A.J., 1973. Some simple, highly reactive, inorganic chlorine derivatives in aqueous-solution. *Trans. Faraday Soc.* **69**, 1597-1607.
- Karamchandani, P., Y. Zhang, and C. Seigneur, 1998. Simulation of sulfate formation in the Mohave Power Project plume, Paper No. 98-RP101A, presented at the 91st Annual Meeting & Exhibition of the Air and Waste Management Association, June 14-18, San Diego, CA.

- Karamchandani, P., L. Santos, I. Sykes, Y. Zhang, C. Tonne, and C. Seigneur, 1999. Development and evaluation of a third-generation reactive plume model, *Environ. Sci. Technol.*, submitted for publication.
- Kumar N., F.W. Lurmann, S. Pandis, and A. Ansari, 1998. Analysis of Atmospheric Chemistry During 1995 Integrated Monitoring Study. Report prepared for the San Joaquin Valleywide Air Pollution Study Agency, c/o the California Air Resources Board, Sacramento, CA by Sonoma Technology, Inc., Petaluma, CA, STI-997214-1791-FR, July.
- Le Henaff, P., 1968. Methodes d'etude et proprietes des hydrates, hemiacetals et hemiacetals derives des aldehydes et des cetones. *Bull. Soc. Chim. Fr.*, 4687-4700.
- Marsh A.R.W. and McElroy W.J., 1985. The dissociation constant and Henry's law constant of HCl in aqueous solution. *Atmos. Environ.* **19**, 1075-1080..
- Marshall, J. S. and W. M. Palmer, 1948. The distribution of raindrops with size, *J. Met.*, **5**, 165-166.
- Martell A.E. and Smith R.M., 1977. *Critical stability constants, Vol 3: other organic ligands*. Plenum, New York.
- Martin, L. R., 1984. Kinetic studies of sulfite oxidation in aqueous solution, in *SO₂, NO and NO₂ Oxidation Mechanisms: Atmospheric Considerations*. Edited by J. G. Calvert. Butterworth, Stoneham, MA, pp.63-100.
- Martin, L. R. and T. W. Good, 1991. Catalyzed oxidation of sulfur dioxide by hydrogen peroxide at low pH, *Atmos. Environ.*, **25A**, 2395-2399.
- Meng, Z., J.H. Seinfeld, P. Saxena and Y.P. Kim, 1995. Atmospheric gas-aerosol equilibrium, IV: Thermodynamics of carbonates, *Aerosol Sci. Technol.*, **23**, 131-154.
- Nenes, T., C. Pilinis, and S.N. Pandis, 1999. Development and testing of a new thermodynamic aerosol module for urban and regional air quality models. *Atmos. Environ.*, in press.
- Pandis, S. and J.H. Seinfeld, J.H., 1989. Sensitivity analysis of a chemical mechanism for aqueous phase atmospheric chemistry, *J. Geophys. Res.*, **94**, 1105-1126.
- Perrin D.D., 1982. *Ionization constants of inorganic acids and bases in aqueous solution*, 2nd Edition. Pergamon Press, New York.

- Pilinis, C. and J.H. Seinfeld 1987. Continued development of a general equilibrium model for inorganic multicomponent atmospheric aerosols, *Atmos. Environ.*, **21**, 2453-2466.
- Scire, J.S., D.G. Strimaitis, R.J. Yamartino and E.M. Insley, 1997. User's Guide for the CALPUFF Dispersion Model (Version 5.0). Earth Tech. Inc., Concord, MA.
- Schwartz S.E., 1984. Gas- and aqueous-phase chemistry of HO₂ in liquid water clouds. *J. Geophys. Res.* **89**, 11589-11598.
- Schwartz S.E. and White W.H., 1981. Solubility equilibrium of the nitrogen oxides and oxyacids in dilute aqueous solution. *Adv. Environ. Sci. Eng.* **4**, 1-45.
- Seigneur, C. and P. Saxena, 1988. A theoretical investigation of sulfate formation in clouds, *Atmos. Environ.*, **22**, 101-115.
- Seigneur C., X.A. Wu, E. Constantinou, P. Gillespie, R.W. Bergstrom, I. Sykes, A. Venkatram, and P. Karamchandani, 1997. Formulation of a second-generation reactive plume and visibility model, *J. Air Waste Manage. Assoc.*, **47**, 176-184.
- Seigneur C., P. Pai, I. Tombach, C. McDade, P. Saxena and P. Mueller, 1999. Modeling of potential power plant plume impacts on Dallas-Fort Worth visibility, *J. Air. Waste Manage. Assoc.*, in press.
- Seinfeld, J.H., 1986. *Atmospheric Chemistry and Physics of Air Pollution*, Wiley, New York.
- Seinfeld J.H. and Pandis S.N., 1998. *Atmospheric chemistry and physics: from air pollution to global change*. J. Wiley, New York.
- Slinn, W. G. N., 1982. Predictions for particle deposition to vegetative canopies, *Atmos. Environ.*, **16**, 1785-1794.
- Smith R.M. and Martell A.E., 1976. *Critical stability constants, Volume 4: inorganic complexes*. Plenum Press, New York.
- Sorensen P.E. and Andersen V.S., 1970. The formaldehyde-hydrogen sulphite system in alkaline aqueous solution: kinetics, mechanism, and equilibria. *Acta Chem. Scand.* **24**, 1301-1306.
- Stewart, D.A. and M.K. Liu, 1981. Development and application of a reactive plume model, *Atmos. Environ.*, **15**, 2377-2393.

- Strader, R., C. Gurciullo, S. Pandis, N. Kumar, and F.W. Lurmann, 1998. Development of Gas-phase Chemistry, Secondary Organic Aerosol, and Aqueous-phase Chemistry Modules for PM Modeling. Report prepared for Coordinating Research Council, Atlanta, GA. by Carnegie Mellon University, Pittsburgh, PA and Sonoma Technology, Inc., Petaluma, CA, STI-997510-1822-FR, October.
- Sykes, R.I. and R.S. Gabruk, 1997. A second-order closure model for the effect of averaging time on turbulent plume dispersion, *J. Appl. Meteor.*, **36**, 165-184.
- Sykes, R.I., S.F. Parker, D.S. Henn, C.P. Cerasoli and L.P. Santos, 1998. "PC-SCIPUFF Version 1.2PD Technical Documentation", ARAP Report No. 718. Titan Corporation, Titan Research & Technology Division, ARAP Group, P.O. Box 2229, Princeton, NJ, 08543-2229.
- Vimont, J.C., 1998. Evaluation of the CALPUFF/CALMET modeling system using Project MOHAVE tracer and implications for sulfate concentrations. In: *Visual Air Quality, Aerosols, and Global Radiation Balance*, Proceedings of AWMA/AGU Specialty Conference, September 9-12, Bartlett, NH, pp. 436-446.
- Walcek, C.J. and G.R. Taylor, 1986. A theoretical method for computing vertical distributions of acidity and sulfate production within cumulus clouds. *J. Atmos. Sci.* **43**, 339-355.
- Zhang, Y., C.H. Bischof, R.C. Easter, P.T. Wu, 1998. Sensitivity analysis of a mixed-phase chemical mechanism using automatic differentiation, *J. Geophys. Res.*, **103**, 18,953-18,979.
- Zhang, Y., C. Seigneur, J.H. Seinfeld, M. Jacobson, S.L. Clegg, and F.S. Binkowski, 1999. A comparative review of inorganic aerosol thermodynamic equilibrium modules: similarities, differences, and their likely causes, *Atmos. Environ.*, in press.

SCICHEM File Formats

SCICHEM File Formats

Final Report, Draft: September 9, 1999

Prepared by
Lynne Santos and R. Ian Sykes
ARAP Group, Titan Research & Technology

Prepared for
EPRI
Southern California Edison
California Energy Commission

EPRI Project Managers
Mary Ann Allan
Naresh Kumar

TABLE OF CONTENTS

Section	Page
1.0 INTRODUCTION.....	1
2.0 INPUT FILES.	4
2.1 INPUT FILE STRUCTURE.	4
2.2 MAIN INPUT FILE.....	4
2.3 RELEASE SCENARIO FILE.....	13
2.4 METEOROLOGY SCENARIO FILE.....	16
2.5 MULTICOMPONENT INPUT FILE.....	20
2.6 SAMPLER LOCATION FILE.....	36
3 METEOROLOGY INPUT.....	37
3.1 OBSERVATION FILE FORMAT.....	37
3.2 MEDOC FORMAT.....	46
3.3 HPAC FORMAT.....	48
3.4 TERRAIN FILE FORMAT.	51
3.5 AMBIENT FILE FORMAT.....	51
4 OUTPUT FILES.	54
4.1 SURFACE OUTPUT FILES.	54
4.2 PUFF FILE.....	57
4.3 SAMPLER TIME-HISTORY FILE.....	60
5 REFERENCES.....	63
APPENDIX.....	65

FIGURES

Figure	Page
Figure 2-1. Sample PC-SCICHEM input file.	6
Figure 2-2. Sample PC-SCICHEM release scenario file.	13
Figure 2-3. Sample PC-SCICHEM meteorology scenario file.	20
Figure 2-4. Sample Control Section of the IMC file.	25
Figure 2-5. Sample Species Section of the IMC file.	28
Figure 2-6. Sample Aqueous Section of the IMC file.	31
Figure 2-7. Sample Equation Section of the IMC file.	33
Figure 2-8. Sample Table Section of the IMC file.	35
Figure 2-9. Example PC-SCICHEM sampler location file.	36
Figure 3-1. Header structure for a meteorology observation file. Records and variables in brackets are optional or required only if nvarp is given.	37
Figure 3-2. General structure of the numerical data in a meteorological observation file. (a) Without nvarp specified; (b) with nvar fixed variables and nvarp profile variables.	45
Figure 3-3. Fortran pseudo-code for reading a formatted MEDOC input file.	47
Figure 3-4. General structure of an HPAC file.	50
Figure 3-5. General structure of an ambient file.	53
Figure 3-5. Fortran statements to write a surface output file timebreak.	54
Figure 3-6. Fortran statements to calculate field values from the surface output file.	57
Figure 4-1. Example of a sampler output file.	61

TABLES

Table	Page
Table 2-1. SCICHEM Species Types.....	26
Table 2-2. Required Species Names for Staged Chemistry	28
Table 3-2. Required species names for the aerosol equilibrium module and aqueous-phase chemistry module	29
Table 2-5. Staged Chemistry Switching Criteria	34
Table 3-1. Meteorological variables and their units recognized in SCICHEM.	41

1.0 INTRODUCTION.

SCIPUFF is a Lagrangian transport and diffusion model for atmospheric dispersion applications. The acronym SCIPUFF stands for Second-order Closure Integrated PUFF and describes two basic aspects of the model. First, the numerical technique employed to solve the dispersion model equations is the Gaussian puff method (Bass, 1980) in which a collection of three-dimensional puffs is used to represent an arbitrary time-dependent concentration field. Second, the turbulent diffusion parameterization used in SCIPUFF is based on the second-order turbulence closure theories of Donaldson (1973) and Lewellen (1977), providing a direct connection between measurable velocity statistics and the predicted dispersion rates. SCIPUFF has been expanded under EPRI sponsorship to include the treatment of nonlinear chemical reactions. SCIPUFF with chemistry is now referred to as SCICHEM.

The Lagrangian puff methodology affords a number of advantages for atmospheric dispersion applications from localized sources. The Lagrangian scheme avoids the artificial diffusion problems inherent in any Eulerian advection scheme, and allows an accurate treatment of the wide range of length scales as a plume or cloud grows from a small source size and spreads onto larger atmospheric scales. This range may extend from a few meters up to continental or global scales of thousands of kilometers. In addition, the puff method provides a very robust prediction under coarse resolution conditions, giving a flexible model for rapid assessment when detailed results are not required. The model is highly efficient for multiscale dispersion problems, since puffs can be merged as they grow and resolution is therefore adapted to each stage of the diffusion process.

SCICHEM implements efficient adaptive time stepping and output grids. Each puff uses a time step appropriate for resolving its local evolution rate, so that the multiscale range can be accurately described in the time domain without using a small step for the entire calculation. The output spatial fields are also computed on an adaptive grid, avoiding the need for the user to specify grid information and providing a complete description of the concentration field within the computational constraints under most conditions.

The generality of the turbulence closure relations provides a dispersion representation for arbitrary conditions. Empirical models based on specific dispersion data are limited in their range of application, but the fundamental relationship between the turbulent diffusion and the velocity fluctuation statistics is applicable for a much wider range. Our understanding of the daytime planetary boundary layer velocity fluctuations provides reliable input for the second-order closure description of dispersion for these conditions. For larger scales and upper atmosphere stable conditions, the turbulence description is based on climatological information, but the closure framework is in place to accept improvement as our understanding of these regimes improves. The closure model has been applied on local scales up to 50km range (Sykes et al., 1988) and also on continental scales up to 3000km range (Sykes et al., 1993).

The second-order closure model also provides the probabilistic feature of SCICHEM through the prediction of the concentration fluctuation variance. In addition to giving a mean value for the concentration field, SCICHEM provides a quantitative value for the random variation in the concentration value due to the stochastic nature of the turbulent diffusion process. This uncertainty estimate is used to provide a probabilistic description of the dispersion result, and gives a quantitative characterization of the reliability of the prediction. For many dispersion calculations, the prediction is inherently uncertain due to a lack of detailed knowledge of the wind field and a probabilistic description is the only meaningful approach.

SCICHEM treats the chemistry by using a passive tracer that carries a set of reactive chemical species, which is referred to as a “multicomponent” material. While the attached species are transported and diffused with the conserved tracer, they are also transformed through chemical reaction. The gas-phase chemical mechanism and rate constants are provided by the user. Options include the use of a “staged” chemical mechanism (Karmachandani et al., 1998) that remains somewhat flexible, except that certain chemical species must be present in the mechanism. The effects of turbulent fluctuations on the binary gas-phase mechanism may be taken into account for user-specified reactions, such as the fast reaction between NO and O₃ (Sykes et al, 1998b). Aqueous-phase chemistry may be optionally included if liquid water content is also provided in the meteorology input. Aerosol equilibrium can also be treated optionally. The aqueous chemistry mechanism and aerosol species equilibrium treatment are fixed in modular subroutines and, therefore, certain chemical species must be present in the gas-

phase mechanism for these options to be used. Wet and dry deposition of the reactive species may also be treated.

Details of the technical approach of the treatment of chemistry in SCICHEM may be found in the EPRI Report entitled “SCICHEM: A new generation plume-in-grid model” (1999) and details of the SCIPUFF dispersion model (with out chemistry) can be found in Sykes et al. (1998a). The purpose of this document is to describe the input and output file formats of SCICHEM. It is not written as a User’s Manual and users are advised to use the ‘Online Help’ when encountering problems or questions when running SCICHEM.

2.0 INPUT FILES.

2.1 INPUT FILE STRUCTURE.

The input data for PC-SCICHEM is constructed by the Graphical User Interface, but consists of Fortran NAMELIST files. There are four input files:

- ProjectName*.INP - the main input parameter file
- ProjectName*.SCN - the release scenario file
- ProjectName*.MSC - the meteorological scenario file
- ProjectName*.IMC - the multicomponent input file (optional)

where *ProjectName* is the identifying name for the PC-SCICHEM calculation. The files are maintained separately so that an arbitrary number of releases can be made, and multiple release material types can be defined. The INP, SCN and MSC file are all generated by providing input to the GUI, however, the IMC file is not generated by the GUI and must be created by the user.

PC-SCICHEM input parameters are specified through namelist groups and unformatted data located in the input, release scenario, meteorology scenario and multicomponent input files. All namelist parameters must be contained within the '**&groupname**' and '**&end**' lines of the given input file. The '**&**' on these lines must be preceded by at least one space in order for the program to recognize this block as namelist input. All lines contained outside of the namelist section are considered comments and are disregarded by PC-SCICHEM, except in the multicomponent input file. Some input parameters have default values; if a parameter does not have a default, the program will abort if the parameter is not included in the namelist.

2.2 MAIN INPUT FILE.

A sample input file is shown in Figure 2-1. The following section describes the namelist parameters and their defaults, if available. Not all of the namelist parameters are shown in the example.

```

$CTRL
  RESTART      = F,
  FILE_RST     = \ \ ,
  PATH_RST     = \ \ \ ,
  TIME_RST     = .000000,
$END
$TIME1
  YEAR_START   = 1979,
  MONTH_START  = 7,
  DAY_START    = 7,
  TSTART       = 8.18330,
  TZONE        = 17.0000,
  LOCAL        = T,
$END
$TIME2
  YEAR_END     = 1979,
  MONTH_END    = 7,
  DAY_END      = 7,
  TEND         = 14.6833,
  TEND_HR      = 6.50000,
  DELT         = 900.000,
  DT_SAVE      = 1800.00,
$END
$FLAGS
  TITLE        = `SCICHEM RUN`,
  CREATE       = F,
  AUDIT_CLASS  = `UNCLASSIFIED`,
  AUDIT_ANALYST= `Anonymous`,
  DYNAMIC      = T,
  DENSE_GAS   = F,
  STATIC       = T,
  MULTICOMP   = T,
  HAZAREA     = `OFF`,
  RUN_MODE    = 0,
$END
$DOMAIN
  CMAP         = `CARTESIAN`,
  XMIN         = -1.00000,
  XMAX         = 60.0000,
  YMIN         = -15.0000,
  YMAX         = 15.0000,
  ZMAX         = 2500.00,
  VRES         = 1.000000E+36,
  HRES         = 1.000000E+36,
  XREF         = .000000,
  YREF         = .000000,
  LON0         = -111.270,
  LAT0         = 36.8800,
$END
$OPTIONS
  T_AVG        = .000000,
  CMIN         = .000000,
  LSPLITZ     = T,
  DELMIN      = 1.000000E+36,
  WWTROP      = 1.000000E-02,
  EPSTROP     = 4.000000E-04,
  SLTROP      = 10.0000,
  UU_CALM     = .250000,
  SL_CALM     = 1000.00,
  NZBL        = 11,
  MGRD        = 2,

```

```

GRDMIN      = .000000,
Z_DOSAGE    = .000000,
SMPFILE     = `samp.loc`,
$END
$MATDEF
MNAME       = `TRAC           `,
CLASS       = `GAS           `,
UNITS       = `ppm-m3        `,
DENSITY     = 1.20000,
GAS_DEPOSITION = .000000,
DECAY_AMP   = .000000,
DECAY_MIN   = .000000,
CONC_MIN    = .000000,
GROUP_DEPOSITION = F,
GROUP_DOSE  = F,
MULTI_COMP  = T,
$END
$MATDEF
MNAME = `DUST           `,
CLASS = `PART          `,
UNITS = `kg            `,
NSG = 4,
DENSITY = 1.00000,
PSIZE = 7.5E-06, 1.25E-05, 1.75E-05, 3.5E-05,
PBOUNDS = 5.0E-06, 1.0E-05, 1.5E-05, 2.0E-05, 5.0E-05,
DECAY_AMP = .000000,
DECAY_MIN = .000000,
CONC_MIN = .000000,
NWPN_DECAY = -1.000000E+36,
GROUP_DEPOSITION = F,
TOTAL_DEPOSITION = F,
GROUP_DOSE = F,
TOTAL_DOSE = F,
MULTI_COMP = F,
FILE_NAME = ``,
FILE_PATH = ``,
$END

```

Figure 2–1. Sample PC-SCICHEM input file.

The namelist group input parameters are defined as follows:

Namelist: **CTRL** - run control flag

- restart* - Flag for run status (LOGICAL). If 'True', the old project file is used to continue the run from the last time break. The default is 'False'.
- file_rst* - name of project used to initialize current project. (CHARACTER*128). If not blank, the current project is run on

from the state defined by the *file_rst* project, puff and surface files. The default is ' ' (blank).

- path_rst* - path for project *file_rst*. (CHARACTER*128). The default is ' '.
- time_rst* - time on the puff and surface files of project *file_rst* used to initialize the current project (REAL*4). The default is the last time.

Namelist: **TIME1** - time domain information

- year_start* - Start year of the calculation (INTEGER*4). If the year is not specified, it is assumed to be that of the first year given in the meteorological input.
- month_start* - Start month of the calculation (INTEGER*4). If the month is not specified, it is assumed to be that of the first month given in the meteorological input.
- day_start* - Start day of the calculation (INTEGER*4). If the day is not specified, it is assumed to be that of the first day given in the meteorological input.
- tstart* - Start time (hours) of the calculation (REAL*4). If the time is not specified, it is assumed to be that of the first time given in the meteorological input.
- tzzone* - Local time of midnight UTC (REAL*4). The default is zero.
- local* - Flag for calculation time convention (LOGICAL). If 'True', the time is taken as local instead of UTC. The default is 'False'.
- time_status* - This variable is not required for this version of the code, however, it will appear if the project is created with the GUI. It is not used.

Namelist: **TIME2** - supplementary time domain input used for restart

- year_end* - Stop year of the calculation (INTEGER*4). If the year is not specified, it is assumed to be the same as the start year.
- month_end* - Stop month of the calculation (INTEGER*4). If the month is not specified, it is assumed to be the same as the start month.

- day_end* - Stop day of the calculation (INTEGER*4). If the day is not specified, it is assumed to be the same as the start day.
- tend* - Stop time (hours) of the calculation (REAL*4). If the time is not specified, it is assumed to be 1 hour past the start time.
- tend_hr* - Duration (hours) of the calculation (REAL*4).
- delt* - Maximum timestep (seconds) of the calculation (REAL*4). The default is 900.
- dt_save* - Amount of time (hours) between output dumps (REAL*4). The output includes the instantaneous fields and the surface accumulation fields, as specified by the user. The default is 6.

Namelist: **FLAGS** - run control and audit information

- title* - Descriptive title of the project (CHARACTER*80). No default is available.
- create* - Flag for full PC-SCICHEM calculation (LOGICAL). If 'True', PC-SCICHEM only initializes the project, but does not start the calculation. The default is 'False'. If a project is created with the GUI, this will be set to 'True'. To run the DOS version, set create to 'False'.
- audit_class* - Classification of the current project (CHARACTER*32). No default is available.
- audit_analyst* - Name of the project analyst (CHARACTER*32). The default is 'anonymous'.
- dynamic* - Flag to including momentum and buoyancy dynamics (LOGICAL). If 'False' then puffs are treated as passive. Only gaseous puffs can carry dynamics; however all puffs will be influenced by the dynamics.
- dense_gas* - Flag to include dense gas effects (LOGICAL). Not required in the current version. Must be 'False'.
- static* - Flag to perform quasi-steady calculation of continuous sources (LOGICAL). The default is 'True'.

- multicomp* - Flag to perform multicomponent chemistry (LOGICAL). Must also have a multicomponent input file (*ProjectName.IMC*).
- hazarea* - Type of hazard area prediction (CHARACTER*4). Not required in the current version. Must be 'OFF'.
- run_mode* - Run mode (INTEGER*4). If set to 0, the standard run mode is used. If set to 1, a fast mode is used. In the fast mode, the vertical and horizontal resolution are coarsened and the merge criteria for puffs is relaxed, leading to fewer puffs and faster computation speed.

Namelist: **DOMAIN**- defines the spatial domain

- cmap* - Type of spatial domain, 'CARTESIAN' or 'LATLON' (CHARACTER*40). The default is 'LATLON'.
- xmin* - Minimum horizontal coordinate (REAL*4). For a LATLON run, this value represents the minimum longitude of the domain in degrees. For CARTESIAN runs, this value represents the western boundary in kilometers.
- xmax* - Maximum longitude (deg) or eastern (km) boundary (REAL*4).
- ymin* - Minimum latitude (deg) or southern (km) boundary (REAL*4).
- ymax* - Maximum latitude (deg) or northern (km) boundary (REAL*4).
- zmax* - Vertical extent (meters) of the calculation domain (REAL*4). The default is 2500.
- vres* - Spacing parameter (meters) that limits the vertical growth of a puff (REAL*4). The default is 250.
- hres* - Spacing parameter that limits the horizontal growth of a puff in the same units as *xmin* (REAL*4). For observational data, the default is 1/10 of the domain. For gridded data, the resolution is taken as that of the meteorology.
- xref* - Cartesian *x*-coordinate (km) of the reference point when CARTESIAN coordinates are specified (REAL*4). The default is zero.

- yref* - Cartesian y-coordinate (km) of the reference point when CARTESIAN coordinates are specified (REAL*4). The default is zero.
- utm_zone* - This variable is not required for this version of the code, however, it will appear if the project is created with the GUI. It is not used.
- lon0* - Longitude of the reference point in degrees, when CARTESIAN coordinates are specified (REAL*4). The default is zero and east is positive.
- lat0* - Latitude of the reference point in degrees, when CARTESIAN coordinates are specified (REAL*4). The default is zero and north is positive.
- domain_status* - This variable is not required for this version of the code, however, it will appear if the project is created with the GUI. It is not used.

Namelist: **OPTIONS** - optional parameters

- t_avg* - Conditional averaging time (seconds) for defining the diffusive component of turbulence (REAL*4). The default is no conditional averaging.
- cmin* - Minimum puff mass (REAL*4) in user-defined units (see *units* under MATDEF). The default is zero.
- lsplitz* - Flag for vertical puff splitting within the planetary boundary layer (LOGICAL). If 'True', puffs are not split in the vertical direction within the boundary layer. The default is 'False'.
- delmin* - Minimum grid size (meters) for the adaptive surface grid (REAL*4). The default is zero.
- wwtrop* - Tropospheric vertical turbulent fluctuations (m^2s^{-2}) used as the minimum value (REAL*4). The default is 0.01.
- sltrop* - Tropospheric vertical length scale (meters) (REAL*4). The default is 10.
- epstrop* - Tropospheric energy dissipation rate (m^2s^{-3}) (REAL*4). The default is 4.0×10^{-4} .

- uu_calm* - Minimum horizontal velocity fluctuation variance (m^2s^{-2}) (REAL*4). The default is 0.25.
- sl_calm* - Horizontal length scale associated with *uu_calm* (meters) (REAL*4). The default is 1000.
- nzbl* - Number of boundary layer vertical grid levels (INTEGER*4). The default is 11.
- mgrd* - Grid resolution parameter that limits the horizontal growth of a puff (INTEGER*4). The horizontal size of the puffs will be limited to $2^{mgrd} \times hres$, where *hres* is specified under the DOMAIN section. The default is 2.
- grdmin* - Minimum grid size (meters) for the puff grid resolution (REAL*4). The default is zero.
- z_dosage* - Elevation at which surface dosages are computed (REAL*4). Default is 0.0
- smpfile* - Name of a file with sampler locations for sampler output (CHARACTER*80). See Section 2.6.
- dt_smp* - Not available in this version of the code (REAL*4). If the project is created with the GUI, the default value of 1.E+36 will appear. It will not be used

Namelist: **MATDEF** - defines material properties (multiple copies of this namelist can be included in the input file to define multiple materials)

- mname* - Material name (CHARACTER*16). Any sixteen character string used to identify the material. No default.
- class* - Material class (CHARACTER*16). Must be 'GAS' (gaseous) or 'PART' (particle).
- nsg* - Number of particle size groups (INTEGER*4). Only used for particle type materials.
- density* - Gaseous or particle material density (kg/m^3) (REAL*4).
- gas_deposition* - Gas deposition velocity (m/s) (REAL*4). Only used for gaseous materials.

- psize* - Array of particle mass mean diameters (microns) (REAL*4). Only used for particle type materials.
- pbounds* - Bin boundaries (microns) that determine the range of particle sizes within the subgroup (REAL*4). Only used for particle type materials.
- group_deposition* - Flag for group deposition (LOGICAL). If 'True', the deposition of each subgroup is included on the output surface deposition file. The default is 'False'.
- total_deposition* - Flag for total deposition (LOGICAL). If 'True', the total deposition of all subgroups is included on the output surface deposition file. The default is 'False'.
- group_dose* - Flag for group dose (LOGICAL). If 'True', the dose of each subgroup is included on the output surface dose file. The default is 'False'.
- total_dose* - Flag for total dose (LOGICAL). If 'True', the total dose of all subgroups is included on the output surface dose file. The default is 'False'.
- units* - Material mass units for labeling plots (CHARACTER*4).
- conc_min* - Minimum concentration of interest for this material (REAL*4).
- decay_amp* - Daytime decay rate (s^{-1}) of the material (REAL*4). The default is zero.
- decay_min* - Nighttime decay rate (s^{-1}) of the material (REAL*4). The default is zero.
- multi_comp* - Flag to attach multiple chemical species to the material (LOGICAL). Must also have a multicomponent input file (*ProjectName.IMC*).
- nwprn_decay* - Not used in this version of the code(REAL*4). If the file is created with the GUI, this variable will appear on the input file as a "not set" value of -1.E+36. It is not used.
- file_name* - Not used in this version of the code(CHARACTER*80). If the file is created with the GUI, this variable will appear on the input file as ' ' (blank). It is not used.

file_path - Not used in this version of the code(CHARACTER*80). If the file is created with the GUI, this variable will appear on the input file as ' ' (blank). It is not used.

2.3 RELEASE SCENARIO FILE.

A sample release scenario file is shown in Figure 2-2. The following section describes the namelist parameters and their defaults, if available. Not all of the namelist parameters are shown in the example.

```

$SCN
TREL      = .000000,
XREL      = .000000,
YREL      = .000000,
ZREL      = 236.000,
CMASS     = 1.00000,
TDUR      = 999.000,
RELTYP    = 'C   ',
NAME_REL   = '   ',
RELMAT    = 'TRAC',
SIGX      = .000000,
SIGY      = 4.20000,
SIGZ      = 4.20000,
UREL      = .000000,
VREL      = .000000,
WREL      = .000000,
WMOM      = 40400.0,
BUOY      = 134000.,
REL_MC    = 117702., 100550., .000000, .000000, .000000,
.000000, .000000, .000000, .000000, .000000, .000000, .000000,
.000000, .000000, .000000, .000000, .000000, .000000, .000000,
.000000, .000000, .000000, .000000, .000000, .000000, .000000,
.000000,
$END

```

Figure 2-2. Sample PC-SCICHEM release scenario file.

The namelist parameters are defined as follows:

- trel* - Release time (hours) (REAL*4). No default is available.
- xrel* - Absolute *x*-coordinate of the release, Cartesian (km) or Lat/Long (degrees) (REAL*4). No default is available.

- yrel* - Absolute y-coordinate of the release, Cartesian (km) or Lat/Long (degrees) (REAL*4). No default is available.
- zrel* - Release height (meters) above the surface (REAL*4). No default is available.
- reltyp* - Type of release, 'C' for continuous, 'I' for instantaneous, 'CM' for continuous moving, or 'CS' for continuous stack (CHARACTER*4). No default is available.
- cmass* - Total mass of material for an instantaneous release or mass flux for a continuous release (REAL*4). In user-defined units (see *units* under MATDEF in the INP file), *units* for instantaneous and *units* per second for continuous, moving or stack. No default.
- size* - Source radius or initial Gaussian spread or stack diameter (meters) (REAL*4). No default is available.
- tdur* - Duration (hours) of release for a continuous release (REAL*4). No default is available.
- name_rel* - Name of the *CLOUDTRANS* file containing the puff data for an instantaneous release (CHARACTER*80). No default is available.
- relmat* - Name identifying the material being released (CHARACTER*4). Must be identical to a name given in the materials list in the input file. No default is available.
- sigx* - x-direction source diameter (meters) (REAL*4). No default is available.
- sigy* - y-direction source diameter (meters) (REAL*4). No default is available.
- sigz* - z-direction source diameter (meters) (REAL*4). No default is available.
- subgroup* - Number of the individual material subgroup for a particle release (INTEGER*4). No default is available. For particle material releases if *subgroup* is equal *nsg*+1 where *nsg* is the number of size bins defined in the MATDEF namelist in *project.inp*, then the *cmass* is distributed among all material bins with a lognormal distribution.

- horiz_uncertainty* - The horizontal uncertainty (m) of the location of the source (REAL*4). The default is zero.
- vert_uncertainty* - The vertical uncertainty (m) of the location of the source (REAL*4). The default is zero.
- urel* - *x*-direction velocity (m/s) for a moving continuous source (REAL*4). No default is available.
- vrel* - *y*-direction velocity (m/s) for a moving continuous source (REAL*4). No default is available.
- wrel* - *z*-direction velocity (m/s) for a moving continuous source (REAL*4). No default is available.
- wmom* - Integrated vertical momentum for the release (m^4 / s^2) for continuous releases and (m^4 / s^2) for instantaneous releases or stack exit velocity (m/s) (REAL*4).
- buoy* - Integrated buoyancy for the release (Cm^3 / s) for continuous releases and (Cm^3) for instantaneous releases or stack exit temperature (C) (REAL*4).
- lognorm_mmd* - The mass-mean diameter of the lognormal distribution for lognormal releases (REAL*4).
- lognorm_sigma* - The sigma of the lognormal distribution for lognormal releases (REAL*4).
- number_random* - The number of copies of this release to be randomly released (INTEGER*4). Default is 1.
- random_spread* - The diameter over which the releases are randomly released (m) (REAL*4). Default is 0.0.
- random_seed* - Random generator seed value (INTEGER*4).
- rel_mc* - Emission rates of the multiple chemical species (REAL*4). Must be in *emission_units* specified on the *ProjectName*.IMC file. Must also be in the order given in the species section of the IMC file (excluding equilibrium species). See Section 2.5.
- opid* - This variable is not required for this version of the code, however, it will appear if the project is created with the GUI. It is not used.

opmod - This variable is not required for this version of the code, however, it will appear if the project is created with the GUI. It is not used.

2.4 METEOROLOGY SCENARIO FILE.

A sample meteorology scenario file is shown in Figure 2-3. The following section describes the namelist parameters and their defaults, if available. Not all of the namelist parameters are shown in the example.

The namelist parameters are defined as follows:

- met_type* - Type of meteorological input, 'OBS', 'GRIDDED', 'MEDOC' or 'FIXED', (CHARACTER*80). If MET_TYPE = 'FIXED', the last line of the MSC file must contain the wind speed and direction, otherwise, the last line must contain the file names of the meteorological input files, as shown in Figure2-3. No default.
- bl_type* - Type of boundary layer input, 'SBL', 'CALC', 'OBS', 'OPER', 'PROF', 'MEDOC', or 'NONE' (CHARACTER*80). No default.
- ensm_type* - Type of large-scale meteorological input, 'INPUT', 'MODEL', 'OBS', 'OPER' or 'NONE' (CHARACTER*80). No default.
- uu_ensm* - Velocity variance (m^2s^{-2}) for calculating the large-scale component of the dispersion (REAL*4). Used only with 'INPUT' large-scale meteorology. The default is 0.25.
- sl_ensm* - Length scale (meters) for calculating the meandering component of the dispersion (REAL*4). Used only with 'INPUT' or 'OBS' large-scale meteorology. The default is 1.0×10^5 .
- sl_haz* - Length scale (meters) for calculating dispersion due to wind uncertainty given as velocity variance on observational meteorology input files (REAL*4). Not required in the current version. The default is 1.0×10^5 .
- zimin* - Minimum daily inversion height (meters) for calculating boundary layer parameters (REAL*4). Used only with 'SBL' boundary layers. No default is available.

<i>zimax</i>	- Maximum daily inversion height (meters) for calculating boundary layer parameters (REAL*4). Used only with 'SBL' boundary layers. No default is available.
<i>hconst</i>	- Minimum daily surface heat flux (Wm^{-2}) for calculating boundary layer parameters (REAL*4). Used only with 'SBL' boundary layers. No default is available.
<i>hdiur</i>	- Maximum daily surface heat flux (Wm^{-2}) for calculating boundary layer parameters (REAL*4). Used only with 'SBL' boundary layers. No default is available.
<i>h_cnp</i>	- Canopy height (meters) (REAL*4). A negative value indicates no vegetative canopy. No default is available.
<i>zruf</i>	- Surface roughness (meters) (REAL*4). No default is available.
<i>albedo</i>	- Fraction of incident light that is reflected by the surface (REAL*4). Used only with 'CALC' boundary layers. No default is available.
<i>bowen</i>	- Ratio of surface sensible heat flux to latent heat flux (REAL*4). Used only with 'calculated' 'CALC' layers. No default is available.
<i>cloud_cover</i>	- Fractional cloud cover where complete overcast is 1 and clear sky is 0 (REAL*4). Used only with 'CALC' boundary layers. No default is available. If the fractional cloud cover is provided on a observational or gridded file, this value will be ignored.
<i>local_met</i>	- Flag specifying the reference time for the Met files (LOGICAL). If 'True' then it is assumed that the times in the Met files are local times. If 'False' the times are assumed to be UTC (GMT) times.
<i>tbin_met</i>	- Observation time bin width in seconds (REAL*4). Observations within a bin are all given the same time. The default is no time binning.
<i>pr_type</i>	- Global precipitation type, 'LGTRAIN', 'MODRAIN', 'HVYRAIN', 'LGTSNOW', 'MODSNOW', 'HVYSNOW' or 'METFILE' (CHARACTER). When not set to 'METFILE', it will

override what has been specified on the meteorological input file for either 'PRATE' or 'PRCP' (see Section 3.1).

- nearest_sfc* - Number of nearest surface observation stations used for meteorology interpolation (INTEGER*4). The default is all.
- nearest_prf* - Number of nearest upper air profile observation stations used for meteorology interpolation (INTEGER*4). The default is all.
- lmc_ua* - Flag to calculate a mass-consistent adjustment to the wind fields (LOGICAL). This is relevant only if *met_type* is 'OBS'. The default is 'False'.
- lout_mc* - Not used in the current version (LOGICAL). If the project is created with the GUI, it will appear in the MSC file. The default is 'False'.
- lout_met* - Flag to output the met fields in a MEDOC-type file (LOGICAL). The default is 'False'.
- tout_met* - Time in seconds to output met fields (REAL*4). The default is the "not set" value of -1.E+36.
- lout_2D* - Flag to output the 2-D fields in a MEDOC-type file (LOGICAL). The default is 'False'.
- lout_3D* - Flag to output the 3-D fields in a MEDOC-type file (LOGICAL). The default is 'False'.
- lformat* - Flag to output the adjusted wind fields in ASCII format (LOGICAL). If 'False', a binary file is created. This is relevant only if *lout_2D* and/or *lout_3D* are 'True'. The default is 'False'.
- file_ter* - Name of file containing terrain information (CHARACTER*80). This is required if *lmc_ua* is 'True'. No default is available.
- alpha_max* - Maximum value of vertical adjustment parameter for mass-consistent wind field calculation (REAL*4). This is relevant only if *lmc_ua* is 'True' and MC-SCICHEM is invoked. The default is 1.
- alpha_min* - Minimum value of vertical adjustment parameter for mass-consistent wind field calculation (REAL*4). This is relevant only

- if *lmc_ua* is 'True' and MC-SCICHEM is invoked. The default is 0.
- max_iter_ac* - Maximum number of iterations allowed for MC-SCICHEM calculation using the point relaxation method (INTEGER*4). The default is 10000.
- max_iter* - Maximum number of iterations allowed for MC-SCICHEM calculation using the FFT method (INTEGER*4). The default is 30.
- ac_eps* - Convergence criterion for MC-SCICHEM calculation using the point relaxation method (REAL*4). The default is 1.0×10^{-2} .
- p_eps* - Convergence criterion for a MC-SCICHEM calculation using the FFT method (REAL*4). The default is 1.0×10^{-5} .
- nzb* - Number of vertical grid levels used for MC-SCICHEM calculation (INTEGER*4). No default is available.
- zb* - Vertical grid levels used for MC-SCICHEM calculation (REAL*4). There must be *nzb* levels specified. No default is available.
- dt_swift* - Update time interval (sec) for the SWIFT mass-consistent wind field calculation. (REAL*4). The default is no time binning. Not required in the current version.
- lswift* - Flag indicating availability of SWIFT mass-consistent wind field module (LOGICAL). Not required in the current version. Must be 'False'.
- nclد* - Number of cloud droplet size sections on observational or MEDOC type files (INTEGER). The default is 0 and currently, the maximum is 1. This is not currently available for editing with the GUI and projects that are created with the GUI may only change this value from the default value by editing the MSC file.
- size_cld* - An array (REAL*4) of cloud droplet sizes (m) corresponding to the cloud droplet sections. Must provide *nclد* sizes. The default is 1.e-5. This is not currently available for editing with the GUI and

projects that are created with the GUI may only change this value from the default value by editing the MSC file.

```
&MET
    MET_TYPE           = 'OBS' ,
    BL_TYPE            = 'CALC' ,
    ENSM_TYPE          = 'NONE' ,
    UU_ENSM            = 0.10 ,
    SL_ENSM            = 0.10 ,
    H_CNP               = -1.0 ,
    ZRUF               = 0.10 ,
    ALBEDO              = 0.14 ,
    BOWEN               = 0.30 ,
    CLOUD_COVER         = 1.00 ,
    LOCAL_MET           = F ,
    NCLD                = 1 ,
    SIZE_CLD            = 1.00E-5 ,
&END
1 $apr_sfc.obs        1 $apr_ua.obs
```

Note: The last line in the figure provides the names of the meteorological input files and must appear as shown (1 \$filename) for MET_TYPE = 'OBS', 'GRIDDED', or 'MEDOC'. For MET_TYPE = 'FIXED', the last line should contain the space-separated wind direction and wind speed.

Figure 2-3. Sample PC-SCICHEM meteorology scenario file.

2.5 MULTICOMPONENT INPUT FILE.

Nonlinear chemistry is performed by defining a multicomponent material that will carry a set of reactive chemical species. The attached chemical species that are transported and diffused with the conserved tracer will also be transformed through chemical reaction. The gas-phase chemical mechanism and rate constants are provided by the user in the multicomponent input file (*ProjectName.IMC*, referred to hereafter as the IMC file).

The IMC file specifies the chemical species names, how they will be modeled, the chemical reactions they will undergo, and the associated reaction rate constants. It is made up of four sections: the control, species, equations and table sections, in any order. Each section begins with “#Section name”, (for example, #Control). All sections are unformatted and need only be space delimited. The section headings are as follows:

Control Section, Species Section, Aqueous Section, Equation Section, and Table Section. An example IMC file is shown in the appendix.

Current options include the use of a staged chemical mechanism (Karamchandani, et. al. 1998) designed for use with mechanisms that describe the photochemical production of ozone. By defining three stages of plume development, a smaller set of reactions can be used near the source, a larger set for the mid-range calculation and the full chemical mechanism at longer ranges. This approach decreases computation time while maintaining the accuracy of the plume chemical development. If the staged chemistry is in use, a further option of using a chemistry puff splitting criteria may be implemented in an attempt to resolve “ozone wings” (initial ozone formation in the plume edges).

Two options are available for the ordinary differential equation (ODE) solver, which are either LSODE or the Young and Boris method. Using LSODE would provide the most accurate solution for the ODEs, but is computationally expensive. The Young and Boris method allows a more rapid solution to the ODEs at some expense of accuracy.

Aerosol equilibrium chemistry may be treated optionally, either by itself or in combination with aqueous-phase chemistry. Aqueous-phase chemistry may be treated if cloud liquid water content has been provided on the meteorological input files. Dry deposition and wet scavenging may be treated with user-supplied deposition velocities and scavenging coefficients.

2.5.1 Multicomponent Control Section.

Under the control section, the following namelist parameters are specified:

- step_ambient* - Specifies whether or not the ambient concentrations will be stepped with the same reaction mechanism as the plume (LOGICAL). Ambient concentrations can be specified in two ways: 1D under the species section and 3D through an ambient file. Only the 1D ambient may be stepped. The default is ‘False’.
- sove_ynb* - Specifies how the chemistry equations will be solved (LOGICAL). If set to ‘True’, the Young & Boris method will be used, otherwise LSODE will be used. The default is ‘False’.

- aqueous* - Specifies whether or not aqueous-phase chemistry will be performed (LOGICAL). Must have certain species defined in the species section, as described in the following section. If set to 'True', the species names (see Table 2-3) will be checked to determine if the aqueous module can be used and if so, aqueous-phase chemistry will be performed in addition to gas phase. Liquid cloud content must be provided on a meteorological input file (Observations or Gridded). The default is 'False'.
- aerosol* - Specifies whether or not aerosol equilibrium chemistry will be modeled (LOGICAL). Must have certain species defined in the species section, as described in the following section. If set to 'True', the species names (see Table 2-3) will be checked to determine if the aerosol module can be used and if so, aerosol equilibrium chemistry will be performed in addition to gas phase. The default is 'False'.
- nsec_aer* - Number of aerosol particle sections (INTEGER). Used with *aerosol* set to 'True'. The default is 1 and currently, the maximum is also 1.
- secbnds_aer(1)* - Section boundaries (m) of the aerosol particles (REAL*4). Used with *aerosol* set to 'True'. Must specify *nsec_aer* + 1 values. The defaults are 0.4e-6 and 0.4e-6 (used to represent a mean aerosol particle diameter of 0.4e-6 m).
- rho_aer* - Density (kg/m³) of the aerosol particles. Used with *aerosol* set to 'True'. The default is 1000.
- ambient_file* - Name of file (CHARACTER*128) that contains the 3D time dependent ambient species concentrations (optional). Must be in the correct format (see Section 3.5). If an ambient file is specified, *step_ambient* must be set to 'False'. The default is no ambient file.
- species_units* - Concentration units (CHARACTER*80) for the ambient concentrations given under the species section and for output concentrations. Options are either 'ppm' or 'molecules/cm³'. The default is 'ppm'.

- emission_units* - Emission rate units (CHARACTER*80). Options are either 'ppm-m³/s', 'molecules-m³/cm³-s', or 'g/s'. Emission rates for the release specified in *rel_mc* in the *Projectname*.SCN file. Aerosol particle species emissions are always assumed to be in g/s. See section 2.3. The default is 'ppm-m³/s'.
- rate_species_units* - Concentration units (CHARACTER*80) for the rate constants given under the equations section. Options are either 'ppm' or 'molecules/cm³'. The *rate_species_units* will be converted to match the *species_units*. The default is 'molecules/cm³'.
- rate_time_units* - Time units (CHARACTER*80) for the rate constants given under the equations section. Options are 'seconds', 'minutes' or 'hours'. The default is 'seconds'.
- rtol* - Relative tolerance (REAL*4) used to solve chemical reaction equations. The default is 1.e-2.
- staged_chem* - Specifies whether the chemical mechanism in the equation section (Section 2.5.4) is staged or not (LOGICAL). Must have certain species defined in the species section (Section 2.5.2). The default is 'False'.
- voc_names(1)* - Used only for staged chemistry. Names (CHARACTER*80) of volatile organic compounds that react with NO₃. No default.
- phno3* - Used only with *staged_chem* set to 'True' (REAL*4). Production rate (% per hour) of HNO₃ due to the reaction of OH and NO₂ that indicates the stage should include acid formation (switch from stage 1 to stage 2). Used both day and night. The default is 0.1% per hour.
- rno3* - Used only with *staged_chem* set to 'True' (REAL*4). Production rate (% per hour) of NO₃ due to the reaction of NO₂ and O₃ that indicates the stage should include acid formation (switch from stage 1 to stage 2). Used at night in conjunction with *cno3*. The default is 0.1% per hour.
- cno3* - Used only with *staged_chem* set to 'True' and in conjunction with *pno3* and *rvocno2* (REAL*4). Concentration of NO₃ (ppm) above which the stage should include acid formation if *pno3* or *rvocno2*

meet their criteria (switch from stage 1 to stage 2). Used only at night. The default is 1.e-8ppm.

- rho2o3* - Used only with *staged_chem* set to 'True' (REAL*4). Ratio (%) of the destruction of NO by HO2 to the destruction of NO by O3 above which the stage should include O3 formation (switch from stage 2 to stage 3). Used day and night in conjunction with *co3*. The default is 0.1%.
- co3* - Used only with *staged_chem* set to 'True' and in conjunction with *rho2o3* (REAL*4). Concentration (ppm) of O3 above which the stage should include ozone formation if *rho2o3* meets its criteria (switch from stage 2 to stage 3). The default is 1.e-3ppm.
- rvocno2* - Used only with *staged_chem* set to 'True' (REAL*4). Ratio (%) of the destruction of NO3 by VOCs to the destruction of NO3 by NO2 above which the stage should include O3 formation (switch from stage 2 to stage 3). Used at night in conjunction with *cno3*. The default is 1%.
- chem_split* - Specifies whether the puffs should use a chemical criteria to split in order to resolve ozone "wings" (LOGICAL). Current split criteria: ozone concentrations are within 20% of the background and plume NO_x concentrations are within 5% of the background. If *chem_split* is set to 'True', then *staged_chem* must also be set to 'True'. The default is 'False'.

```

#CONTROL
&CONTROL
  step_ambient = .false.
  aqueous = .true.
  aerosol = .true.
  nsec_aer = 1
  secbnds_aer(1) = 2.5e-6,10.e-6
  rho_aer = 1.
  ambient_file = 'ambient.dat'
  species_units = 'ppm'
  rate_species_units = 'ppm'
  rate_time_units = 'seconds'
  rtol = 1.e-3
  staged_chem = .true.
  voc_names(1) = 'HCHO','ALD2','OLE','CRES','ISOP'
  phno3 = 0.1
  pno3 = 0.1
  cno3 = 1.e-8
  rho2o3 = 0.1
  co3 = 1.e-3
  rvocno2 = 1.0
  chem_split = .true.
&END

```

Figure 2-4. Sample Control Section of the IMC file.

The control section namelists begin with “\$CONTROL” and end with “\$END”. If parameters are not set under this section, the default values will be assumed. An example of a control section is shown in Figure 2-4.

2.5.2 Multicomponent Species Section.

Each line of the species section gives the species name, the species type (F, S, P, A, or E), the ambient concentration (ppm or molecules/cm³), the absolute tolerance (ppm or molecules/cm³), the gas deposition velocity (m/s), the wet scavenging coefficient (s⁻¹), and the molecular weight (g/mole) to be used in solving for the concentration. There are no defaults for these parameters. The species types are shown in Table 2-1.

Table 2-1. SCICHEM Species Types.

<i>F</i>	Fast	Species concentrations change rapidly and species rate equations will be integrated using LSODE.
<i>S</i>	Slow	Species concentrations change slowly and will be integrated explicitly using a predictor-corrector scheme.
<i>P</i>	Particle	Species concentrations are determined through aerosol equilibrium. Species name must match aerosol particles set by aerosol module.
<i>E</i>	Equilibrium	Species concentrations are assumed to be at steady-state.
<i>A</i>	Ambient	Species concentrations do not change by the reaction, such as H ₂ O or O ₂ .

The wet scavenging coefficient, s (s⁻¹), is used to define the scavenging rate, sr (s⁻¹), as:

$$sr = s (R/R_0)$$

where R is the precipitation rate in mm/hr and R_0 is the reference precipitation rate of 1 mm/hr. The scavenging rate is applied to the gas-phase species after the gas-phase chemistry has been advanced. If the aqueous-phase chemistry module is turned on, the wet scavenging coefficient will be ignored and the wet removal will be carried out inside the aqueous-phase module. Scavenging coefficients for aerosol particles are ignored. Particle scavenging rates are determined internally based on particle size and precipitation rate based on the approach of Seinfeld (1986). Dry deposition velocities for aerosol particles are also ignored and dry deposition is computed internally following the approach of Slinn (1982).

Every species that appears in the equation section must also appear in the species section. The ambient concentration of H₂O may be set on the species line to a desired concentration or set to -1.0 to be set internally by the meteorological conditions. When set internally, the H₂O concentration is obtained from the humidity given in the meteorological input files or a default value of 30% relative humidity is used. Note that if species other than H₂O are specified as ambient, such as O₂, the correct ambient concentration must be given on the species line. Ambient concentrations for equilibrium species are calculated internally based on the chemical mechanism and the other ambient

concentrations, and therefore, the value entered will not be used. If an ambient file has been specified under the control section, the ambient concentrations given here in the species section will be overridden by the 3D ambient file.

Molecular weights are used to convert the gas-phase emissions to the desired species units. Emission rates that are provided in 'g/s' will be converted to either 'ppm-m³/s' or 'molecules-m³/cm³-s' using the molecular weight, depending on whether *species_units* has been set to ppm or molecules/cm³, respectively. It is not essential to provide molecular weights for non-emitted species, however, since species emission rates are not checked initially to identify emitted species versus non-emitted species, all 'Fast' and 'Slow' species must have non-zero molecular weights provided on the IMC file. Molecular weights are not required for equilibrium species or for particle species, since equilibrium concentrations are determined from the 'Fast' and 'Slow' species concentrations and aerosol particle species concentrations are always assumed to be in µg/m³ and the emission rates in g/s.

An example of a species section is shown in Figure 2-5. In the example, only HNO₃ has a nonzero deposition velocity and wet scavenging coefficient and therefore, there will be no deposition or scavenging of any species other than HNO₃. HNO₃ is modeled as a fast species with a background concentration of zero and a relative tolerance of 1.e-8. The deposition velocity is 0.02 m/s and the wet scavenging coefficient is 6.e-5 s⁻¹. The ambient H₂O concentration will be determined from the meteorological input data. Molecular weights of non-emitted, equilibrium and ambient species have been set to an arbitrary value of 99.99.

#Species	Type	Ambient	Atol	Dep	Wet Scav	MW
NO	F	0.0	1.e-8	0.00	0.000	30.01
O3	F	0.1	1.e-8	0.00	0.000	48.00
NO2	F	0.0	1.e-8	0.00	0.000	46.01
HNO3	F	0.0	1.e-8	0.02	6.e-5	63.00
RCHO	F	0.50	1.e-8	0.00	0.000	99.99
RH	S	12.0	1.e-8	0.00	0.000	99.99
PAN	F	0.0	1.e-8	0.00	0.000	121.0
OH	F	0.0	1.e-12	0.00	0.000	99.99
HO2	E	0.0	1.e-12	0.00	0.000	99.99
RO2	E	0.0	1.e-12	0.00	0.000	99.99
C2O3	E	0.0	1.e-12	0.00	0.000	99.99
H2O	A	-1.0	1.e-6	0.00	0.000	99.99

Figure 2-5. Sample Species Section of the IMC file.

If staged chemistry is turned on, the species in Table 2-2 must appear in the species section. If either the aerosol equilibrium chemistry is turned on (aerosol is equal to 'True' under the control section) or the aqueous-phase chemistry is turned on (aqueous is equal to 'True' under the control section), or both, the species shown in Table 2-3 must appear in the species section, even if they do not all appear in the gas phase mechanism (for example the aerosol species).

Table 2-2. Required Species Names for Staged Chemistry

Chemical	Required Species Name
Nitric Oxide (NO)	NO
Nitrogen Dioxide (NO2)	NO2
Nitrate Radical (NO3)	NO3
Dinitrogen Pentoxide (N2O5)	N2O5
Nitric Acid (HNO3)	HNO3
Ozone (O3)	O3
Hydroxyl Radical (OH)	OH
Hydroperoxy Radical (HO2)	HO2
Volatile Organic Compounds (VOCs)	As named in the control section

For multiple particle sections (*nsec_aer* greater than 1), the aerosol species names must appear in the species section of the IMC file with the section number. For example, when three sections are desired (*nsec_aer* is equal to 3), the user must list CRUS01, CRUS02, and CRUS03 and likewise for the other aerosol particles. Note that *nsec_aer* will specify the number of sections for all the aerosol particle species. The species list

will be searched for aerosol_name01 to aerosol_namensec_aer using the format (A,i2.2) where the aerosol_name refers to CRUS, ASO4, ANO3, ANH4, ANA, ACL, AMG, ACA, or APOT. However, recall that currently, the maximum number of aerosol particle sections is 1. For nsec_aer equal to 1, the user may optionally leave off the section number from the name. The required names for either aqueous chemistry or aerosol equilibrium will be as they appear in Table 3-2.

Table 3-2. Required species names for the aerosol equilibrium module and aqueous-phase chemistry module

Chemical	Required Species Name
Sulfur dioxide (SO ₂)	SO2
Hydrogen peroxide (H ₂ O ₂)	H2O2
Formaldehyde (HCHO)	FORM
Formic Acid (HCOOH)	FA
Nitrous acid (HNO ₂)	HONO
Nitric Oxide (NO)	NO
Nitrogen Dioxide (NO ₂)	NO2
Ozone (O ₃)	O3
Peroxyacyl Nitrate (CH ₃ C(O)OONO ₂)	PAN
Carbon Dioxide(CO ₂)	CO2
Hydroxyl Radical (OH)	OH
Hydroperoxy Radical (HO ₂)	HO2
Nitrate Radical (NO ₃)	NO3
Toluene-hydroxyl radical adduct	TO2
NO-to-NO ₂ operation	XO2
Crustal Material (particulate) ¹	CRUS01 or CRUS ²
Aerosol Sulfate ¹	ASO401 or ASO4 ²
Aerosol Nitrate ¹	ANO301 or ANO3 ²
Aerosol Ammonia ¹	ANH401 or ANH4 ²
Aerosol Sodium ¹	ANA01 or ANA ²
Aerosol Chloride ¹	ACL01 or ACL ²
Aerosol Magnesium ¹	AMG01 or AMG ²
Aerosol Calcium ¹	ACA01 or ACA ²
Aerosol Pottasium ¹	APOT01 or APOT ²
Sulfuric Acid (H ₂ SO ₄)	SA
Nitric Acid (HNO ₃)	HNO3
Ammonia (NH ₃)	NH3
Hydrogen chloride (HCl)	HCL

Note: ¹ Aerosol particles must be specified as species type “P” (particle).

² For nsec_aer equal to 1, the section number may be optionally removed from the aerosol particle names.

2.5.3 Multicomponent Aqueous Section.

The aqueous section of the IMC file specifies parameters that will be used in the aqueous-phase module (using *aqueous* in the control section set to 'True'). The aqueous variables may be provided as an option and this section does not even have to appear on the IMC file. If it does not appear on the file, the default values will be used in the aqueous module. The following variables may be specified:

- debug* - Debug flag (LOGICAL). If set to 'True', messages from the aqueous module are printed to the log file. The default is 'False'.
- lradical* - Choice of whether or not to use aqueous-phase free radical chemistry (LOGICAL). If set to true, the aqueous-phase free radical chemistry will be performed during the daytime hours. Otherwise, it is not performed at all. The default is true.
- dactiv* - Dry activation diameter (m) (REAL*4). The default is 3.0e-7.
- fdist(1)* - Fraction of mass change that will go to each aerosol particle size section (REAL*4). Must specify *nsec_aer* values. The default is 1. For future applications when *nsec_aer* is greater than 1, the default is to have the mass equally distributed.
- kiron* - Choice of expression for iron and manganese chemistry (INTEGER*4). If *kiron* is 0, there is no iron and manganese chemistry. If *kiron* is 1, the method of Martin and Good (1991) is used. If *kiron* is 2, the method of Martin (1984) is used. The default is 1.
- firon* - Fraction of crustal material that is iron (REAL*4). The default is 1.e-2.
- fman* - Fraction of crustal material that is manganese (REAL*4). The default is 2.e-3.
- chlorine* - Choice of turning off chlorine chemistry (REAL*4). If set to 0, chlorine chemistry will be turned off. The default is 1.0.
- so2min* - Minimum SO₂ concentration (ppm) for the aqueous calculation (REAL*4). The default is 1.0e-6.

- lwcm_{in}* - Minimum liquid water content (g/m³) for the aqueous calculation (REAL*4). The default is 5.0e-2.
- atol_x* - Absolute error tolerance for numerical integration (REAL*4). The default is 1.0e-4.
- rtol_x* - Relative error tolerance for numerical integration (REAL*4). The default is 1.0e-3.
- dtmax_{sec}* - Maximum time step (seconds) for numerical integration (REAL*4). The default is 120.
- xtol* - Relative error tolerance for nonlinear solver (REAL*4). The default is 1.0e-3.

The aqueous section namelist begins with “\$AQUEOUS” and end with “\$END”. If parameters are not set under this section, the default values will be assumed. An example of a control section is shown in Figure 2-6.

```
#Aqueous
$AQUEOUS
  debug = .true.
  lradical = .true.
  dactiv = 3.000000e-07,
  fdist = 1.0,
  kiron = 1,
  firon = 1.000000e-02,
  fman = 2.000000e-03,
  chlorine = 1.00000,
  so2min = 1.000000e-06,
  lwcmin = 5.000000e-02,
  atolx = 1.000000e-04,
  rtolx = 1.000000e-03,
  dtmaxsec = 120.000,
  xtol = 1.000000e-03,
$END
```

Figure 2-6. Sample Aqueous Section of the IMC file.

2.5.4 Multicomponent Equation Section.

Each line of the equations section gives the equation number followed by the chemical reaction. Species names must be placed in square brackets, such as [NO], and

stoichiometric coefficients are given in parentheses, as in (2.0) [NO]. The maximum number of reactants is 2 and the maximum number of products is 10. The reaction is ended by a semi-colon followed by the reaction rate coefficient type. The following rate coefficient types are available:

- 0 radiation dependent
- 1 constant
- 2 temperature dependent
- 3 temperature and pressure dependent
- 4 temperature dependent and multiplied by the concentration of H2O

For the radiation dependent rate constants, a table must be provided listing the rate constants as a function of zenith angle. For the others, the necessary constants are given after the type number. After type 1, the rate constant itself is then given. For type 2, constants A, then B are given, satisfying the following equation:

$$k = A e^{B/T}$$

For type 3, constants k_0 , m_0 , k_∞ and m_∞ are given, such that:

$$k = \frac{k_0 T^{m_0} [M]}{1 + [k_0 T^{m_0} [M] / k_\infty T^{m_\infty}]} F^z$$

where

$$z = 1 + \log_{10} \frac{k_0 T^{m_0} [M]}{k_\infty T^{m_\infty}} F^{-1}$$

$$F = 0.60$$

$$[M] = 7.413 \times 10^{21} \frac{P}{T}$$

and $[M]$ is the concentration of air in molecules/cm³.

Rate constant type 4 is used for water dependent rate constants. It follows the same form as those for type 2. This type must be used for the case when 2 reactants are also reacting with H2O, since the maximum number of reactants is 2. If the rate constant

is a constant, instead of using type 1 for 2 species reacting with water, use type 2 with B = 0. The rate constant will be multiplied by the concentration of water.

Spaces must separate different components of the equation line. A plus sign (“+”) is used to separate species, a minus sign followed by a greater-than sign (“->”) must be used to denote the end of the reactants and the beginning of the products and a semi-colon (“;”) begins the rate constant information.

An example equation section is shown in Figure 2-7. In the example, k1 is radiation dependent, k2 = 2.28e-10, k3 = 1.40e-03*exp(1175/T), k4 is given by the temperature-pressure dependent equation above with = 4.50e-23, = -3.3, = 1.50e-12 and = 0, and k5 = [H2O]*2.20e-38*exp(5800/T). The concentration and time units of the rate constants must be the same for all and are specified in the control section. The maximum number of reactions is 100.

A reaction will be modeled as turbulent if a “t” is placed in front of the equation number. A correlation between the two reactants will be evaluated and used in determining the reaction rate. If this option is used, both reactants must be specified as “fast” in the species section.

```
#Equations
1  [O3] -> [O] ; 0
2  [O1D] + [H2O] -> (2.0) [OH] ; 1 2.28e-10
3  [O] -> [O3] ; 2 1.40e-3 1175.
4  [OH] + [SO2] -> [SULF] + [HO2] ; 3 4.50e-23 -3.3 1.5e-12 0.0
5  (2.0) [HO2] -> [H2O2] ; 4 2.20e-38 5800.
```

Figure 2-7. Sample Equation Section of the IMC file.

Staged Chemistry

To minimize the computational burden for a multicomponent project that is simulating the formation of ozone through the interaction of emitted nitric oxide (NO) and ambient Volatile Organic Compounds (VOCs), the reactions can be partitioned in stages. The first stage contains the smallest number of reactions. The second stage contains the reactions from first stage, as well as additional reactions, and is the stage

where acid formation is important. The final stage is the stage where ozone formation is important and this stage contains all reactions. The criteria for advancing the puff chemical stage are shown in Table 2-5.

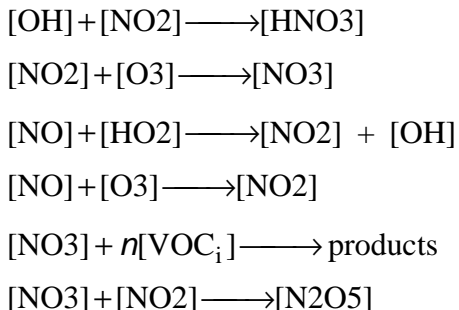
Table 2-5. Staged Chemistry Switching Criteria

	Day	Night
Stage 1 to Stage 2 (Acid formation)	$[\text{OH}] \geq \frac{P_{\text{hno3}}}{k_1}$ <p>where</p> $[\text{OH}] + [\text{NO}_2] \xrightarrow{k_1} [\text{HNO}_3]$	<p>Day criteria or</p> $[\text{O}_3] \geq \frac{P_{\text{no3}}}{k_2}$ <p>and</p> $[\text{NO}_3] \geq C_{\text{no3}}$ <p>where</p> $[\text{NO}_2] + [\text{O}_3] \xrightarrow{k_2} [\text{NO}_3]$
Stage 2 to Stage 3 (Ozone formation)	$\frac{k_3[\text{HO}_2]}{k_4[\text{O}_3]} \geq R_{\text{HO}_2/\text{O}_3}$ <p>and</p> $[\text{O}_3] \geq C_{\text{o}_3}$ <p>where</p> $[\text{NO}] + [\text{HO}_2] \xrightarrow{k_3} [\text{NO}_2] + [\text{OH}]$ <p>and</p> $[\text{NO}] + [\text{O}_3] \xrightarrow{k_4} [\text{NO}_2]$	<p>Day criteria or</p> $\frac{\sum k_i[\text{VOC}_i]}{k_5[\text{NO}_2]} \geq R_{\text{VOC}/\text{NO}_2}$ <p>and</p> $[\text{NO}_3] \geq C_{\text{no3}}$ <p>where</p> $[\text{NO}_3] + [\text{VOC}_i] \xrightarrow{k_i} \text{products}$ <p>and</p> $[\text{NO}_3] + [\text{NO}_2] \xrightarrow{k_5} [\text{N}_2\text{O}_5]$
<p>Note: Reaction numbers shown above are used for demonstration purposes only and are not required reaction numbers. There are no required reaction numbers.</p>		

Phno3, *Pno3*, *Rho2o3*, *Rvocno2*, *Co3*, *Cno3* and *VOC* names are specified on input in the control section of the IMC file (see Section 2.5.1). Requirements for the use of the staged chemistry include having specific species defined in the Equation Section and the reactions appearing above in the Equation Section.

Required species are: NO, NO2, NO3, N2O5, HNO3, O3, OH, HO2, and VOCs.

Required reactions are the following:



Equations for a stage must be followed by a minus sign, '-', or a dashed line. There must be 3 stages shown in the equations section when using staged chemistry. The example IMC file in the Appendix shows a staged chemical mechanism.

2.5.5 Multicomponent Table Section.

Radiation dependent rate constants appear in the table section. The table is of the form:

0, zenith angles(i) , i = 1, no. zenith angles
 equation number, radiation constants(i), i = 1, no. zenith angles

A zero in the equation number field will indicate that the values to follow are the zenith angles. Each line must begin with a zero or an equation number.

#Table				
0	0.0	30.0	60.0	88.0
1	4.83e-4	4.54e-4	3.55e-4	1.00e-10

Figure 2-8. Sample Table Section of the IMC file.

An example of a radiation constant table is shown in Figure 2-8. In the example, $k_1 = 3.55e-4$ at a zenith angle of 60 degrees. The zenith angle is 0 degrees at noon and 90 degrees at sunrise and sunset. The maximum number of zenith angles that can be input are 20. The radiation dependent rate constants are set to zero before sunrise and after

sunset. Every equation that has a rate constant type 0 must have a corresponding entry in the table section.

2.6 SAMPLER LOCATION FILE.

Time history of concentration at a set of sampler locations can be obtained by specifying a sampler location file on the input data (Section 2.1). The location file is an ASCII text file containing the concentration variable of interest and a set of coordinate locations. The format for the file is:

matname, igrp : Material name (CHARACTER) and subgroup identifier (INTEGER*4), free format but separated by white space. The material name must correspond to one of the names defined in the *MATDEF* namelists in the input file (Section 11.1.2). The subgroup identifier is optional and can be used to select a particular size group for a particle material. A value of zero (default value if **igrp** is missing) implies total concentration for the specified material, i.e., sum over all subgroups.

x, y, z : List of sampler locations (one per line) free format. The horizontal location is in project coordinates; the vertical location is in meters above ground level.

The sample file illustrated in Figure 2-9 defines sampler out put for the gas material TRAC at 5 locations. Assuming the project is in lat/lon coordinates, there are 3 samplers on an East-West line at 38°N from 105°W to 107°W all at 2m above the ground, and 2 more samplers at 4m and 8m height at (105°W, 38°N).

TRAC 1
-105. 38. 2.
-106. 38. 2.
-107. 38. 2.
-105. 38. 4.
-105. 38. 8.

Figure 2-9. Example PC-SCICHEM sampler location file.

3 METEOROLOGY INPUT.

3.1 OBSERVATION FILE FORMAT.

A meteorological observation input file consists of a header section that specifies the file type, the number of observation variables, their names and units, followed by the numerical data.

```
[# comment]
...
ftype
nvar [nvarp]
name1 name2 name3 ... namenvar
unit1 unit2 unit3 ... unitnvar
[pname1 pname2 pname3 ... pnamenvarp]
[punit1 punit2 punit3 ... punitnvar]
missing [zref]
```

Figure 3-1. Header structure for a meteorology observation file. Records and variables in brackets are optional or required only if **nvarp** is given.

The header structure is shown in Figure 3-1 and individual records are described in the following.

comment : Optional comments are indicated by '#' in the first column. There is no limit to the number of comment lines.

ftype : The file type which can be 'PROFILE' or 'SURFACE'. (Only these two types are recognized by SCICHEM.) A *SURFACE* file has only one observation for each station and is typically associated with near-surface measurements of wind and/or boundary layer parameters such as surface heat flux or mixing-layer height. A *PROFILE* file generally has more than one observation height at a station and is used when vertical profiles of wind, temperature, etc. are available, e.g. from upper air soundings.

nvar : The number of observation variables given in the file, read with free format. If **nvarp** is given, then **nvar** is the number of fixed variables for a *PROFILE* file. Fixed variables are not functions of height and these are indicated in Table 11-1. **nvar** must be at least 4 (station id, time and horizontal position are the minimum requirements). **nvar** + **nvarp** cannot exceed 30 for a *PROFILE* file; **nvar** cannot exceed 22 for a surface file.

nvarp : The number of profile observation variables, read with free format. This is an option for *PROFILE* files only. Profile variables typically vary with height. Examples are height, pressure, temperature, humidity and wind velocity. The minimum number is 3 (height and velocity).

name₁, ... , name_{nvar} : The observation variable names are read using **(30a8)** format. There must be **nvar** names specified and the order here determines the order in which variables are given in each record of the numerical data. Names recognized in SCICHEM are defined in Table 3-1; multiple specific names indicate synonyms. Other names will be ignored without causing an error so that input files with variables not needed in SCICHEM may still be used. If **nvarp** is given, these are the names of the fixed variables. Acceptable fixed variable names are indicated in Table 3-1. Not all combinations of recognized variable names are permitted. This is discussed below.

unit₁, ... , unit_{nvar} : The observation variable units are read using **(30a8)** format. Only certain variables require that units be specified; otherwise blank spaces are acceptable. Variables requiring units are indicated in Table 3-1 along with those units recognized by SCICHEM. An error message is given if a unit is unrecognized (but only for those requiring units).

pname₁, ... , pname_{nvarp} : The profile observation variable names are read as described for **name**, if **nvarp** is given. There must be **nvarp** names specified.

punit₁, ... , punit_{nvarp} : The profile observation variable units are read as described for **unit**, if **nvarp** is given.

missing : A character string of up to 8 characters used to indicate a missing or bad value in the numerical data.

zref : Optionally, the reference height in meters above the surface can be specified for *SURFACE* observations. If the reference height is omitted, a standard value of 10m is assumed, unless the height for each observation is specified in the data record.

The minimum requirements for meteorological observation files are that the station ID, time, location, wind speed and height (for a *PROFILE* file only) must be specified. Additionally, if certain input options are chosen, such as observational large-scale variability or observational or profile boundary layer then specific combinations of variables must be given. In particular, then, the following variables (or some combination thereof) are required as a minimum:

- 1) ID,
- 2) time (TIME, HOUR, YEAR, MONTH, DAY, YYMMDD, JDAY),
- 3) wind velocity (U, V, WSPD, SPEED, SPD, DIR, WDIR),
- 4) horizontal location (X, Y, LON, LAT),
- 5) Z if file type is PROFILE,
- 6) UL, VL and UVL if observational large-scale variability is specified (ENSM_TYPE='OBS'),
- 7) Both ZI and HFLUX together or PGT or MOL if observational boundary layer is specified (BL_TYPE='OBS'),
- 8) UU, VV, WW, WT, SL, and SZ if profile boundary layer is specified (BL_TYPE='PROF').

Cloud names are read with (A5,1.1) format to determine which cloud droplet size section the variable refers to, however, if *ncl*d (specified on the MSC file) is 1, either 'CLOUD' or 'CLOUD1' may be given in the header. If *ncl*d is less than the number of sections given on the observation file, a warning is displayed and the sections greater than *ncl*d will be ignored.

Some combinations of variables, particularly those concerning time, are not allowed, are mutually exclusive or result in some of the variables being ignored. Also, the presence or absence of certain variables dictates that others be given. These situations are now enumerated:

- 1) Specifying TIME supersedes HOUR, DAY, MONTH, YEAR, YYMMDD and JDAY. No error message is given, but all other time variables are ignored.

- 2) HOUR must be specified in the absence of TIME. HOUR must be combined with either YYMMDD, the combination of DAY, MONTH, YEAR or JDAY. Note that YYMMDD supersedes DAY, MONTH, YEAR, which supersedes JDAY. All three variables DAY, MONTH and YEAR must be given together.
- 3) X and Y must be specified together. X and Y supersede LON and LAT.
- 4) LON and LAT must be specified together and are required if X and Y are not given.
- 5) U and V must be specified together. U and V supersede WSPD, etc. and DIR or WDIR.
- 6) WSPD, etc. and DIR or WDIR must be specified together and are required in the absence of U and V.
- 7) UL, VL and UVL must be specified together. These can only be used in combination with U and V; an error occurs if they are used with WSPD and WDIR.
- 8) MOL supersedes PGT and HFLUX; PGT supersedes HFLUX.

The numerical data are given after the header section in the order dictated by the list of variable names. The general structure of the numerical data is shown in Figure 3-2. If **nvarp** is given, individual profiles must be separated by the fixed data record, which must begin with the string "ID:". Vertical profiles must be given with height monotonically increasing. This is also true for time and it is further necessary that all observations at a particular time be grouped together. All **nvar** and **nvarp**, if applicable, variables for each station and/or height at a particular time must be contained on a single line of no more than 256 characters. The figure illustrates that all nz heights for station id_1 at $time_1$ are given before station id_2 and that data from all $nsta$ stations at $time_1$ are given before $time_2$.

Table 3-1. Meteorological variables and their units recognized in SCICHEM.

Variable Description	Specific Name	Units
Station ID ^{1,2}	ID	None
Time ² (intended for laboratory or other idealized situations where date and time of day is irrelevant)	TIME	HOURS HRS MIN SEC
Time of Day ²	HOUR	HOURS ³
Year ²	YEAR	None
Month ²	MONTH	None
Day ²	DAY	None
Year-Month-Day ²	YYMMDD	None
Julian Day ²	JDAY	None
X-location ²	X	KM ³
Y-location ²	Y	KM ³
Longitude ²	LON	E ⁴ W
Latitude ²	LAT	N ⁴ S
Wind Speed	WSPD or SPEED or SPD	KNOTS KTS M/S MPH
Wind Direction	DIR or WDIR	DEG ³

Table 3-1. Meteorological variables and their units recognized in SCICHEM.

Variable Description	Specific Name	Units
Velocity along X- or Longitude-Axis	U	KNOTS KTS M/S MPH
Velocity along Y- or Latitude-Axis	V	KNOTS KTS M/S MPH
Height	Z	M FEET FT
Pressure	P	MB ³
Temperature	T	C K F
Humidity	H HUMID Q	GM/GM G/G GM/KG G/KG %
Boundary Layer Mixing Height ²	ZI	M FEET FT
Pasquill-Gifford-Turner Stability Class ²	PGT	None ⁵

Table 3-1. Meteorological variables and their units recognized in SCICHEM.

Variable Description	Specific Name	Units
Surface Heat Flux ²	HFLUX	K-M/S C-M/S W/M/M W/M2
Monin-Obukhov Length ²	MOL	M
Precipitation. Index ^{2,6}	PRCP	None
Precipitation Rate ^{2,7}	PRATE	MM/HR
Fractional Cloud Cover ²	FCC	None
Cloud Liquid Water Content ⁸	CLOUD or CLOUD1 to CLOUD <i>n</i> cl <i>d</i>	G/M3
U-Velocity Std. Deviation, Large-Scale Variability	UL	KNOTS KTS M/S MPH
V-Velocity Std. Deviation, Large-Scale Variability	VL	KNOTS KTS M/S MPH
Large-Scale Variability Velocity Correlation Coefficient	UVL	None
Shear-Driven Lateral Velocity Variance	UU	M2/S2
Shear-Driven Lateral Velocity Variance	UU	M2/S2

Table 3-1. Meteorological variables and their units recognized in SCICHEM.

Variable Description	Specific Name	Units
Buoyancy-Driven Lateral Velocity Variance	VV	M2/S2
Vertical Velocity Variance	WW	M2/S2
Boundary Layer Heat Flux	WT	K-M/S C-M/S
Turbulence Scale (Buoyancy-Driven)	SL	M
Turbulence Scale (Shear-Driven)	SZ	M

Notes:

- ¹ ID can be an 8 character alphanumeric string if it is the first variable given, otherwise it must be an integer.
- ² variable can be specified as fixed data on a *PROFILE* file.
- ³ unit assumed regardless of input.
- ⁴ default unit if none specified.
- ⁵ standard PGT classes converted to numerical values, i.e. class A = 1, B = 2, ..., G = 7 (non-integer values are permitted).
- ⁶ precipitation index specified as follows: light rain 1, moderate rain 2, heavy rain 3, light snow 4, moderate snow 5 and heavy snow 6.
- ⁷ precipitation rate only specifies a liquid form of precipitation (i.e., not frozen).
- ⁸ if *ncl* is 1, variable may be specified as either CLOUD or CLOUD1.

```

var1 ... id1    ... time1 ... z1    ... varnvar      (a)
...
var1 ... id1    ... time1 ... znz ... varnvar
var1 ... id2    ... time1 ... z1    ... varnvar
...
var1 ... idnsta ... time1 ... znz ... varnvar
var1 ... id1    ... time2 ... z1    ... varnvar
...

```

```

ID: id1... time1 ... varnvar      (b)
var1 ... z1 ... varnvarp
...
var1 ... znz ... varnvarp
ID: id2... time1 ... varnvar
var1 ... z1 ... varnvarp
...
var1 ... znz ... varnvarp
...
ID: idnsta... time1 ... varnvar
var1 ... z1 ... varnvarp
...
var1 ... znz ... varnvarp
...
ID: id1... time2... varnvar
var1 ... z1 ... varnvarp
...
var1 ... znz ... varnvarp
...

```

Figure 3-2. General structure of the numerical data in a meteorological observation file. (a) Without **nvarp** specified; (b) with **nvar** fixed variables and **nvarp** profile variables.

3.2 MEDOC FORMAT.

A MEDOC file contains a header section followed by numerical data for each time. A sample Fortran code that reads the data for a single time break is illustrated in Figure 3–3. The first record must be either ‘FFFFFFFF’ for a formatted file or ‘BBBBBBBB’ for a binary file. The binary file is read with code identical to that shown in Figure 3–3, absent the format statements. The definitions of the input variables for the rest of the records are as follows:

IMAX, JMAX, KMAX : Number of grid points in the (x , y , z) directions, respectively.

NREPER : Number of special points. This information is not used for the SCICHEM input and NREPER can be set to zero.

NVAR3D : Number of three-dimensional fields.

NAM3D : Names of the three-dimensional variables. SCICHEM requires at least the 2 horizontal velocity component fields, with the names ‘U’, ‘V’. SCICHEM will also read the vertical velocity component, ‘W’ (required if terrain elevation is given as a two-dimensional field), potential temperature ‘T’ or absolute temperature ‘TA’. In addition, humidity ratio, ‘H’, and cloud liquid water content, ‘CLD’ or ‘CLD1’ to ‘CLD n cl d ’ may be specified. Velocities are assumed to be in ms^{-1} , temperature in $^{\circ}\text{K}$ and humidity and cloud liquid water content in grams moisture per grams dry air. Cloud names are read with (A3,1.1) format to determine which cloud droplet size section the variable refers to, however, if n cl d (specified on the MSC file) is 1, ‘CLD’ may be given in the header. If n cl d is less than the number of sections given on the MEDOC file, a warning is displayed and the sections greater than n cl d will be ignored. All other names are ignored.

NVAR2D : Number of two-dimensional fields.

NAM2D : Names of the two-dimensional variables. SCICHEM recognizes the following two-dimensional fields if provided: terrain elevation in meters (required if vertical velocity is given), ‘REL’ or ‘TOPO’; planetary boundary layer height (above surface) in meters, ‘ZI’ or ‘PBL_HITE’; surface heat flux in watts per square meter, ‘HFLX’ or ‘SFC_HTFX’, precipitation rate in millimeters per hour, ‘PRATE’ or ‘PRECIP’, and fractional cloud cover, ‘FCC’ or ‘CC’. All other variables are ignored.

```

C      RECORD 1 - FILE FORMAT ('FFFFFFF' or 'BBBBBBB')
      READ (1,9001) FFLAG
C
C      RECORD 2 - NAME OF CODE - NOT USED IN SCICHEM
      READ (1,9001) CODENAME
C
C      RECORD 3 - TIME
      READ (1,9002) IDAY,IMONTH,IYEAR,IHOUR,IMIN,ISEC
C
C      RECORD 4 - INITIAL TIME OF CALCULATION - NOT USED IN SCICHEM
      READ (1,9002) JDAY,JMONTH,JYEAR,JHOUR,JMIN,JSEC
C
C      RECORD 5 - NUMBER OF GRID POINTS, KEY POINTS, VARIABLES
      READ (1,9002) IMAX,JMAX,KMAX,NREPER,NVAR3D,NVAR2D
C
C      RECORD 6 - NOT USED FOR SCICHEM
      READ (1,9002) IDUM,IDUM,IDUM,IDUM,IDUM,IDUM
C
C      RECORD 7 - NOT USED FOR SCICHEM
      READ (1,9002) IDUM,IDUM,IDUM
C
C      RECORD 8 - GRID AND TIMING INFORMATION (KMAX+11 VALUES)
      READ (1,9003) (SZ(K),K=1,KMAX),DX,DY,XO,YO,LAT,LON,
&                  DUM,DUM,DUM,DUM,ZTOP
C
C      RECORD 9 - NAMES AND UNITS (NREPER+2*NVAR3D+2*NVAR2D VALUES)
      READ (1,9001) (NAMDUM,N=1,NREPER),
&                  (NAM3D(N),N=1,NVAR3D),(NAMDUM,N=1,NVAR3D),
&                  (NAM2D(N),N=1,NVAR2D),(NAMDUM,N=1,NVAR2D)
C
C      RECORD 10 - NOT USED IN SCICHEM
      READ (1,9003) (DUM,N=1,3*NREPER)
C
C      RECORD 11 - 3D VARIABLES
&                  (NVAR3D SETS OF IMAX*JMAX*KMAX VALUES)
      DO 21 N=1,NVAR3D
21      READ (1,9003) ((VAR3D(I,J,K,N),I=1,IMAX),J=1,JMAX),K=1,KMAX)
C
C      RECORD 12 - 2D VARIABLES (NVAR2D SETS OF IMAX*JMAX VALUES)
      DO 41 N=1,NVAR2D
41      READ (1,9003) ((VAR2D(I,J,N),I=1,IMAX),J=1,JMAX)
C
9001 FORMAT(6(A8,1X))
9002 FORMAT(6(I12,1X))
9003 FORMAT(6(F12.4,1X))

```

Figure 3-3. Fortran pseudo-code for reading a formatted MEDOC input file.

SZ : Array of **KMAX** vertical grid coordinates in meters. **SCICHEM** assumes a terrain-following coordinate transformation as described in Section 8.3.2.

DX, DY : Horizontal grid spacing in meters.

XO, YO : Horizontal grid origin (SW corner) coordinates in km.

LAT, LON : Horizontal grid origin (SW corner) coordinates in degrees.

ZTOP : Vertical meteorology domain height in meters. If the parameter is not specified, the domain height is assumed to be **SZ(KMAX)**.

The MEDOC file format described in Figure 3-3 is more general than that used by SCICHEM. Variables not used in the SCICHEM application are indicated as dummy variables in the figure.

3.3 HPAC FORMAT.

An HPAC file contains a header section specifying grid parameters and the number of variables, followed by the numerical data. The general format structure is illustrated in Figure 3-4.

The header variables in the first record are read with a **(4f10.0, 5i5)** format and are defined as follows:

xlon0, xlat0 : Origin of the longitude/latitude grid (lower left corner) in degrees E and N, respectively.

dx, dy : Grid spacing in degrees of longitude and latitude, respectively.

nx, ny : Number of grid points in the longitude and latitude directions, respectively.

nz : Number of vertical grid levels.

nt : Number of time breaks.

nvar : Number of variables. If **nvar** = 4, the field variables are assumed to be, in order, *u*-wind component (east-west, ms^{-1}), *v*-wind component (north-south, ms^{-1}), temperature ($^{\circ}\text{C}$) and relative humidity (%). If **nvar** = 5, the field variables are assumed to be, in order, *u*-wind component (east-west, ms^{-1}), *v*-wind component (north-south, ms^{-1}), vertical velocity (ms^{-1}), temperature ($^{\circ}\text{C}$) and relative humidity (%). Also, if

nvar = 5, SCICHEM checks if a terrain elevation file exists. This is discussed below. If **nvar** is missing, the default value is 4 and the field variables are assumed accordingly.

```

xlon0, xlat0, dx, dy, nx, ny, nz, nt, nvar
z1, z2, ... znz
p1, p2, ... pnz
(month, day, year, time)1
  title1
    var1((((i, j, k), i=1, nx), j=1, ny), k=1, nz)
    ...
  titlenvar
    varnvar((((i, j, k), i=1, nx), j=1, ny), k=1, nz)
(month, day, year, time)2
  title1
    var1((((i, j, k), i=1, nx), j=1, ny), k=1, nz)
    ...
  titlenvar
    varnvar((((i, j, k), i=1, nx), j=1, ny), k=1, nz)
(month, day, year, time)nt
...

```

Figure 3-4. General structure of an HPAC file.

The next record(s) gives the **nz** vertical grid levels, read using **(10f8.0)** format. The following record(s) contains the corresponding pressures and is also read with **(10f8.0)** format.

The numerical data follows the first three records (or $3 + 2 * \text{int}[(\mathbf{nz} - 1) / 10]$ if **nz** > 10). As illustrated in Figure 3-4, each time break is headed by a record giving **month**, **day**, **year**, **hour**, and **minutes**, read with **(1x, i2, 1x, i2, 1x, i2, ix, i2, i2)** format. Figure 3-4 also shows that a title record, read with **(a12)** format, precedes the data for each field variable. This record normally contains the field variable name and units, but SCICHEM does not check consistency between this title and the assumed variables and order described above. The field data itself is read using **(10f8.0)** format so that the number of records for each field is $\text{int}[(\mathbf{nx} * \mathbf{ny} * \mathbf{nz} - 1) / 10] + 1$. The indexing order of the fields is shown in Figure 3-4.

3.4 TERRAIN FILE FORMAT.

The terrain input file is an ASCII text file containing a grid description header followed by terrain elevation data defined on a regular two-dimensional grid. The header consists of two records:

grid_type, **param1**, **param2** : the grid type (CHARACTER*8) can be 'LATLON', 'UTM', 'KM', 'METERS' or 'M'. If **grid_type** is LATLON, the two numerical parameters are not required. For UTM grids, **param1** (INTEGER) contains the UTM zone number; the other parameter is not required. For all other types, if **param1** (REAL) and **param2** (REAL) are specified, they contain the longitude and latitude of the grid origin, respectively. The numerical parameters are in free format.

x0, **y0**, **dx**, **dy**, **nx**, **ny** : the grid origin (REAL) for the east-west coordinate (**x0**), the grid origin (REAL) for the north-south coordinate (**y0**), grid spacings (REAL) (**dx** and **dy**) and number of grid points in the coordinate directions (INTEGER) (**nx** and **ny**). **x0** and **y0** are in degrees if **grid_type** is LATLON, otherwise they are in kilometers. **dx** and **dy** are in the same units as the origin coordinates unless **grid_type** is METERS or M in which case they are in meters.

The terrain elevation data (in meters) is read using the following Fortran statements:

```
      read (1,1000) ((height(i,j),i=1,nx),j=1,ny)
1000  format(12i6)
```

The location (i, j) is taken to be at $x0+(i-1)*dx$ and $y0+(j-1)*dy$.

3.5 AMBIENT FILE FORMAT.

Three-dimensional time-dependent ambient concentrations may be provided to a multicomponent project. The file is specified in the *ambient_file* parameter in the control section of the IMC file. If this is done, the ambient concentrations given in the species section of the IMC file will be ignored and instead read from the ambient file. Ambient concentrations for all integrated species (fast or slow) must be provided in the order that they appear in the IMC file, followed by the concentrations of ambient species (such as water or oxygen), also in the order that they appear on the IMC file. In other words, the

order will be the list of species as it is given under the species section *excluding* the equilibrium species, since they will be determined internally based on the rate equations.

If the domain goes further than what is provided in the ambient file, SCICHEM will use the nearest point in space. Likewise, if the calculation begins before the time given on the ambient file, the first time will be used and if it begins after the last time on the file, the last time will be used. A three-dimensional ambient file must hold a minimum of one point in space at one time. Units for the concentrations are set in *species_units* under the control section.

To use the relative humidity provided in the meteorological observation file for the concentrations of water, negative concentrations for water must be specified on the 3D ambient file. This will indicate the water concentrations should be calculated internally. If relative humidity is not provided on the observation file, a default value of 30% is assumed.

The 3D ambient file contains a header section followed by numerical data for each time. The general format structure is illustrated in Figure 3-5 which shows the FORTRAN code used to read the file.

```

C      RECORD 1 - NO. OF TIMES, GRID POINTS,
C      GRID SPACING, AND ORIGIN
READ (1,9000)      NT, NX, NY, NZ, DX, DY, DZ, X0, Y0

C      (LOOP OVER TIMES)
      DO N=1,NT

C      RECORD 2 - TIME
C      (YEAR, MONTH AND DAY SPECIFIED IN PROJECTNAME.INP)
      READ (1,9002)  IYEAR, IMONTH, IDAY, HOUR

C      ----OR----

C      RECORD 2 - TIME
C      (YEAR, MONTH AND DAY NOT SPECIFIED IN
C      PROJECTNAME.INP)
      READ (1,9004)  HOUR

C      (LOOP OVER SPECIES)
C      RECORD 3 - 3D AMBIENT DATA
      DO M = 1,NAMB
        READ(1,9005) (((AMB(I,J,K,N,M),I=1,NX),J=1,NY),K=1,NZ)
      END DO

      END DO

9000  FORMAT(4(I4,1X),5(F12.2,1X))
9002  FORMAT(I4,2(I2,2X),F12.4)
9004  FORMAT(F12.4)
9005  FORMAT(6(1PE12.4,1X))

```

Figure 3-5. General structure of an ambient file.

4 OUTPUT FILES.

4.1 SURFACE OUTPUT FILES.

If deposition or dose parameters are set to true in the material definition (*group_deposition*, *total_deposition*, *group_dose*, and *total_dose* under the MATDEF namelist of the INP file, see Section 2.2), the surface integrals of dose and deposition are stored as adaptive grid files with multiple timebreaks. The dose integral, χ_T , is stored in the surface file, *project.dos*, and the deposition, χ_D , in *project.dep*. These files are direct-access binary files with a record length of 512 bytes (128 words), and consist of a number of timebreaks. Each timebreak contains a header record followed by the field data. The Fortran statements to write a timebreak are illustrated in Figure 3-5.

```
C----- HEADER RECORD
      write(nwrt,rec=ir) time, ngrid, nx, ny, xorg, yorg, dx, dy,
      $                  nvar, (names(i),i=1,nvar), iversion

C----- GRID INDEX ARRAY
      do ii = 1,ngrid,128
        j1 = min0(ii+127,ngrid)
        ir = ir + 1
        write(nwrt,rec=ir) (iref(j), j=ii,j1)
      end do

C----- FIELD DATA ARRAYS
      do ivar = 1,nvar
        do ii = 1,ngrid,128
          j1 = min0(ii+127,ngrid)
          ir = ir + 1
          write(nwrt,rec=ir) (fields(j,ivar), j=ii,j1)
        end do
      end do
```

Figure 3-5. Fortran statements to write a surface output file timebreak.

The header record consists of the variables:

time	(real*4)	time of the field in hours from the beginning of the calculation
ngrid	(integer*4)	total number of grid cells in the adaptive grid. A value of zero indicates the end of the file.

(nx, ny)	(integer*4)	number of base grid points in the (x, y)-direction
(xorg, yorg)	(real*4)	origin coordinates of the base grid
(dx, dy)	(real*4)	grid spacings of the base grid
nvar	(integer*4)	number of field variables
names	(char*4)	array of field variable identifying names
iversion	(integer*4)	PC-SCICHEM version number

The variable names are constructed from the input material list but do not contain direct reference to the material identifier names. The field names are 4-character identifiers, and the first character denotes the type of field. **M** denotes the mean field, **V** denotes the fluctuation variance, and **S** denotes the correlation length scale. Note that the scale variable is multiplied by the fluctuation variance on the output file, since the integral value is weighted by the variance. Units for the various fields are dependent on the type of surface field, but are based on the material mass units (as specified as part of the material properties definitions) and SI units. For gaseous materials or individual particle size bins, the remaining three characters of the name contain the unique type descriptor number, as defined in Section 11.4. For particle materials with multiple size bins, the total particulate mass variables are represented by a two-character integer, containing the material identifier number, and the last character of the name is **T**. The material identifier is simply the position in the list of *MATDEF* namelists in the *ProjectName*.INP file, as described in Section 11.1. Thus, the total mean deposition for the first material in the input file would be named as **M01T**, while the variance of the fifth particle size bin for the first material would be **V005**.

The adaptive grid structure is described by the integer*4 index array, **iref**, and the field data is stored in the real*4 array **fields**. For each grid cell, **iref** points to the first refinement sub-cell, if it exists. If the grid cell, **i**, is not refined, then **iref(i) = 0**. The first **nx*ny** cells are the base grid, so **ngrid** is necessarily greater than or equal to **nx*ny**. The centers of these cells are located at

$$x_i = \mathbf{xorg} + (i - 0.5) * \mathbf{dx}, \quad i = 1, \mathbf{nx}$$

$$y_j = \mathbf{yorg} + (j - 0.5) * \mathbf{dy}, \quad j = 1, \mathbf{ny}$$

and the location (x_i, y_j) corresponds to cell number $(j - 1) * \mathbf{nx} + i$ in the adaptive grid.

If a cell is refined, then the **iref** array contains the grid cell number of the first of four sub-cells with half the grid size of the parent cell. Suppose i_0 is the parent cell number, with grid sizes Δx_0 and Δy_0 and center location (x_0, y_0) . The parent cell may be a base grid cell but is not necessarily so since the refinement process can be continued without limit. The four sub-cells are numbered consecutively as $\{i_1 + k : k = 0, 3\}$ where **iref**(i_0) = i_1 . The sub-cells are numbered as shown in Figure 3-5 (i.e., lower left is zero, then lower right, upper left, upper right), and have center locations

$$(x_0 \pm \Delta x_0/4, y_0 \pm \Delta y_0/4)$$

and grid size $(\Delta x_0/2, \Delta y_0/2)$.

Each cell has a complete set of field variables associated with it, so the local field value has contributions from all levels of refinement. A simple estimate of the field value at a given location (**xp**, **yp**) can be obtained using the pseudo-code illustrated in Figure 3-6. Note that this example uses a recursive subroutine call to scan the list of refinements. The **field** array in the example represents any one of the **nvar** variables in the **fields** array on the file. This estimate simply adds contributions from successive refinement levels without any interpolation across grid cells.

```

xx = (xp-xorg)/dx
yy = (yp-yorg)/dy

i0 = int(yy)*nx + int(xx) + 1

cval = 0.0

call sum_point_val(i0,xx,yy,cval)
c ---- cval contains the local field value
c-----
subroutine sum_point_val(i0,xc,yc,cval)

cval = cval + field(i0)
c *** Check for refinement

if (iref(i0) .ne. 0) then
  xc = 2.*(xc - int(xc))
  yc = 2.*(yc - int(yc))
  i1 = iref(i0) + 2*int(yc) + int(xc)
  call sum_point_val(i1,xc,yc,cval)
end if

return
end

```

Figure 3-6. Fortran statements to calculate field values from the surface output file.

4.2 PUFF FILE.

The puff file, *project.puf*, is a binary file containing the complete puff data at a number of time breaks together with boundary layer and continuous source information for restart purposes. The file is written using the unformatted Fortran write statement:

```

write(lun_puf) t,
$      npuf, ((puff(i).r(j), j=1, 43), i=1, npuf),
$      npaux, (paux(i), i=1, npaux-1),
$      nspecies,
$      nxbl, nybl, dxbl, dybl,
$      xbl(i=1, nxbl), ybl(i=1, nybl),
$      zibl(i=1, nxbl*nybl),
$      ncrel, (c_plen(i), i=1, ncrel),
$      nsrcaux, (src_aux(i), i=1, nsrcaux)

```

where

t	(real*4)	time of the data in seconds from the beginning of the calculation
npuf	(integer*4)	total number of puffs
puff(i).r(*)	(real*4)	floating point data for puff i
npaux	(integer*4)	total number of puff auxiliary data values + 1
paux(*)	(integer*4)	floating point data auxiliary puff data
nspecies	(integer*4)	number of multicomponent chemistry species
nxbl,nybl	(integer*4)	horizontal dimensions of meteorology grid
dxbl,dybl	(real*4)	horizontal grid intervals of meteorology grid
xbl(*),ybl(*)	(real*4)	horizontal grid locations of meteorology grid
zibl(*)	(real*4)	boundary layer depth on meteorology grid
ncrel	(integer*4)	total number of active continuous releases
c_plen(*)	(real*4)	length scale associated with each release
nsrcaux	(integer*4)	total number of source auxiliary data values
src_aux(*)	(real*4)	auxiliary source data

The floating point puff data is stored as follows:

j=1-3	$\bar{x}, \bar{y}, \bar{z}$	puff centroid coordinates
j=4-9	σ_{ij}	puff spread moments, in the order $\sigma_{xx}, \sigma_{xy}, \sigma_{xz}, \sigma_{yy}, \sigma_{yz}, \sigma_{zz}$
j=10-15	α_{ij}	puff inverse moments, in the order $\alpha_{xx}, \alpha_{xy}, \alpha_{xz}, \alpha_{yy}, \alpha_{yz}, \alpha_{zz}$

j=16	$\ \sigma\ $	determinant of the puff spread moments
j=17	Q	puff mass
j=18	$\langle c^2 \rangle$	integrated mean square concentration
j=19	$\langle x' u' c' \rangle_L$	Large-scale diagonal-xx turbulent flux moment
j=20	X_{12}	cross-xy turbulent flux moment
j=21	$\langle y' v' c' \rangle_L$	Large-scale diagonal-yy turbulent flux moment
j=22	$\langle y' v' c' \rangle_B$	Buoyancy-driven diagonal-yy turbulent flux moment
j=23	$\langle y' v' c' \rangle_S$	Shear-driven diagonal-yy turbulent flux moment
j=24	$\langle z' w' c' \rangle$	diagonal-zz turbulent flux moment
j=25	$\langle w' c' \rangle$	vertical turbulent drift moment
j=26	$\langle \bar{c}^2 \rangle$	squared mean concentration from overlap calculation
j=27-28	Λ_c, Λ_{cH}	horizontal concentration fluctuation length scales
j=29	Λ_{cV}	vertical concentration fluctuation length scale
j=30	$2T_c$	correlation time scale for the puff concentration fluctuations
j=31	f_A	linear decay factor
j=32	z_i	local mixed layer depth
j=33	z_c	puff vertical cap height; used to control puff splitting within the planetary boundary layer
j=34-36	$\bar{u}, \bar{v}, \bar{w}$	ambient wind velocity for use with Adams-Bashforth scheme

The following 7 data values are integers stores as floating point values:

j=37	<i>type</i>	an identifier for the puff material and size bin type
j=38-39	<i>next, prev</i>	pointers for the linked list on the spatial grid
j=40	<i>grid</i>	grid refinement level for the spatial grid
j=41	<i>tlev</i>	refinement level for the puff time step
j=42	<i>tnxt</i>	pointers for the linked list for time stepping
j=43	<i>iaux</i>	pointer into the auxiliary array for additional puff data. The number of data values in the array for any given puff

in dependent on the material type and on the overall *dynamics* flags

There may be additional puff data values for each puff, depending on the user's options. These variables would appear in the following order:

j=1	$\langle \bar{c}_T^2 \rangle$	mean square total concentration (for multiple size bin particle materials)
j=2	$\langle \bar{c}_T \rangle^2$	squared mean total concentration (for multiple size bin particle materials)
j=3-10		buoyancy parameters
Next nspectot values		multicomponent species masses
Next nspectot values		multicomponent species puff overlap concentrations
Next ncorrt values		multicomponent species correlations
Next nspectot values		multicomponent species end of chemistry concentrations
j=11+3*nspectot+ncorrt		inverse puff volume
j=12+3*nspectot+ncorrt		puff chemical stage

The puff *type* identifier is simply allocated sequentially in the order that materials are specified in the *ProjectName*.INP file. Thus, the first material is *type* = 1 if it is a gas, or the N_{bin} size bins are *type* = 1 up to *type* = N_{bin} for a particle material. Identifiers for the second material are then allocated beginning with the next available value for *type*.

4.3 SAMPLER TIME-HISTORY FILE.

The sampler time history file is an ASCII text file containing the instantaneous concentration field statistics for the selected material at the locations specified in the sampler location file described in Section 2.6. The output file consists of a header section followed by a single data record for each model time step. The output interval is the large time step as specified in the input file. The header records are

Record 1: The number of variables per data record .

Record 2: A list of variable names(CHARACTER*8), 10 per line.

Record 3: A title string containing the project name

The data records contain the time (in seconds from the start of the calculation) and $3 + n_{spectot}$ (total number of multicomponent species) + n_{corrt} (total number of species correlations) data values for each sampler location:

Data Record: time, $\overline{\theta}, \overline{c'^2}, T_c, \overline{c}_{species}, \overline{c'_A c'_B}$ for location-1, $\overline{\theta}, \overline{c'^2}, T_c, \overline{c}_{species}, \overline{c'_A c'_B}$ for location-2, etc., where $\overline{c}, \overline{c'^2}, T_c$ refer to the tracer where the three data values are mean concentration, concentration variance, and correlation time scale (in seconds), respectively, and $\overline{c}_{species}, \overline{c'_A c'_B}$ refer to the multicomponent species concentrations and species fluctuation correlations, respectively. Species names as they appear on the multicomponent input file are used as variable names for both the mean concentration and the species correlations.

An example of the sampler output file is given in Figure 4-1. The output shows 2 sampler locations, showing 16 variables per record. The output time interval is 10 seconds and the data records shown continue beyond the page width. There are 3 multicomponent species, NO, O3 and NO2.

16	C001	V001	T001	NO01	O301	NO201	C002	V002	T002
T									
NO02	O302	NO202	C002	V002	T002				
Sampler time histories for TRAC for project test									
10.00000	0.0000000E+00								
20.00000	0.0000000E+00								
30.00000	1.0000000E-03	1.2000000E-05	1.0000000E+00	0.0000000E+00	0.0000000E+00	0.0000000E+00	0.0000000E+00	0.0000000E+00	0.0000000E+00
40.00000	1.5000000E-03	2.0000000E-05	1.2000000E+00	0.0000000E+00	0.0000000E+00	0.0000000E+00	0.0000000E+00	0.0000000E+00	0.0000000E+00
50.00000	2.0000000E-03	3.0000000E-05	1.8000000E+00	0.0000000E+00	0.0000000E+00	0.0000000E+00	0.0000000E+00	0.0000000E+00	0.0000000E+00
60.00000	4.0000000E-03	4.0000000E-05	2.0000000E+00	0.0000000E+00	0.0000000E+00	0.0000000E+00	0.0000000E+00	0.0000000E+00	0.0000000E+00
.....									
.....									

Figure 4-1. Example of a sampler output file.

If the reaction between NO and O3 had been specified as turbulent, NOO301 and NOO302 would appear on the output file, and would represent the fluctuation correlation, $\overline{NO' O3'}$. This is used internally in the code to define a turbulent rate factor as:

$$f_t = 1 + \frac{\overline{NO' O3'}}{\overline{NO} \overline{O3}}$$

which multiplies the reaction rate based on the mean concentrations, as follows:

$$r = f_t k \overline{NO} \overline{O3}$$

where k is the reaction rate coefficient and r is the effective reaction rate.

5 REFERENCES.

- Bass, A. (1980), "Modelling long range transport and diffusion", Second Joint Conf. on Appl. of Air Poll. Met., AMS & APCA, New Orleans, LA, pp193-215.
- Donaldson, C. du P. (1973), "Atmospheric turbulence and the dispersal of atmospheric pollutants", *AMS Workshop on Micrometeorology*, ed. D. A. Haugen, Science Press, Boston, pp313-390.
- EPRI (1999), "SCICHEM: A new generation Plume-in-Grid Model", Palo Alto, CA. EPRI Report No. TR-113097.
- Karamchandani, P., A. Koo and C. Seigneur (1998), "A reduced gas-phase kinetic mechanism for atmospheric plume chemistry", *Environ. Sci. Technol.*, **32**, 1709-1720.
- Lewellen, W. S. (1977), "Use of invariant modeling", *Handbook of Turbulence*, ed. W. Frost and T. H. Moulden, Plenum Press, pp237-280.
- Martin, L. R. (1984), "Kinetic studies of sulfite oxidation in aqueous solution", in *SO₂, NO and NO₂ Oxidation Mechanisms: Atmospheric Considerations*. Edited by J. G. Calvert. Butterworth, Stoneham, MA, pp.63-100.
- Martin, L. R. and T. W. Good (1991), "Catalyzed oxidation of sulfur dioxide by hydrogen peroxide at low pH", *Atmos. Environ.*, **25A**, 2395-2399.
- Seinfeld, J.H. (1986). *Atmospheric Chemistry and Physics of Air Pollution*, Wiley, New York.
- Slinn, W. G. N. (1982). "Predictions for particle deposition to vegetative canopies", *Atmos. Environ.*, **16**, 1785-1794.
- Sykes, R. I., W. S. Lewellen, S. F. Parker and D. S. Henn (1988), "A hierarchy of dynamic plume models incorporating uncertainty, Volume 4: Second-order Closure Integrated Puff", EPRI, EPRI EA-6095 Volume 4, Project 1616-28.
- Sykes, R. I., S. F. Parker, D. S. Henn and W. S. Lewellen (1993), "Numerical simulation of ANATEX tracer data using a turbulence closure model for long-range dispersion", *J. Appl. Met.*, **32**, 929-947.

Sykes, R.I., S.F. Parker, D.S. Henn, C.P. Cerasoli and L.P. Santos (1998a). "PC-SCIPUFF Version 1.2PD Technical Documentation", ARAP Report No. 718. Titan Corporation, Titan Research & Technology Division, ARAP Group, P.O. Box 2229, Princeton, NJ, 08543-2229

Sykes, R. I., L. P. Santos and D. S. Henn (1998b), "Large Eddy Simulation of a turbulent reacting plume in a convective boundary layer", *Proc. 10th Conference on Appl. of Air Pollut. Meteor.*, Jan. 11-16, 78th Annual AMS Meeting, Phoenix, AZ, 539-543.

APPENDIX.

EXAMPLE IMC FILE

A sample IMC file is shown below. The equation section shows equations wrapped for the purpose of this display, but these equations must be on one line.

```
#Control
$CONTROL
  aqueous = .true.
  aerosol = .true.
  nsec_aer = 1
  secbnds_aer(1) = 2.5e-6,10.e-6
  rho_aer = 1000.,
  step_ambient = .false.
  emission_units = 'g/s'
  species_units = 'ppm'
  rate_species_units = 'ppm'
  rate_time_units = 'min'
  rtol = 1.e-3
  staged_chem = .true.
  voc_names(1) = 'HCHO', 'ALD2', 'OLE', 'CRES', 'ISOP'
  phno3 = 0.1
  pno3 = 0.1
  cno3 = 1.e-8
  rho2o3 = 0.1
  co3 = 1.e-3
  rvocno2 = 1.0
$END

#Aqueous
$AQUEOUS
  debug = .true.,
  lradical = .true.,
  dactiv = 3.000000e-07,
  fdist = 1.0,
  kiron = 1,
  firon = 1.000000e-02,
  fman = 2.000000e-03,
  chlorine = 1.00000,
  so2min = 1.000000e-06,
  lwcmn = 5.000000e-02,
  atolx = 1.000000e-04,
  rtolx = 1.000000e-03,
  dtmaxsec = 120.000,
  xtol = 1.000000e-03,
$END

#Species,Type,Ambient,Tolerance,deposition vel,wet scav,mw
NO          F          1.0000E-04          1.0000E-08          0.0          0.0          30.01
SO2         F          0.0000E+00          1.0000E-08          0.0          0.0          64.07
NO2         F          1.0000E-05          1.0000E-08          0.0          0.0          46.01
O3          F          3.4000E-02          1.0000E-08          0.0          0.0          48.00
OLE         F          7.0000E-04          1.0000E-08          0.0          0.0          32.00
PAR         F          3.5000E-02          1.0000E-08          0.0          0.0          16.00
```

TOL	F	7.0000E-04	1.0000E-08	0.0	0.0	112.00
XYL	F	0.0000E+00	1.0000E-08	0.0	0.0	128.00
FORM	F	3.0000E-03	1.0000E-08	0.0	0.0	30.03
FA	F	3.0000E-03	1.0000E-08	0.0	0.0	46.03
ALD2	F	5.0000E-04	1.0000E-08	0.0	0.0	32.00
ETH	F	2.0000E-03	1.0000E-08	0.0	0.0	32.00
CRES	F	0.0000E+00	1.0000E-08	0.0	0.0	16.00
MGLY	F	0.0000E+00	1.0000E-08	0.0	0.0	16.00
OPEN	F	0.0000E+00	1.0000E-08	0.0	0.0	16.00
PAN	F	2.0000E-04	1.0000E-08	0.0	0.0	121.00
CO	S	2.0000E-01	1.0000E-08	0.0	0.0	28.00
HONO	F	0.0000E+00	1.0000E-08	0.0	0.0	47.00
H2O2	F	1.0000E-03	1.0000E-08	0.0	0.0	34.00
HNO3	F	1.0000E-03	1.0000E-08	0.0	0.0	63.00
ISOP	F	1.0000E-03	1.0000E-08	0.0	0.0	80.00
SA	F	0.0000E+00	1.0000E-08	0.0	0.0	98.00
CRUS	P	0.9500E+00	1.0000E-08	0.0	0.0	99.99
ASO4	P	0.9500E+00	1.0000E-08	0.0	0.0	96.00
ANO3	P	0.9500E+00	1.0000E-08	0.0	0.0	62.00
ANH4	P	0.9500E+00	1.0000E-08	0.0	0.0	18.00
ANA	P	0.39316240	1.0000E-08	0.0	0.0	23.00
ACL	P	0.60683760	1.0000E-08	0.0	0.0	35.50
AMG	P	0.0000E+00	1.0000E-08	0.0	0.0	55.00
ACA	P	0.0000E+00	1.0000E-08	0.0	0.0	40.00
APOT	P	0.0000E+00	1.0000E-08	0.0	0.0	39.00
HCL	S	4.0000E-04	1.0000E-08	0.0	0.0	36.50
NH3	S	1.0000E-03	1.0000E-08	0.0	0.0	17.00
NO3	E	0.0000E+00	1.0000E-12	0.0	0.0	99.99
N2O5	E	0.0000E+00	1.0000E-12	0.0	0.0	99.99
C2O3	E	0.0000E+00	1.0000E-12	0.0	0.0	99.99
XO2	E	0.0000E+00	1.0000E-12	0.0	0.0	99.99
XO2N	E	0.0000E+00	1.0000E-12	0.0	0.0	99.99
CRO	E	0.0000E+00	1.0000E-12	0.0	0.0	99.99
O	E	0.0000E+00	1.0000E-12	0.0	0.0	99.99
OH	E	0.0000E+00	1.0000E-12	0.0	0.0	99.99
O1D	E	0.0000E+00	1.0000E-12	0.0	0.0	99.99
HO2	E	0.0000E+00	1.0000E-12	0.0	0.0	99.99
ROR	E	0.0000E+00	1.0000E-12	0.0	0.0	99.99
TO2	E	0.0000E+00	1.0000E-12	0.0	0.0	99.99
CO2	A	3.5000E+02	1.0000E-08	0.0	0.0	44.00
H2O	A	-1.0	1.0000E-06	0.0	0.0	18.02

#Table

	0.	15.	30.	45.	60.	75.
0	0.	15.	30.	45.	60.	75.
80.	86.	87.	88.			
1	5.4420E-01	5.3460E-01	5.0520E-01	4.4820E-01	3.5040E-01	1.8120E-01
	4.1280E-02	6.0000E-04	6.0000E-09	6.0000E-09		
23	1.0320E-01	1.0140E-01	9.5400E-02	8.4000E-02	6.4200E-02	3.1740E-02
	7.2000E-03	6.0000E-05	6.0000E-09	6.0000E-09		
8	2.8980E-02	2.8560E-02	2.7240E-02	2.4960E-02	2.1300E-02	1.5000E-02
	5.6820E-03	6.0000E-05	6.0000E-09	6.0000E-09		
9	2.1300E-03	1.9620E-03	1.5180E-03	9.0000E-04	3.2760E-04	3.2520E-05
	5.1180E-07	6.0000E-09	6.0000E-09	6.0000E-09		
31	4.9560E-04	4.7880E-04	4.2900E-04	3.4380E-04	2.2440E-04	8.3400E-05
	1.5360E-05	6.0000E-07	6.0000E-09	6.0000E-09		
42	2.6040E-04	2.4600E-04	2.0580E-04	1.4400E-04	7.3200E-05	1.6380E-05
	1.4580E-06	6.0000E-08	6.0000E-09	6.0000E-09		
35	1.9260E-03	1.8540E-03	1.6380E-03	1.2840E-03	7.8600E-04	2.5080E-04
	3.6360E-05	6.0000E-07	6.0000E-09	6.0000E-09		
36	3.1200E-03	3.0420E-03	2.7960E-03	2.3460E-03	1.6440E-03	6.7200E-04
	1.3740E-04	6.0000E-06	6.0000E-12	6.0000E-12		

```

14 1.14E+01    1.128E+01    1.086E+01    1.02E+01    8.94E+00    6.42E+00
2.238E+00    6.0000E-03    6.0000E-09    6.0000E-09
71 8.8200E-03    8.7000E-03    8.3400E-03    7.6800E-03    6.4800E-03    4.0140E-03
1.0260E-03    6.0000E-05    6.0000E-09    6.0000E-09
66 1.7411E-02    1.6760E-02    1.4808E-02    1.1607E-02    7.1054E-03    2.2672E-03
3.2869E-04    5.4240E-06    5.4240E-08    5.4240E-08
#Equations -- from ROME
20 [NO] + [NO] -> (2.00) [NO2] ; 2 2.599E-05 5.3000E+02
3 [NO] + [O3] -> [NO2] ; 2 2.643E+03 -1.3700E+03
1 [NO2] -> [NO] + [O] ; 0 0.000E+00 0.0000E+00
2 [O] -> [O3] ; 2 8.383E+04 1.1750E+03
-----
8 [O3] -> [O] ; 0 0.000E+00 0.0000E+00
9 [O3] -> [O1D] ; 0 0.000E+00 0.0000E+00
10 [O1D] -> [O] ; 2 1.148E+10 3.9000E+02
11 [O1D] + [H2O] -> (2.00) [OH] ; 2 3.260E+05 0.0000E+00
22 [NO] + [OH] -> [HONO] ; 2 6.555E+02 8.0600E+02
23 [HONO] -> [NO] + [OH] ; 0 0.000E+00 0.000E+00
26 [NO2] + [OH] -> [HNO3] ; 2 1.5370E+03 7.1300E+02
28 [NO] + [HO2] -> [NO2] + [OH] ; 2 5.484E+03 2.4000E+02
31 [H2O2] -> (2.00) [OH] ; 0 0.0000E+00 0.0000E+00
35 [HCHO] -> (2.00) [HO2] + [CO] ; 0 0.0000E+00 0.0000E+00
36 [HCHO] -> [CO] ; 0 0.0000E+00 0.0000E+00
42 [RHCO] -> [XO2] + (2.00) [HO2] + [CO] + [HCHO]; 0 0.00E+00 0.00E+00
79 [SO2] + [OH] -> [SA] + [HO2]; 2 6.489E+02 1.60E+02
44 [C2O3] + [NO2] -> [PAN]; 2 3.840E+03 3.8000E+02
45 [PAN] -> [C2O3] + [NO2]; 2 1.2000E+18 -1.3500E+04
43 [C2O3] + [NO] -> [NO2] + [XO2] + [HCHO] + [HO2] ; 2 5.150E+04 -1.80E+02
7 [NO2] + [O3] -> [NO3] ; 2 1.760E+02 -2.4500E+03
14 [NO3] -> (0.89) [NO2] + (0.89) [O] + (0.11) [NO] ; 0 0.00E+00 0.00E+00
15 [NO] + [NO3] -> (2.00) [NO2] ; 2 1.909E+04 2.5000E+02
16 [NO3] + [NO2] -> [NO] + [NO2] ; 2 3.660E+01 -1.2300E+03
17 [NO3] + [NO2] -> [N2O5] ; 2 7.849E+02 2.5600E+02
19 [N2O5] -> [NO3] + [NO2] ; 2 2.110E+16 -1.0897E+04
18 [N2O5] + [H2O] -> (2.00) [HNO3] ; 2 1.900E-06 0.0000E+00
76 [XO2] + [NO] -> [NO2]; 1 1.2000E+04 0.0000E+00
77 [XO2] + [XO2] ->; 2 2.5500E+01 1.3000E+03
29 [HO2] + [HO2] -> [H2O2] ; 2 8.7390E+01 1.1500E+03
30 [HO2] + [HO2] -> [H2O2] ; 4 7.6900E-10 5.8000E+03
-----
4 [NO2] + [O] -> [NO] ; 2 1.375E+04 0.0000E+00
5 [NO2] + [O] -> [NO3] ; 2 2.303E+02 6.8700E+02
6 [NO] + [O] -> [NO2] ; 2 3.233E+02 6.0200E+02
12 [OH] + [O3] -> [HO2] ; 2 2.344E+03 -9.4000E+02
13 [HO2] + [O3] -> [OH] ; 2 2.100E+01 -5.8000E+02
21 [NO] + [NO2] -> (2.00) [HONO] ; 4 1.600E-11 0.0000E+00
24 [HONO] + [OH] -> [NO2] ; 2 9.770E+03 0.0000E+00
25 [HONO] + [HONO] -> [NO] + [NO2] ; 2 1.5000E-05 0.0000E+00
27 [HNO3] + [OH] -> [NO3] ; 2 7.601E+00 1.0000E+03
32 [OH] + [H2O2] -> [HO2] ; 2 4.7200E+03 -1.8700E+02
33 [CO] + [OH] -> [HO2] ; 2 3.2200E+02 0.0000E+00
34 [HCHO] + [OH] -> [HO2] + [CO] ; 1 1.5000E+04 0.0000E+00
37 [HCHO] + [O] -> [OH] + [HO2] + [CO] ; 2 4.3020E+04 -1.5500E+03
38 [HCHO] + [NO3] -> [HNO3] + [HO2] + [CO] ; 1 9.3000E-01 0.0000E+00
39 [RHCO] + [O] -> [C2O3] + [OH] ; 2 1.7390E+04 -9.8600E+02
40 [RHCO] + [OH] -> [C2O3] ; 2 1.0370E+04 2.5000E+02
41 [RHCO] + [NO3] -> [C2O3] + [HNO3] ; 1 3.7000E+00 0.0000E+00
46 [C2O3] + [C2O3] -> (2.00) [XO2] + (2.00) [HCHO] + (2.00) [HO2] ; 1 3.7E+03
47 [C2O3] + [HO2] -> (0.79) [HCHO] + (0.79) [XO2] + (0.79) [HO2] + (0.79) [OH]
; 1 9.6E+03
48 [OH] -> [XO2] + [HCHO] + [HO2] ; 2 6.521E+03 -1.71E+03
49 [PAR] + [OH] -> (0.87) [XO2] + (0.13) [XO2N] + (0.11) [HO2] + (0.11)
[RHCO] + (-0.11) [PAR] + (0.76) [ROR] ; 1 1.2030E+03 0.0000E+00
50 [ROR] -> (1.10) [RHCO] + (0.96) [XO2] + (0.94) [HO2] + (0.04) [XO2N] +
(0.02) [ROR] + (-2.10) [PAR] ; 2 6.2510E+16 -8.0000E+03
51 [ROR] -> [HO2]; 1 9.5450E+04 0.0000E+00
52 [ROR] + [NO2] ->; 1 2.2000E+04 0.0000E+00
53 [O] + [OLE] -> (0.63) [RHCO] + (0.38) [HO2] + (0.28) [XO2] + (0.30) [CO]

```

```

      + (0.20) [HCHO] + (0.02) [XO2N] + (0.22) [PAR] + (0.20) [OH]
      ; 2 1.7560E+04 -3.2400E+02
54 [OH] + [OLE] -> [HCHO] + [RHCO] + [XO2] + [HO2] + (-1.00) [PAR]
      ; 2 7.7400E+03 5.0400E+02
55 [O3] + [OLE] -> (0.50) [RHCO] + (0.74) [HCHO] + (0.33) [CO] + (0.44) [HO2]
      + (0.22) [XO2] + (0.10) [OH] + (-1.00) [PAR] ; 2 2.104E+01 -2.105E+03
56 [NO3] + [OLE] -> (0.91) [XO2] + [HCHO] + [RHCO] + (0.09) [XO2N] + [NO2]
      + (-1.00) [PAR]; 1 1.135E+01 0.00E+00
57 [O] + [ETH] -> [HCHO] + (0.70) [XO2] + [CO] + (1.70) [HO2] + (0.30) [OH]
      ; 2 1.5400E+04 -7.9200E+02
58 [OH] + [ETH] -> [XO2] + (1.56) [HCHO] + [HO2] + (0.22) [RHCO]
      ; 2 3.0010E+03 4.1100E+02
59 [O3] + [ETH] -> [HCHO] + (0.42) [CO] + (0.12) [HO2]
      ; 2 1.8560E+01 -2.6330E+03
60 [TOL] + [OH] -> (0.08) [XO2] + (0.36) [CRES] + (0.44) [HO2]
      + (0.56) [TO2]; 2 3.1060E+03 3.2200E+02
61 [TO2] + [NO] -> (0.90) [NO2] + (0.90) [HO2] + (0.90) [OPEN]
      ; 1 1.2000E+04 0.0000E+00
62 [TO2] -> [CRES] + [HO2] ; 1 2.5000E+02 0.0000E+00
63 [OH] + [CRES] -> (0.40) [CRO] + (0.60) [XO2] + (0.60) [HO2] + (0.30) [OPEN]
      ; 1 6.1000E+04 0.0000E+00
64 [CRES] + [NO3] -> [CRO] + [HNO3]; 1 3.2500E+04 0.0000E+00
65 [CRO] + [NO2] -> ; 1 2.0000E+04 0.0000E+00
66 [OPEN] -> [C2O3] + [HO2] + [CO] ; 0 0.0000E+00 0.0000E+00
67 [OPEN] + [OH] -> [XO2] + (2.00) [CO] + (2.00) [HO2] + [C2O3] + [HCHO]
      ; 1 4.4000E+04 0.0000E+00
68 [OPEN] + [O3] -> (0.03) [RHCO] + (0.62) [C2O3] + (0.70) [HCHO] + (0.03)
      [XO2] + (0.69) [CO] + (0.08) [OH] + (0.76) [HO2] + (0.20) [MGLY]
      ; 2 8.0310E-02 -5.0000E+02
69 [XYL] + [OH] -> (0.70) [HO2] + (0.50) [XO2] + (0.20) [CRES] + (0.80)
      [MGLY] + (1.10) [PAR] + (0.30) [TO2] ; 2 2.4530E+04 1.1600E+02
70 [MGLY] + [OH] -> [XO2] + [C2O3]; 1 2.6000E+04 0.0000E+00
71 [MGLY] -> [C2O3] + [HO2] + [CO]; 0 0.0000E+00 0.0000E+00
72 [ISOP] + [O] -> (0.6) [HO2] + (0.80) [RHCO] + (0.55) [OLE] + (0.5)
      [XO2] + (0.5) [CO] + (0.45) [ETH] + (0.9) [PAR]; 1 2.70E+04 0.0E+00
73 [ISOP] + [OH] -> [XO2] + [HCHO] + (0.67) [HO2] + (0.4) [MGLY] + [ETH] +
      (0.2) [RHCO] + (0.13) [XO2N] ; 1 1.4200E+05 0.0000E+00
74 [ISOP] + [O3] -> [HCHO] + (0.4) [RHCO] + (0.55) [ETH] + (0.2) [MGLY] +
      (0.44) [HO2] + (0.1) [OH] + (0.06) [CO] + (0.1) [PAR]
      ; 1 1.8000E-02 0.0000E+00
75 [ISOP] + [NO3] -> [XO2N]; 1 4.70E+02 0.0000E+00
78 [XO2N] + [NO] -> ; 1 1.0000E+03 0.0000E+00
82 [SO2] -> [SA] ; 1 0.0000E+00 0.0000E+00
83 [XO2] + [HO2] -> ; 2 1.135E+02 1.30E+03
-----

```

